Belgian Physical Society
general scientific meeting

28 May 2025

BPS
Belgian Physical Society

UCLouvain

Belgian Physical Society general scientific meeting 2025
28 May, Louvain-la-Neuve

Venue

Auditoires Croix du Sud, place Croix du Sud, 1348 Louvain-la-Neuve

Local Organizing Committee (UCLouvain)

Xavier Urbain
Gwenhaël Wilberts Dewasseige
Matthieu Génévriez
Benoît Hackens
François Massonnet

Scientific Committee

Jozef Ongena	Ecole Royale Militaire - Koninklijke Militaire School
Gilles Rosolen	Université de Mons
Spencer Jolly	Université libre de Bruxelles
Michael Tytgat	Vrije Universiteit Brussel
Peter Schlagheck	Université de Liège
Ewald Janssens	KU Leuven
Jacques Tempere	UAntwerpen
Fabrice Louche	Ecole Royale Militaire - Koninklijke Militaire School
Kristel Crombé	Ugent/Ecole Royale Militaire - Koninklijke Militaire School
Michèle Coeck	SCK/Centre d'Etude de l'Energie Nucléaire
Henk Vrielinck	Universiteit Gent
Gwendolyn Lacroix	Université de Mons
Jean Jodogne	Inst.R.Météo-Kon.Meteo.Inst.
Yves Caudano	Université de Namur
Raymond Koch	Ecole Royale Militaire - Koninklijke Militaire School
Karolien Lefever	Royal Belgian Institute for Space Aeronomy
Bart Cleuren	U Hasselt
Alberto Mariotti	Vrije Universiteit Brussel
Xavier Urbain	Université catholique de Louvain
Dirk Saeys	VELEWE

PL Plenary Session
CAT Catering
PS Poster Session
SP Sponsor Booth

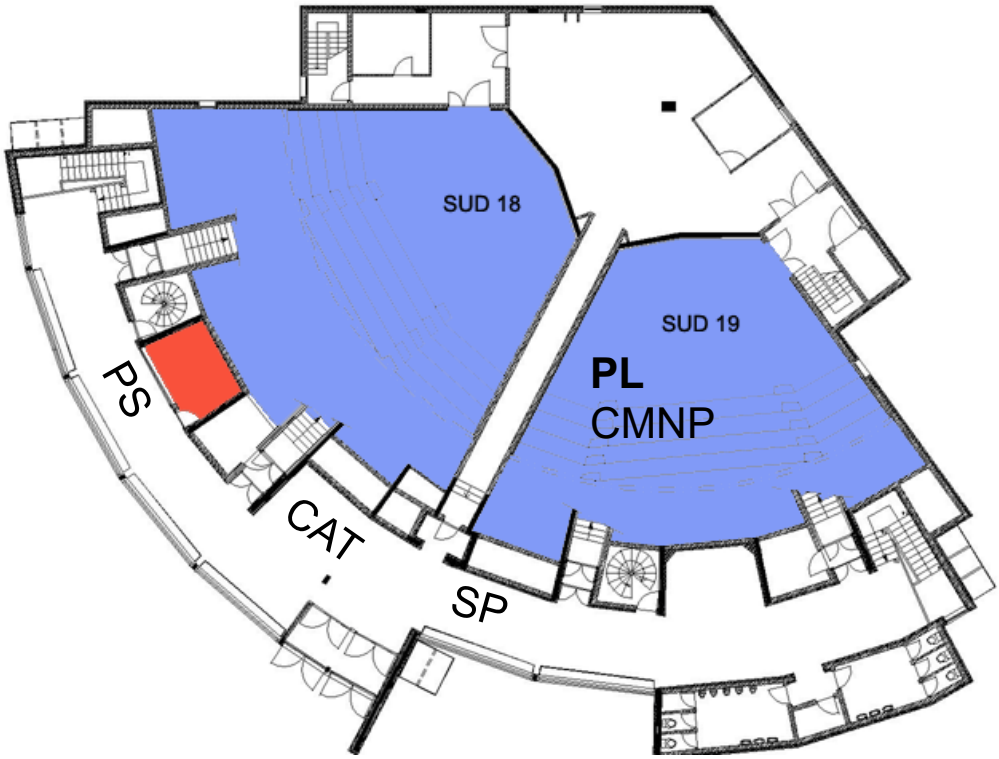

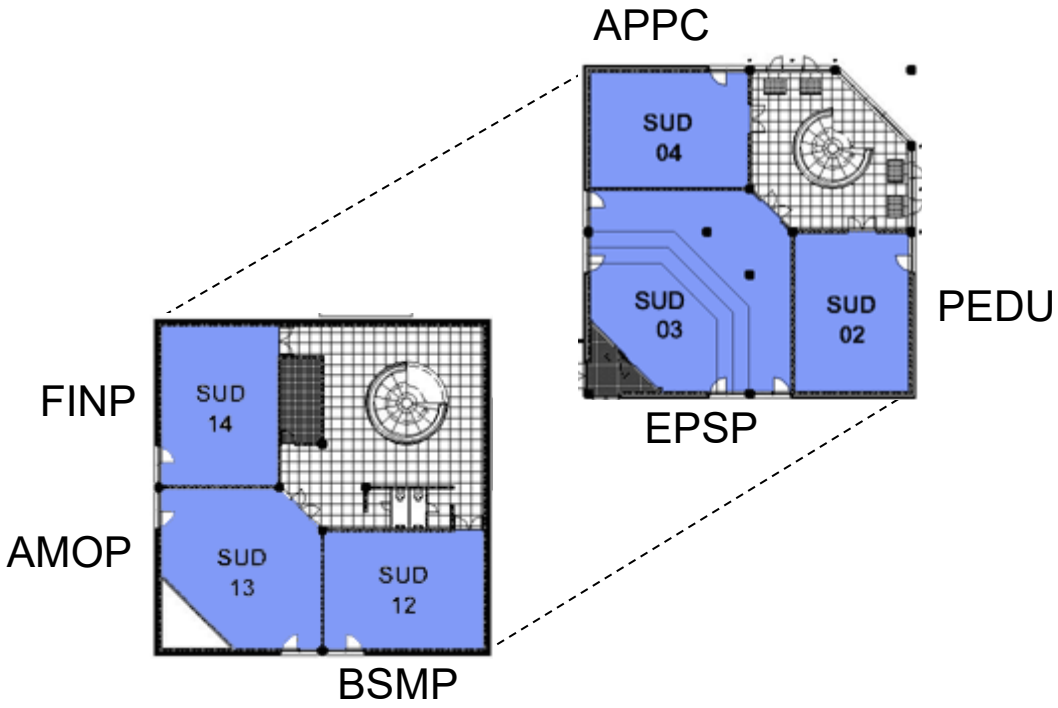

EPSP Earth & Planetary Sciences and Plasma Physics
CMNP Condensed Matter and Nanostructure Physics
APPC Astroparticle Physics and Cosmology
FINP Fundamental Interactions, Nuclear and Particle Physics
AMOP Atomic, Molecular & Optical Physics and Photonics
BSMP Biological, Statistical and Mathematical Physics
PEDU Physics and Education

This conference is organized with the generous support of

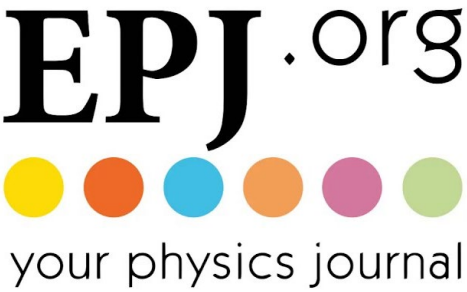

General Scientific Meeting of the Belgian Physical Society

8:30 Registration and coffee

9:00 – 10:50 Plenary lectures

9:00 Welcome address

9:10 **Antoine Browaeys** (CNRS, Inst. d'Optique, Institut de France)
Assembling quantum matter one atom at a time P1

10:00 **Tim Palmer** (Oxford University, Royal Society)
Chaos, noise and uncertainty: enemies or allies for predicting weather and climate? P2

10:50 Coffee break

11:15 – 12:25 Young Speaker Contest

11:15 Introduction of the European Physical Journal (EPJ)

11:25 **Elena Petrova** *(*KULeuven)
High-frequency waves in the upper solar atmosphere as observed by Solar Orbiter/EUI P3

11:45 **Anupama K Xavier** (KMI)
Comparative predictability of eastern and western north pacific blocking events P4

12:05 **Jonathan Mauro** (UCLouvain)
Model-agnostic interpretation of the first KM3NeT Ultra-High-Energy event within the Global Neutrino Landscape P5

12:25 Conference picture

12:30 – 14:30 Walking lunch and posters

14:30 – 17:15 Parallel sessions

- Earth and Planetary Sciences, and Plasma Physics
- Condensed Matter and Nanostructure Physics
- Astroparticle Physics and Cosmology
- Fundamental Interactions, Nuclear and Particle Physics
- Atoms, Molecules, Optics and Photonics
- Biological, Medical, Statistical and Mathematical Physics
- Physics and Education

17:30 – 18:30 Closing ceremony

Master Thesis, Best Poster & Young Speaker prizes & reception

A – **Earth & Planetary Sciences and Plasma Physics**

Chairs: Kristel Crombé (UGent) and François Massonnet (UCLouvain)

Parallel session

14:30 **Laurent Masse** (CEA, France)
Inertial Confinement Fusion: Ignition and What Next? A1

15:00 Yangyang Zhang (UGent)
Bayesian Techniques for Optimization of Nuclear Diagnostics: A Case Study on the WEST Tokamak A2

15:15 **Alexander Haumann** (Alfred Wegener Institute/Ludwig-Maximilians-Universität München, Germany)
What goes around comes around: A changing Southern Ocean A3

15:45 break

16:00 Benjamin Richaud (UCLouvain)
Does increased spatial resolution improve the simulation of Antarctic sea ice? A4

16:15 Eva Lemaire (UCLouvain)
Investigating Iceberg–Sea Ice Interactions in the Southern Ocean Using NEMO-ICB A5

16:30 Jerome Sauer (UCLouvain)
Extreme Arctic sea ice lows investigated with a rare event algorithm A6

16:45 Noé Pirlet (UCLouvain)
Impact of a representation of Antarctic landfast ice on the shelf water properties simulated by NEMO4-SI³ A7

17:00 Antoine Honet (ULB)
Estimation of atmospheric lifetime and emissions of NH_3 sources from 15 years of satellite data A8

Posters

Francis Feba (UCLouvain) *Antarctic Sea Ice Response to Wind Perturbation Experiments* A9

Annelies Sticker (UCLouvain) *Drivers of Arctic Rapid Sea Ice Loss Events in CESM2* A10

B – **Condensed Matter and Nanostructure Physics**

Chairs: Clément Merckling (KULeuven/IMEC) and Benoît Hackens (UCLouvain)

Parallel session

14:30 **Maëlle Kapfer** (Univ. Paris-Saclay, France) *Programming twist angle and strain gradient in two-dimensional materials* B1

15:00 Oriane de Leuze (UCLouvain) *Charge transport in 2D flakes networks: the case of Ti3C2Tx* B2

15:15 Yaojia Wang (KU Leuven) *Supercurrent interference in a kagome superconductor* B3

15:30 Amirmostafa Amirjani (KU Leuven) *Inverse design of plasmonic metasurface using machine learning* B4

15:45 break

16:00 **Vincent Meunier** (Pennsylvania State University, USA) *Electromechanical coupling at the nanoscale: The ubiquitous case of flexoelectricity* B5

16:30 Danny Vanpoucke (U Hasselt) *Straining group-IV color centers in diamond: Using density functional theory to model the Zero-Phonon-Line shift* B6

16:45 Matthew Houtput (U Antwerpen) *First principles theory of nonlinear long-range electron-phonon interaction* B7

17:00 Simon Dubois (UCLouvain) *Inference based model Hamiltonians balancing accuracy, interpretability and data efficiency* B8

Posters

Serghei Klimin (U Antwerpen) *Analytic Methods for Polarons in a Non-Parabolic Conduction Band* B9

Wu Heng (KU Leuven) *The global critical current effect of superconductivity* B10

Diego Fossion (UCLouvain) *Properties of Kondo cloud modulations in quantum dots coupled to cavities* B11

Pauline Castenetto (U Hasselt) *Identification and characterisation of the reaction path of β-O-4 dimerisation of monolignols by means of first-principles calculations* B12

E. Aylin Melan (U Hasselt) *From DFT to GW: Benchmarking the Electronic Structure of Diamond* B13

Lisa Siciliani (Sciensano/U Antwerpen) *Physicochemical characterisation of iron oxides and hydroxides applied as food additive E 172* B14

Emerick Y. Guillaume (U Namur) *Multiscale modelling of LTO PVD growth* B15

Fernando Massa Fernandes (UCLouvain) *Real-time gas sensing with lead-sulfide quantum-dots* B16

Thijs van Wijk (U Hasselt) *Calculating the vibrational spectrum of the GeV defect in Diamond* B17

Célia Delaive (ULiège) *Creating NOON states with ultracold atoms using time crystals* B18

Michael Tzvetkov (UCLouvain) *Study of out-of-plane electronic transport in multilayer graphene films by C-AFM* B19

Sofiane Arib (UCLouvain) *Estimation of electrical conductivity anisotropy in MXenes by CAFM modeling* B20

Arnaud Dochain (UCLouvain) *Observation of fast atom diffraction through suspended graphene* B21

Valentin Fonck (UCLouvain) *A Scanning Thermal Microscope at cryogenic temperatures* B22

C – **Astroparticle Physics and Cosmology**

Chairs: Juan Antonio Aguilar Sánchez (ULB) and Gwenhaël Wilberts Dewasseige (UCLouvain)

Parallel session

14:30 Aart Heijboer (NIKHEF/University of Amsterdam)
Observation of the first ultra-high energy cosmic neutrino C1

15:00 Soumen Roy (UCLouvain)
Parametrized test of general relativity with gravitational waves including higher harmonics and precession C2

15:20 Leonardo Ricca (UCLouvain)
Multi-Messenger Search for Neutrino and Gravitational-Wave Emissions from Binary Black Holes Near Active Galactic Nuclei C3

15:40 Jef Heynen (UCLouvain)
Using the null stream to detect strongly lensed gravitational waves C4

16:00 break

16:15 Emile Moyaux (UCLouvain)
Neutrino energy distributions of astrophysical sources: the GRB example C5

16:35 Nhan Chau (ULB)
Dark matter search in the Galactic Center with IceCube Upgrade C6

16:55 Guillaume Lhost (UMONS)
Late inspiral of eccentric asymmetric binaries C8

Posters

Eliot Genton (UCLouvain) *Prospective Sensitivity to WIMP Dark Matter with the IceCube Upgrade* C9

Christoph Raab (UCLouvain) *Low-latency neutrino follow-up combining diverse IceCube selections* C10

Mathieu Lamoureux (UCLouvain) *Multi-messenger astrophysics with the ACME consortium* C11

Mathieu Lamoureux (UCLouvain) *Multi-messenger astrophysics with the ACME consortium* C11

Marco Scarnera (UCLouvain/Université Paris Cité) *Probing neutrino yield from different gamma-ray burst populations using the entire ANTARES data set* C12

Thomas Delmeulle (ULB) *Studying Muon Bundles for Improved EHE Neutrino Identification in IceCube* C13

Marine Vilarino (ULB) *Cosmic Ray Simulation for Background Rate Estimation in the ARA Detector using the FAERIE Framework* C14

D – **Fundamental Interactions, Nuclear and Particle Physics**

Chairs: Nick Van Remortel (UAntwerpen) and Alberto Mariotti (ULB)

Parallel Session

14:30 **Agi Koszorus** (KULeuven, invited)
Laser spectroscopy of radioactive probes: study of the nuclear force and searches for new physics D1

15:05 Martin Delcourt (CERN)
How Belgium is ensuring the CMS tracker data performance D2

15:25 Aloke Kumar Das (ULB)
The Belgian contribution to the CMS Silicon Strip Tracker Upgrade D3

15:45 break

15:55 Sumaira Ikram (UCLouvain)
Development of a portable particle detector for imaging with cosmic ray muons D4

16:15 Felipe Figueroa Vilar del Valle (UMONS)
Dual Models revisited: A bootstrap perspective D5

16:35 ZeQiang Wang (UCLouvain)
The Brief Talk of τ g-2 for Future Colliders D6

16:55 Cyrille Chevalier (UMONS)
Glueballs with two and three constituent gluons within the helicity formalism D7

Posters

Arjun Chaliyath (CERN) *High precision automated metrology of the 2S modules for the CMS phase-II tracker upgrade* D8

Dora Geeraerts (VUB) *The ScIDEP Muon Radiography Project at the Egyptian Pyramid of Khafre* D9

Zahraa Zaher (UCLouvain) *Differentiable Optimization of Muon Scattering Tomography Detector Designs* D10

E – **Atoms, Molecules, Optics and Photonics**

Chairs: Tatevik Chalyan (VUB) and Matthieu Génévriez (UCLouvain)

Parallel session

14:30 **John Fourkas** (University of Maryland, USA) *Is visible light the way forward for cutting-edge nanolithography?* E1

15:00 Spencer Jolly (ULB) *Propagation of space-time optical beams in multimode fibers* E2

15:15 Sélim Chaabani (ULiège) *Going to 2.1 μm for Space Quantum Key Distribution* E3

15:30 Julien Grondin (UCLouvain) *Construction and Characterization of a Ca Magneto-Optical Trap for Rydberg Physics* E4

15:45 break

16:00 Robbe Van Duyse (KU Leuven) *High precision optical spectroscopy using trapped Sr ions* E5

16:15 Alexandr Bogomolov (UCLouvain) *High resolution spectrum of D_2O-CO_2 van der Waals complex around the 3OD vibrational excitation* E6

16:30 Mhamad Hantro (UMONS) *Impact of Higher Order Effects in the Far-field for Dipole-Forbidden Transitions near Plasmonic Structures* E7

16:45 Adrien Debacq (UNamur) *Finite-Difference Time-Domain Analysis of Stimulated Emission in NZI Materials* E8

17:00 Sébastien Mouchet (UMONS) *Nature-Inspired Strategies for Infrared Control and Thermal Insulation* E9

Posters

Arthémise Altman (UCLouvain) *Spectroscopy of methanol in the near-infrared at the 10^{-13} level* E10

Yves Caudano (UNamur) *Weak values as stereographic projections* E11

Simon Dengis (ULiège) *NOON states creation with ultracold atoms via geodesic counterdiabatic driving* E12

Julien Bouchat (UNamur) *Weak measurements and Goos-Hänchen effects in the case of uniaxial anisotropic media* E13

Alisée Bouillon (UCLouvain) *Electron transfer between ultra-long range Rydberg molecules and heavy-Rydberg molecules* E14

Steve Smeets (UMONS) *Two-photon molecular emitters enhanced with nanoantennas* E15

Hippolyte Stassart (ULiège) *Study of the optical coupling between luminescent quantum dots and gold nanorods* E16

Loris Cavenaile (UMONS) *Achieving Optical Transparency: Simulations of Light Scattering in Biological Tissues* E17

Simon Collignon (UCLouvain) *Rest frequency determination of the 12.2 GHz methanol maser line with sub-kHz accuracy* E18

Xavier Huet (ULB) *Rovibronic spectra of carbon monoxide dication* CO^{2+} E19

Xavier Urbain (UCLouvain) *Resolving the fine structure branching ratio in* K^- *photodetachment* E20

F – **Biological, Medical, Statistical & Mathematical Physics**

Chairs: Bart Cleuren (U Hasselt) and Edmond Sterpin (UCLouvain)

Parallel session

14:30 **Enrico Carlon** (KU Leuven)
DNA Topology: from single molecules to chromosomal structure F1

15:00 **Bram Carlier** (KU Leuven)
Towards in vivo radiation sensing using radiation-sensitive ultrasound contrast agents F2

15:30 Charlotte Rossi (U Namur)
TOF-SIMS as a tool to study the alteration of membrane lipids in breast cancer cells after X-Ray and UHDR proton irradiation F3

15:45 Khalil El Achi (UCLouvain)
Design of a new 2D amorphous Silicon-based detector for Particle Therapy F4

Posters

Éléonore Martin (UMONS) *Monte Carlo study of high-field transverse relaxation induced by iron oxide nanoparticles coated by a slow water diffusion layer* F5

Gijs Vanoppen (U Hasselt) *Electrical stress on metallic nanoring based networks for flexible transparent electrodes* F6

G – **Physics and Education**

Chair: Gabriel Dias de Carvalho Junior (UCLouvain)

Parallel Session

14:30 Michaël Lobet (UNamur)
Interaction between students and AI in a physics course: Towards modelling a learning practice G1

15:00 **Carlos Fiolhais** (Coimbra University)
"The Fun of Physics": a book for informal education G2

15:45 break

16:00 Anna Benecke (UCLouvain)
The Physics Project Days - A workshop to promote gender equality in physics G3

16:25 Brigitte Van Tiggelen (Science History Institute, Philadelphia)
"Women in their element" – What happens when the history of the periodic system focuses on women? G4

16:50 Elsa Tartinville (UCLouvain) and Gabriel Dias de Carvalho Junior (UNamur, UCLouvain)
Understanding Nuclear Physics at different stages or education: looking for operational invariants G5

Assembling quantum matter one atom at a time

Antoine Browaeys[1]

[1] *Laboratoire Charles Fabry, Institut d'Optique, CNRS,*
2 avenue A. Fresnel, 91127 Palaiseau, France

Over the last twenty years, physicists have learned to manipulate individual quantum objects: atoms, ions, molecules, quantum circuits, electronic spins... It is now possible to build "atom by atom" a synthetic quantum matter. By controlling the interactions between atoms, one can study the properties of these elementary many-body systems: quantum magnetism, transport of excitations, superconductivity... and thus understand more deeply the N-body problem. More recently, it was realized that these quantum machines may find applications in the industry, such as finding the solution of combinatorial optimization problems.

This talk will present an example of a synthetic quantum system, based on laser-cooled ensembles of individual atoms trapped in microscopic optical tweezer arrays. By exciting the atoms into Rydberg states, we make them interact, even at distances of more than ten micrometers. In this way, we study the magnetic properties of an ensemble of more than a hundred interacting ½ spins, in a regime in which simulations by usual numerical methods are already very challenging. Some aspects of this research led to the creation of a startup, Pasqal.

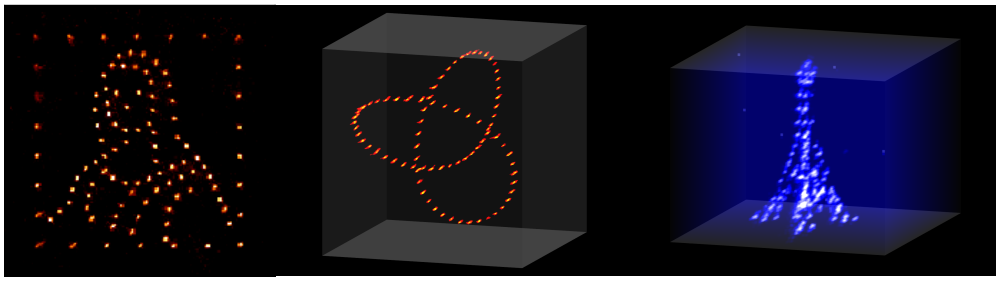

Figure 1: Fluorescence images of individual atoms trapped in various optical tweezers arrays. Each point corresponds to an atom.

Chaos, noise and uncertainty: enemies or allies for predicting weather and climate?

T. Palmer

[1]*Oxford Martin Institute and Jesus College, Oxford University, Oxford, United Kingdom*

The solutions to the physical equations that govern the dynamics of weather and climate exhibit chaotic behavior. In this lecture, Prof. Palmer will explore how chaos, noise, and uncertainty, initially seen as obstacles, can be exploited as constructive resources to enhance prediction capabilities from days to decades.

High-frequency waves in the upper solar atmosphere as observed by Solar Orbiter/EUI

Elena Petrova

Centre for mathematical Plasma Astrophysics, Mathematics Department, KU Leuven, Celestijnenlaan 200B bus 2400

Since the Sun's temperature was first measured, scientists have faced the challenge of explaining the abrupt rise in temperature observed from the chromosphere - the middle layer of the atmosphere - to the corona, its outermost layer. Despite being farther from the Sun's hot core, the corona is significantly hotter than the underlying layers, a puzzling phenomenon known as the coronal heating problem. Understanding how energy is transported and dissipated across these layers remains one of the key unsolved questions in solar physics.

Among the proposed explanations, wave-based mechanisms have gained significant attention, particularly the role of magnetohydrodynamic (MHD) waves in transferring and depositing energy. These waves are generated in the Sun's lower atmosphere and can travel upwards, potentially contributing to heating processes in the corona. However, the detection and characterization of these waves - especially at the small scales where energy dissipation is expected to occur - have been limited by instrumental constraints such as their temporal and spatial resolution.

In this study, we investigate two key aspects of wave-driven heating: the presence of high-frequency kink waves within small-scale coronal structures and the propagation of Alfvén waves from the lower atmosphere to the corona. First, we analyze high-frequency transverse waves detected in short coronal loops using the High Resolution Imager in extreme ultraviolet (HRIEUV) of the Extreme Ultraviolet Imager (EUI) onboard Solar Orbiter. The telescope's exceptional temporal and spatial resolution allowed us to observe waves with shorter periods than previously recorded, and our energy estimates suggest that these waves could play a crucial role in maintaining the temperature of the quiet solar corona.

Secondly, we turn our attention to the transport of energy from the lower layers of the Sun, focusing on Alfvén waves - one of the few wave modes capable of propagating efficiently from the photosphere to the corona. Using the superior resolution of our instruments, we successfully detected these rotational wave motions, a challenging task for imaging-based tools. To reinforce our analysis, we combined data from two additional instruments aboard Solar Orbiter - SPectral Imaging of the Coronal Environment (SPICE) and the Polarimetric and Helioseismic Imager (PHI). We also addressed instrumental challenges related to the point spread function (PSF) of SPICE by performing forward modeling analyses to generate synthesized raster images, ensuring the reliability of our derived Doppler maps.

These findings provide critical insights into how wave-based mechanisms contribute to the long-standing coronal heating problem. By detecting high-frequency kink waves with sufficient energy to heat the quiet corona and confirming the presence of propagating Alfvén waves that transport energy across atmospheric layers, we offer new observational evidence supporting wave-driven heating models. Additionally, our methodological advancements, such as addressing instrumental limitations through forward modeling, pave the way for more precise future studies of solar dynamics.

Comparative predictability of eastern and western north pacific blocking events

Anupama K Xavier[1,2], Oisín Hamilton[1,2] Davide Farandaand[3,4,5] Stéphane Vannitsem[1]

[1]*Royal Meteorological Institute, meteo et climato dynamique, Uccle, Belgium*
[2]*Université catholique de Louvain, Pl. de l'Université 1, 1348 Ottignies-Louvain-la-Neuve*
[3]*Laboratoire des Sciences du Climat et de l'Environnement, UMR 8212 CEA-CNRS-UVSQ, Université Paris-Saclay, IPSL,91191 Gif-sur-Yvette, France*
[4]*London Mathematical Laboratory, 8 Margravine Gardens London, W6 8RH, UK*
[5]*Laboratoire de Météorologie Dynamique/IPSL, École Normale Supérieure, PSL Research University, Sorbonne Université,École Polytechnique, IP Paris, CNRS, Paris, 75005, France*

North Pacific blocking patterns, defined by persistent high-pressure systems that disrupt atmospheric circulation, are pivotal elements of mid-latitude weather dynamics. These blocking events play a significant role in shaping regional weather extremes, such as prolonged cold spells or heatwaves, and can redirect storm tracks across the Pacific. For instance, the 2021 Pacific Northwest heatwave demonstrated the profound impact of blocking on terrestrial temperatures, where an upstream cyclone acted as a diabatic source of wave activity, intensifying the blocking system. This led to heat-trapping stable stratification, which elevated surface temperatures to unprecedented levels (Neal et al., 2022). Similarly, marine heatwaves in the Northeast Pacific have been linked to high-latitude blocking events, which weaken westerly winds, suppress southward Ekman transport, and enhance ocean stratification, thereby increasing sea surface temperatures (Niu et al., 2023). The predictability of North Pacific blocking events is governed by the intricate interplay of large-scale atmospheric dynamics, ocean-atmosphere interactions, and internal variability (Smith et al., 2020).

This study investigates the differences in predictability between eastern and western North Pacific blocking events, using a modified version of the Davini et al. (2012) blocking index to distinguish their geographical locations. Identified blocking events were tracked using a block-tracking algorithm until they dissipated. Predictability was assessed by identifying an analogue pair for each blocking event. Specifically, after classifying blocks as eastern or western, geopotential height maps for each event were compared to all other days in the dataset. The analogue pair for an event was defined as the day with the smallest root mean square (RMS) distance. Predictability was then evaluated by averaging the error evolution of the tracks between events in each analogue pair.

Using CMIP6 model simulations, the study revealed that eastern blocks are significantly more persistent and stable than their western counterparts. Eastern blocks exhibited longer durations and greater resistance to atmospheric variability, resulting in improved forecast accuracy. In contrast, western blocks were found to be more transient and challenging to predict due to their susceptibility to dynamic instabilities.

[1] Davini, P. *et al.*, 2012. Bidimensional diagnostics, variability, and trends of Northern Hemisphere blocking, *Journal of Climate*, **25(19)**, pp.6496-6509.

[2] Neal, E. *et al.*, 2022. The 2021 Pacific Northwest heat wave and associated blocking: Meteorology and the role of an upstream cyclone as a diabatic source of wave activity, *Geophysical Research Letters*, **49(8)**, p.e2021GL097699.

[3] Niu, X., Chen, Y. and Le, C., 2023. Northeast Pacific marine heatwaves associated with high-latitude atmospheric blocking, *Environmental Research Letters*, **19(1)**, p.014025.

Model-agnostic interpretation of the first KM3NeT Ultra-High-Energy event within the Global Neutrino Landscape

J. Mauro[1], C. Argüelles[2], G. W. De Wasseige[1], N. Kamp[2], M. Lamoureux[1], P.A. Sevle Myhr[1] and A. Y. Wen[2] for the KM3NeT Collaboration

[1] *UCLouvain, Centre for Cosmology, Particle Physics and Phenomenology, Chemin du Cyclotron, 2, Louvain-la-Neuve, 1348 Belgium*
[2]*Harvard University, Department of Physics and Laboratory for Particle Physics and Cosmology, Lyman Laboratory, 17 Oxford St., Cambridge, MA 02138 USA*

On February 13th, 2023, the KM3NeT/ARCA telescope [1] detected a neutrino candidate with an estimated energy in the hundreds of PeVs [2], surpassing prior observations by the IceCube Neutrino Observatory by more than one order of magnitude. We review this ultra-high-energy neutrino detection in light of null observations above tens of PeV from the IceCube [3] and Pierre Auger [4] observatories. Assuming an isotropic E^{-2} flux, we combine data from all three experiments to obtain a joint-fit flux of $E^2\phi^{1\mathrm{f}}_{\nu+\bar{\nu}} = 7.5 \times 10^{-10}\ \mathrm{GeV\,cm^{-2}\,s^{-1}\,sr^{-1}}$ in the 90% energy range of the KM3NeT event. Furthermore, we present the first combination of positive observations of high-energy neutrinos from different experiments. Specifically, we discuss how the ultra-high-energy data fit with the IceCube measurements at lower energies, either with a single power law or with a broken power law, allowing for the presence of a new component in the spectrum. We find a slight preference for a break in the PeV regime when including IceCube's "High-Energy Starting Events" [5] sample, while no such preference emerges in the other cases considered [6, 7]. Finally, we discuss the prospects that may lead to resolving the apparent discrepancy between experiments and better characterizing the neutrino landscape at ultra-high energies [8].

[1] S. Adrian-Martinez *et al* (KM3NeT) 2016 *J. Phys. G* **43** 084001
[2] S. Aiello *et al* (KM3NeT) 2025 *Nature* **638** 376–382
[3] M. Meier (IceCube) 2024 in *58th Rencontres de Moriond on Very High Energy Phenomena in the Universe* arXiv:2409.01740 [astro-ph.HE]
[4] A. Abdul Halim *et al* (Pierre Auger) 2023 *PoS* **ICRC2023** 1488
[5] R. Abbasi *et al* (IceCube) 2021 *Phys. Rev. D* **104** 022002
[6] R. Abbasi *et al* (IceCube) 2022 *Astrophys. J.* **928** 50
[7] R. Abbasi *et al* (IceCube) 2024 *Phys. Rev. D* **110** 022001
[8] O. Adriani *et al* (KM3NeT) 2025 arXiv:2502.08173 [astro-ph.HE]

Recent breakthrough in Inertial Confinement Fusion

L. Masse[1]

[1]*CEA/DAM/DIF, Arpajon France*

In august 2021 the Lawrence Livermore National Laboratory in California USA claimed to have reached the threshold of laser fusion ignition on the National Ignition Facility (NIF). Few months later the tokamaks EAST in China and Jet in UK established new fusion energy and plasma temperature records in Magnetic Confinement Fusion. In the same time a young company reached for the first time 100 millions Kelvin in a facility built on private funds, proving how active fusion research is.
In this talk we will present the fundamentals of thermonuclear fusion and the different approaches to control thermonuclear fusion reactions. We will explain what those recent records really mean and how the different approaches and projects compare to each others. The presentation will concentrate then on the 10 years journey leading to the recent breakthrough obtained on NIF. Last, we will discuss the impact of these results on the Inertial Confinement Fusion community and the long term perspectives.

Bayesian Techniques for Optimization of Fusion Diagnostics: A Case Study on the WEST Tokamak.

Y. Zhang[1], J. De Rycke[1], D. Mazon[2], G. Verdoolaege[1] and the WEST team

[1]*Ghent University, Ghent, 9000, Belgium*
[2]*IRFM, CEA, Saint Paul-lez-Durance, 13108, France*

Nuclear fusion devices like tokamaks and stellarators are complex systems operating under extreme physical conditions. As a consequence, direct measurements are typically unfeasible, and diagnostics rely primarily on indirect observations, which inherently present significant inverse problems. Accurate diagnostic systems are therefore critical for obtaining precise magnetic and kinetic information necessary for the reliable operation and safety control of these fusion reactors. However, these diagnostic systems are often constrained by practical limitations such as budget and space restrictions, emphasizing the importance of optimizing their design.

In this study, we present an example of design optimization applied to the pick-up coil diagnostic system on the WEST tokamak, utilizing advanced Bayesian techniques. By employing mutual information as the evaluation metric, we demonstrate that the number of pick-up coils can be substantially reduced without compromising the accuracy of key physical parameters. While Bayesian methods have already proven highly effective in addressing inverse problems such as sensor fusion (integrated data analysis) and solving partial differential equations, this work further shows their strength in system optimization tasks relevant to fusion research.

What goes around comes around: A changing Southern Ocean

F. A. Haumann[1,2]

[1]*Alfred Wegener Institute Helmholtz Centre for Polar and Marine Research, Bremerhaven, 27570, Germany*
[2]*Ludwig-Maximilians-Universität München, Munich, 80333, Germany*

The Southern Ocean plays a vital role in the global climate system as it connects the global surface waters with the deep ocean. In fact, in this region about 80% of the global subsurface waters return to the surface and are renewed through ice-ocean and atmosphere-ocean interactions. In this process, climatically relevant constituents like carbon and heat are exchanged and lead to melting of ice and affect near-surface warming and atmospheric CO_2 concentrations. While this system has slowed global surface warming since the preindustrial era by taking up a major share of the anthropogenic heat and CO_2, it remains uncertain if the system will continue to provide such a service in future, in particular in light of the recently observed drastic sea ice decline. In this presentation, I will outline the most recent changes that have occurred in the coupled Southern Ocean ice-ocean system and motivate the need for a currently planned large international campaign (Antarctica InSync) to better understand this system.

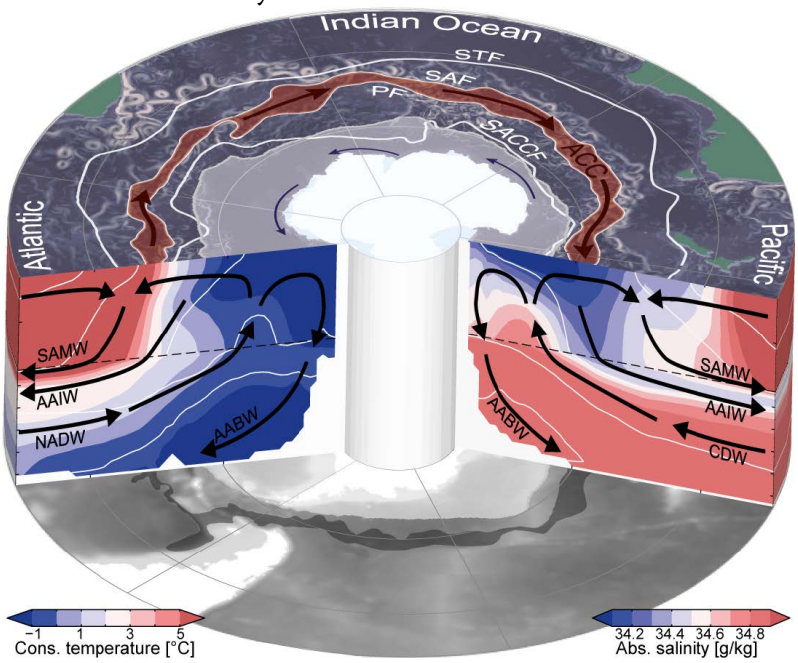

Figure 1: Schematic of the Southern Ocean overturning circulation, water masses, and stratification: the top shows the main fronts (STF: Subtropical Front, SAF: Subantarctic Front, PF: Polar Front, SACCF: Southern ACC Front; white), the Antarctic Circumpolar Current (ACC; red), the Antarctic Coastal Current (blue), the winter sea ice extent (September; gray), and ocean velocity (background). AABW, Antarctic Bottom Water; NADW, North Atlantic Deep Water; CDW, Circumpolar Deep Water; AAIW, Antarctic Intermediate Water; SAMW, Subantarctic Mode Water. Source: Haumann et al. (2016).

[1] Haumann, F. A. 2016 *ETH Zurich: Doctoral Thesis* doi: 10.3929/ethz-b-000166276

Does increased spatial resolution improve the simulation of Antarctic sea ice?

B. Richaud[1], F. Massonnet[1], T. Fichefet[1], D. Topál[1], A. Barthélemy[1] and D. Docquier[2]

[1]*Earth and Climate Research Center, Earth and Life Institute, Université catholique de Louvain, Louvain-la-Neuve, Belgium*
[2]*Dynamical Meteorology and Climatology Unit, Royal Meteorological Institute of Belgium, Brussels, Belgium*

The Antarctic total sea ice extent has rapidly evolved over the past decade, with a stagnating or slowly increasing extent until 2015 followed by a important drop. The sea ice state has not recovered since then, and co-occurred with warm ocean subsurface temperatures, therefore hypothesised to have driven the recent decline in sea ice extent. Using the global ocean–sea ice model NEMO4.2-SI[3] in the same setup but at three different horizontal resolutions (namely, 1/12°, 1/4° and 1°), we thoroughly examine the sea ice states and underlying oceanic conditions simulated by the model. We then compare how increased spatial resolution, allowing for the simulation of finer-scale physical processes such as ocean eddies, impacts the modelled sea ice thickness and concentration distribution, as well as the different ice mass fluxes. A particular attention is being paid to the influence of ocean heat content anomalies, as increased horizontal resolution provides a more realistic simulation of heat inflow accross the Antarctic Circumpolar Current through the resolution of eddies generated downstream of bathymetric features. This study highlights the benefits of increased spatial resolution for realistically simulating the Antarctic sea ice cover and weighs them with the associated computational cost. The decomposition of the ice mass budget into its different thermodynamic and dynamic terms puts forward the often downplayed role of the ocean in determining the interannual variability of Antarctic sea ice and provides a stepping stone for further studies.

Investigating Iceberg–Sea Ice Interactions in the Southern Ocean Using NEMO-ICB

E. Lemaire[1], F. Massonnet[1], T. Fichefet[1], N. Pirlet[1], P. Mathiot[2], J. Marini Marson[3], and A. Olivé Abelló[2],

[1]*Earth and Climate, Earth and Life Institute, Université Catholique de Louvain, Louvain-la-neuve, 1348, Belgium*
[2]*Institut des Géosciences de l'Environnement, Université Grenoble Alpes, Grenoble, 38000, France*
[3]*Centre for Earth Observation Science (CEOS), Department of Environment and Geography, Clayton H. Riddell Faculty of Environment, Earth, and Resources, University of Manitoba, Winnipeg, MB R3T 2N2, Canada*

Icebergs, formed by the calving of the Antarctic ice sheet, are among the most emblematic natural features of the polar regions. Their presence in the Southern Ocean, an essential carbon and heat sink, raises important questions about their role in the future evolution of the ocean and climate. As the mass balance of the Antarctic ice sheet continues to decline, it is crucial to better understand how iceberg-sea ice interactions influence ocean dynamics and sea ice variability in the Southern Ocean.

In this study, we use the NEMO version 4.2.2 ocean model coupled to the ICB module (Iceberg) to investigate these interactions. Our approach has two main objectives: (1) We assess the impact of icebergs on the ocean and sea ice by running two 30-year regional hindcast simulations of the Southern Ocean, one with the ICB module enabled and the other with the module disabled. This allows us to isolate the influence of iceberg dynamics on sea ice concentration and thickness, along with ocean physical properties such as surface temperature and salinity. And (2) by implementing a sea ice locking process in the ICB module after Lichey and Hellmer (2001) [1] we aim to better represent the mechanical interactions between icebergs and sea ice, particularly when icebergs become 'trapped' by thick, highly concentrated sea ice. Sea ice locking has a major impact on the distribution of freshwater fluxes in the ocean, by influencing the trajectory of icebergs.

This study is a first step towards improving our understanding of the coupled iceberg-sea ice-ocean system and its implications for the future evolution of the Southern Ocean in a changing climate.

[1] Lichey C and Hellmer H. 2001 *Journal of Glaciology* 47, no. 158 (January 2001): 452–60. https://doi.org/10.3189/172756501781832133.

Extreme Arctic sea ice lows investigated with a rare event algorithm

J. Sauer[1], F. Ragone[2], F. Massonnet[1], J. Demaeyer[3], G. Zappa[4]

[1]*Earth and Climate Research Center, Earth and Life Institute, Université catholique de Louvain, Louvain-la-Neuve, Belgium*
[2]*School of Computing and Mathematical Sciences, University of Leicester, Leicester, United Kingdom*
[3]*Royal Meteorological Institute of Belgium, Brussels, Belgium*
[4]*National Research Council of Italy, Institute of Atmospheric Sciences and Climate, Bologna, Italy*

Various studies identified possible drivers of extreme Arctic sea ice lows, such as observed in the summers of 2007 and 2012, including preconditioning, feedback mechanisms, the oceanic heat transport and the atmospheric circulation. However, a robust quantitative statistical analysis of extreme Arctic sea ice lows is hindered by the small number of events that can be sampled in observations and numerical simulations with computationally expensive climate models. Recent studies tackled the problem of sampling climate extremes by using rare event algorithms, i.e., computational techniques developed in statistical physics to reduce the computational cost required to sample rare events in numerical simulations [1]. Here we apply a rare event algorithm to ensemble simulations with the coupled climate models Planet Simulator (PlaSim) [2] and European community Earth-System-Model version 3 (EC-Earth3) [3] to investigate extreme negative summer pan-Arctic sea ice area anomalies in present-day climate conditions. Owing to the algorithm, we produce sea ice lows with probabilities of two orders of magnitude smaller than feasible with direct sampling, and we compute statistically significant composite maps of dynamical quantities conditional on the occurrence of these extremes. We exploit the improved statistics to study precursors of extremely negative summer sea ice area anomalies, including a surface energy budget analysis to disentangle the oceanic and atmospheric forcing on the sea ice. Likewise, we investigate the linkage between extreme negative sea ice area anomalies and the dominant modes of atmospheric circulation variability, as well as between the extremes and the preconditioning through the winter-spring sea ice state.

[1] Ragone F. and Bouchet F., 2021: Rare event algorithm study of extreme warm summers and heatwaves over Europe, Geophys. Res. Lett., **48(12**), doi:10.1029/2020GL091197.
[2] Fraedrich K., Jansen H., Kirk E., Luksch U., and Lunkeit F., 2005: The Planet Simulator: Towards a user friendly model, Meteorologische Zeitschrift, **14(3)**, 299-304, doi:10.1127/0941-2948/2005/0043.
[3] Döscher R., Acosta M., Alessandri A., Anthoni P., Arneth A., Arsouze T., Bergmann T. Bernadello R., Bousetta S., Caron L., et al., 2022: The EC-Earth3 Earth System Model for the Climate Model Intercomparison Project 6, Geoscientific Model Development, **15(7)**, 2973-3020, doi:10.5194/gmd-2020-446.

Impact of a representation of Antarctic landfast ice on the shelf water properties simulated by NEMO4-SI³

N. Pirlet[1], T. Fichefet[1], M. Vancoppenolle[2] and C. de Lavergne[2]

[1]*ELI/ELIC, UCLouvain, Louvain-la-Neuve, Belgique*
[2]*LOCEAN Laboratory, Sorbonne University, Paris, France*

The formation of dense water in the Southern Ocean plays a key role in the global overturning circulation of the ocean, and thus affects the distributions of heat, carbon, oxygen and nutrients across the World Ocean. However, the simulation of dense water properties by climate models remains problematic. These models often generate dense water in incorrect locations and for wrong reasons, primarily through deep convection in the center of the Weddell and Ross Seas. We hypothesize that this inability to simulate the formation and fate of dense water stems partly from the erroneous or absent representation of coastal polynyas and their key drivers, particularly landfast ice. A recent study presented a restoring method that accurately represents Antarctic landfast ice and demonstrated its essential role in shaping coastal polynyas and enhancing sea ice production in the NEMO4-SI3 model. Here, building on this study, we investigate the impact of this landfast ice representation on water mass properties simulated by the model over the Antarctic continental shelf. We perform two simulations: one with the landfast ice scheme activated and one with this scheme turned off. A comparison of the simulation results confirms the expected densification of water masses within polynyas when landfast ice is represented. However, the results also reveal unexpected regions of fresher water beneath landfast ice, which influence the polynya dynamics downstream. On a circumpolar scale, incorporating landfast ice enhances the model's agreement with observations, particularly in terms of bottom salinity, temperature and mixed layer depth. Notably, the mixed layer depth undergoes significant changes, which in turn affect the Southern Ocean's coastal dynamics and lead to enhanced ice shelf melting. Overall, representing landfast ice improves the simulation of dense water formation and shelf ocean dynamics, thereby advancing our understanding of key physical processes in these critical regions.

Estimation of atmospheric lifetime and emissions of NH_3 sources from 15 years of satellite data

A. Honet[1], L. Clarisse[1], M. Van Damme[1,2], C. Clerbaux[1,3], and P. Coheur[1]

[1]*Université libre de Bruxelles (ULB), Brussels Laboratory of the Universe (BLU-ULB), Spectroscopy, Quantum chemistry and Atmospheric Remote Sensing (SQUARES) Brussels, Belgium*
[2]*Royal Belgian Institute for Space Aeronomy (BIRA-IASB) Brussels, Belgium*
[3]*LATMOS/IPSL, Sorbonne Université, UVSQ, CNRS Paris, France*

Ammonia (NH_3) is a short-lived atmospheric constituent with devastating effects on air quality and environment. Its global concentration is however continuously increasing and there is therefore a need to pinpoint the emitters. Once the emitters are localized, quantitative estimates of the amount of gas emitted per source as well as its atmospheric lifetime is of primary importance. Here, we present an update of the catalogue of NH_3 sources first published in [1]. We used measurements from Infrared Atmospheric Sounding Interferometer (IASI) instrument, carried on the MetOp satellites. The sources are identified from supersampled high-resolution maps [2] for the whole IASI satellite activity period (2008-2022). Identification challenges arise for emerging/disappearing sources and for sources near regions often affected by wildfires. For this reason, we also analyzed supersampled maps representing smaller time periods (5 years) and maps where months of intense wildfires periods were removed. Overall, we identified more than 750 sources and classified them into 12 categories including agriculture, industries (fertilizer, soda ash, coke and steel), urban or natural.

In addition, we present the results of fitting to the line densities (spatial integrals of wind-rotated supersampled maps) an exponentially modified Gaussian to estimate both the lifetime and emission of sources. We discuss the results of the fitting procedure and particularly the criteria used to ensure good quality fits. The input parameters for the fit (fitting interval, windspeed, source location, …) result in uncertainties in the derived lifetimes and emissions. These uncertainties are assessed through propagation of uncertainty of the input parameters and combined into a total uncertainty. Of the 769 sources in the catalogue, 43 are fitted satisfactorily. We analyze the seasonal variations in lifetime and emission of these according to the source type and location. Finally, we use the average derived lifetime to estimate the emissions for all the sources from catalogue on a yearly basis. We discuss the evolution of emissions for several specific cases and global trends for agriculture and industry.

[1] Van Damme, M. *et al.* Nature **564**, 99–103 (2018).
[2] Clarisse, L. *et al.* Atmos. Meas. Tech., 12, 5457–5473 (2019).

Antarctic Sea Ice Response to Wind Perturbation Experiments

Feba F*. & H. Goosse
Universite catholique de Louvain
Belgium

* feba.francis@uclouvain.be

The sea ice extent (SIE) in the Southern Ocean experienced a drop in the late 1970s, though less pronounced compared to the one post-2016. Though several studies explain the drop since 2016, the 1970s decline is critical in understanding the long-term variability of SIE. To investigate the underlying mechanisms for this decline, we conducted wind perturbation experiments using the general circulation model EC-Earth3. We perturb the model by adding wind stress anomalies derived from ERA5 to the model winds. Using this technique, we simulate the evolution of SIE over the period 1958-2023. Our analyses show that the perturbation induces a drop in the 1970s despite the control (no-perturbation) run showing no such trend. This strongly indicates the important role of winds in driving the drop, though ocean processes and other feedback mechanisms may also contribute to the decline. The SIE shows spatial heterogeneity in the variations driven by the wind. Presently, we are conducting multiple ensemble simulations to evaluate the influence of initial conditions on the results.

Drivers of Arctic Rapid Sea Ice Loss Events in CESM2-lessmelt

A. Sticker[1], F. Massonnet[1], T. Fichefet[1] and A. Jahn[2,3]

[1]*Earth and Life Institute, Earth and Climate, Université catholique deLouvain, Louvain-la-Neuve, 1348, Belgium*
[2]*Department of Atmospheric and Oceanic Sciences, University of Colorado Boulder, Boulder, CO, USA*
[3]*Institute for Arctic and Alpine Research, University of Colorado Boulder, Boulder, CO, USA*

The decline in summer Arctic sea ice extent that has been underway for several decades is set to continue until summer Arctic sea ice disappears completely by the middle of the century, according to the latest climate projections. Based on observations and these climate model projections, the rate at which sea ice is retreating is not linear: the decrease in the Arctic sea ice cover is marked by periods of abrupt sea ice decline. Specifically, it has been suggested that these rapid ice loss events (RILEs) will become a frequent phenomenon in the coming decades. The causes of such events remain poorly understood, and we are still unable to reliably predict their evolution. By running sensitivity simulations with the CESM2 model, our objective was to investigate the predictability of RILEs and the factors that contribute to their onset. Simulations initialized in the year of the event demonstrate predictive skills, whereas those initialized one to two years earlier exhibit limited predictive capability. Additional simulations are designed to explore the role of sea ice mean state and previous oceanic conditions in driving these events.

Towards improved seasonal to interannual predictions of Arctic sea ice through Data Assimilation and dedicated reanalysis

A. Delhasse[1] and F. Massonnet[1]

[1]*Earth & Life Institute (ELI), Earth & Climate (ELIC), UCLouvain, Louvain-La-Neuve,1348, Belgium*

The Arctic is undergoing a rapid transition towards a new climatic state, characterized by nearly ice-free summer conditions by the 2050s. Projections suggest that summer sea ice retreat will not follow a linear trend, but will instead feature pronounced sub-decadal fluctuations, including abrupt declines occurring within 3–5 years during rapid sea ice loss events. Understanding the precursors, mechanisms, and predictability of these events is essential for improving climate projections and guiding adaptation strategies. The ArcticWATCH project (https://arcticwatch-erc.github.io/) aims to develop a seasonal to interannual prediction tool dedicated to the study and prevention of this kind of events.

Within the framework of this project, we implement data assimilation (DA) into the NEMO-SI3 model using an Ensemble Kalman Filter (EnKF) method to achieve two primary objectives: 1) enhance polar ocean and sea ice initial conditions for predictions with the Earth System Model (ESM) EC-Earth, and 2) develop a near-real-time reanalysis product dedicated to sea ice applications and monitoring, including precursors of rapid ice loss events. The ensemble is generated by perturbing ERA5 atmospheric reanalysis fields (25 members) used to force NEMO. Initially, monthly sea ice concentration data from the OSISAF dataset (1979–present) were assimilated, leading to significant improvements in NEMO-SI3's performance, particularly in simulating late-summer sea ice conditions. The comparison between simulations with and without data assimilation highlights model deficiencies in capturing specific sea ice states or events, enabling us to better identify key processes that need improvement to enhance accuracy of our model.

Block minima modeling of Antarctic's sea ice extent extremes

A. Tytgat[1], F. Massonnet[1] and A. Kiriliouk[2]

[1]*Earth and Climate Center, Earth and Life Institute, Université catholique de Louvain, Louvain-la-Neuve, 1348, Belgium*
[2]*Namur Institute for Complex Systems (NaXys), Université de Namur, Namur, 5000, Belgium*

The Antarctic sea ice extent (SIE) has exhibited unusual variability in recent years, including record lows in annual minima observed in 2017, 2022, 2023, and 2024. This marks a sharp contrast with the sea ice extent evolution between 1979 and 2015, during which yearly mean sea ice extent slightly increased despite global warming. Such events raise critical questions about their probabilities under current and future conditions, as well as the potential factors driving such events. To address these questions, we use block-minima models to analyze and interpret the yearly minima of the Antarctic SIE. Additionally, we extend this approach to the five regional basins that constitute the Antarctic, aiming to shed some light on their contributions to the recent extreme events. Our results suggest that the trend in SIE yearly minima is best captured by a piecewise linear model for the mean, and an increasing scale parameter over time, and that the recent record lows, though unprecedented, were not highly improbable given recent trends. The regional analysis indicates that the Ross Sea, Weddell Sea and Western Pacific Ocean basins are the primary contributors to the recent decline in total SIE.

The WarmAnoxia project

M. Crucifix[1], A. C Da Silva[2], L. Sablon[1], J. Gérard[2] and J. Huygh [3]

[1]*Earth and Life Institute, UCLouvain, Louvain-la-Neuve, BE-1348, Belgium*
[2]*SedClim, Université de Liège, Liège, BE-4000, Belgium*

The Devonian period (419 to 359 million years ago) stands as a critical epoch in Earth's geological history, marked by significant climatic and environmental transformations. During this era, 29 instances of ocean anoxic or hypoxic conditions have been identified and documented. The dynamics of these Ocean Anoxic Events (OAEs) and their underlying mechanisms have been investigated over the last decades. It has been hypothesized that the cyclical nature of anoxia in geological records can be attributed to astronomical cycles. These cycles involve changes in the rotation of the Earth's axis and the geometry of its orbit, impacting seasonal variations and the level of incoming solar radiation, thereby affecting the global climate on geological timescales. In the WarmAnoxia Research project (funded by the FNRS), we have initiated an investigation that relies on:

[1] Production of plausible astronomical scenarios for the Devonian;

[2] Modelling of deep-ocean dynamics and biogeochemical responses to changes in continental configuration and orbital forcing throughout the Devonian using a modelling framework called cGENIE;

[3] Numerical simulation of regolith dynamics and nutrient flows to the ocean using a realistic climate model (HadSM3) coupled with a model of the regolith dynaimcs, based on physical principles.

We combine modelling and geological evidence to provide constraints on the timing and duration of anoxia with respect to astronomical forcing (specifically, the timing of so-called "nodes" of eccentricity) and to investigate possible physical and biogeochemical mechanisms that would explain this link.
The poster showcases mid-term results generated by this project.

Arctic landfast ice simulation with brittle rheology and probabilistic grounding

A. Lambotte[1], T. Fichefet[1], F. Massonnet[1], P. Rampal[2], L. Brodeau[2]

[1]*UCLouvain, ELI, ELIC, Louvain-la-Neuve, Belgium*
[2]*IGE/CNRS, Grenoble, France*

Landfast ice, sea ice that is mechanically immobilized for several weeks along the coasts, significantly influences the underlying ocean by affecting the occurrence of polynyas and the formation of dense water. However, it remains poorly represented in current numerical models. In the Arctic, the presence of landfast ice is mainly due to sea ice arching between islands and grounding, when thick sea ice ridges reach the seabed. Therefore, an accurate simulation of landfast ice relies on a grounding parameterization and on a sea ice rheology producing realistic coastal sea ice thickness and sustaining ice arching.
In this study, we use the ocean–sea ice model NEMO-SI3 at a quarter-degree horizontal resolution. For the grounding parameterization, we use the probabilistic seabed–ice keel interaction from Dupon et al. (2022) [1]. We show that leveraging realistic sub-grid-scale bathymetry distributions helps to efficiently represent landfast ice cover in deep waters (e.g., the Kara Sea). We also compare two rheologies: a brittle one (i.e., the Brittle Bingham Maxwell, or BBM), newly implemented in NEMO-SI3 [2], and a standard elastic–viscous–plastic rheology (i.e., the aEVP), which is widely used in sea ice models and modified with a tensile strength, as in Lemieux et al. (2016) [3].

[1] Frédéric Dupont, Dany Dumont, Jean-François Lemieux, Elie Dumas-Lefebvre and Alain Caya (2022), A probabilistic seabed–ice keel interaction model, *The Cryosphere*, **16**, 1963–1977

[2] Laurent Brodeau, Pierre Rampal, Einar Ólason and Véronique Dansereau (2024), Implementation of a brittle sea ice rheology in an Eulerian, finite-difference, C-grid modeling framework: impact on the simulated deformation of sea ice in the Arctic, *Geosci. Model Dev.*, **17**, 6051–6082

[3] Lemieux, J.-F., F. Dupont, P. Blain, F. Roy, G. C. Smith, and G. M. Flato (2016), Improving the simulation of landfast ice by combining tensile strength and a parameterization for grounded ridges, *J. Geophys. Res. Oceans*, **121**, 7354–7368

How predictable was the recent decade-long pause in Arctic summer sea ice retreat?

Patricia DeRepentigny[1], François Massonnet[1], Roberto Bilbao[2] and Stefano Materia[2]

[1]*Earth & Life Institute, UCLouvain, Louvain-la-Neuve, 1348, Belgium*
[2]*Barcelona Supercomputing Center, Barcelona, 08034, Spain*

The Earth has warmed significantly over the past 40 years, and the fastest rate of warming has occurred in and around the Arctic. The warming of northern high latitudes at a rate of almost four times the global average [1], known as Arctic amplification, is associated with sea ice loss, glacier retreat, permafrost degradation, and expansion of the melting season. Since the mid-2000s, summer sea ice has exhibited a rapid decline, reaching record minima in September sea ice area in 2007 and 2012. However, after the early 2010s, the downward trend of minimum sea ice area appears to decelerate [2, 3]. This apparent slowdown and the preceding acceleration in the rate of sea ice loss are puzzling in light of the steadily increasing rate of greenhouse gas emissions of about 4.5 ppm yr^{-1} over the past decade [4] that provides a constant climate forcing. Recent studies suggest that low-frequency internal climate variability may have been as important as anthropogenic influences on observed Arctic sea ice decline over the past four decades [5, 6].

Here, we investigate how predictable this decade-long pause in Arctic summer sea ice decline was within the context of internal climate variability. To do so, we first assess how rare this deceleration of Arctic sea ice loss is by comparing it to trends in historical simulations from the Coupled Model Intercomparison Project Phase 6 (CMIP6). We also use simulations from the Decadal Climate Prediction Project (DCPP) contribution to CMIP6 to determine if initializing decadal prediction systems from estimates of the observed climate state substantially improves their performance in predicting the slowdown in Arctic sea ice loss over the past decade. As the DCPP does not specify the data or methods to be used to initialize forecasts or how to generate ensembles of initial conditions, we also assess how different formulations affect the skill of the forecasts by analyzing differences between models. This work provides an opportunity to attribute this pause in Arctic sea ice retreat to internal variability or radiative external forcings, something that observation analysis alone cannot achieve.

[1] Rantanen M *et al* 2022 *Commun. Earth Environ.* **3** 168
[2] Swart NC *et al* 2015 *Nature Clim. Change* **5** 86–89
[3] Baxter I *et al* 2019 *Journal of Climate* **32** 8583–8602
[4] Friedlingstein P *et al* 2023 *Earth System Science Data* **15** 5301–5369
[5] Dörr JS *et al* 2023 *The Cryosphere* **17** 4133–4153
[6] Karami MP, Koenigk T and Tremblay B 2023 *Environ. Res.: Climate* **2** 025005

40 Years of ICRF Operation on JET: Achievements and Challenges

P. Dumortier[1], I. Monakhov[2], P. Jacquet[2], F. Durodié[1], E. Lerche[1], JET Contributors* and the EUROfusion Tokamak Exploitation Team§

[1]LPP-ERM/KMS, TEC partner, Brussels, Belgium
pierre.dumortier@rma.ac.be
[2]UKAEA, Culham, UK
** See author list of C.F. Maggi et al 2024 Nucl. Fusion 64 112012*
§ See author list of E. Joffrin et al., 2024 Nucl. Fusion 64 112019

After 40 years of successful operation and multiple Deuterium-Tritium (D-T) campaigns, the Joint European Torus (JET) concluded its operations in December 2023. From the outset, Ion Cyclotron Range of Frequency (ICRF) heating was identified as a key auxiliary heating system, with the first ICRF system becoming operational in 1985. This system underwent significant development, culminating in a high-power (32MW installed), wideband (23-57 MHz range), and highly versatile system. The A2 antennas, installed during the 1993 shutdown, operated successfully until the end of JET's operation, demonstrating an impressive 30-year service without major issues.

This contribution provides an overview of the JET RF system's evolution over its lifetime, highlighting selected technological achievements and operational challenges. It addresses the rationale behind the development and operation of the ICRF system, including the implementation and operation of load-resilient systems (3dB hybrid coupler, External Conjugate-T, ILA), as well as the operational limits and system protection measures, such as the specific mode of operation for Ion Cyclotron Wall Conditioning (ICWC). The impact of transitioning from a carbon wall to the beryllium and tungsten ITER-Like Wall on the system's operation and the challenges posed by D-T operations are also emphasized.

Finally, key lessons learned from the technical challenges, constraints, and achievements of the JET experience are highlighted, with an eye towards the design and operation of ICRF systems in future machines.

Almost-off-the-shelf tools for ICRH modelling

D. Van Eester[1], V. Maquet [1], B. Reman[1], E.A. Lerche[1], P.U. Lamalle[1]

[1]*Laboratory for Plasma Physics, LPP-ERM/KMS, 1000 Brussels, Belgium*
d.van.eester@fz-juelich.de, Vincent.Maquet@ulb.be, Bernard.Reman@mil.be, ealerche@msn.com

Studying the dynamics of the wave-particle interaction underlying Ion Cyclotron Resonance Heating in tokamaks or stellarators requires the development and solving of the relevant wave equation. Over the last decades, a large number of authors have contributed to pushing the realism of the models forward (see e.g. [1-6] and references therein) so a lot of detailed expressions – with various degrees of realism while concentrating on specific subtopics, each deserving attention - are available for exploitation. Similarly, gradually more sophisticated tools become available for solving partial differential equations in complex geometries. Combining the strength of both offers perspectives for the development and exploitation of "almost-off-the-shelf" tools with high degree of efficiency as well as richness of physics.

Crudely speaking, there are 2 main challenges when modelling wave heating in magnetic confinement devices while attempting to capture key aspects of the dynamics of the wave-particle interaction of RF created or fusion-born fast particle populations:

(i) the perpendicular dynamics requires accounting for finite temperature (finite Larmor radius) effects, and

(ii) charged particles move more freely along than across the magnetic field; when the magnetic field varies along the orbit, the associated modification of the dielectric response needs to be accounted for.

The present contribution summarizes some recent work aimed at adopting this mixed-tool approach, highlighting opportunities as well as bottlenecks. In particular, it is the somewhat more pen-and-paper counterpart of recent work by V. Maquet [7], the latter putting the focus on the numerical aspects.

1. P. U. Lamalle et al. "Dielectric kernels for Maxwellian tokamak plasmas", *AIP Conference Proceedings* **2254**, 100001 (2020)
2. P. U. Lamalle et al., "Integral dielectric kernel approach to modelling RF heating in toroidal plasmas", 25th Topical Conference on *Radio-Frequency Power in Plasmas* (2025)
3. B.C.G. Reman et al., "Integral dielectric kernel implementation to model RF heating in toroidal plasmas", 25th Topical Conference on *Radio-Frequency Power in Plasmas* (2025)
4. P.U. Lamalle et al., "High-frequency dielectric integral kernels for Maxwellian tokamak plasmas", to be submitted
5. P. U. Lamalle et al., "On the high-frequency kernel dispersion functions of Maxwellian plasmas", to be submitted
6. B.C.G. Reman et al., "Implementation of high-frequency kernel dispersion function of Maxwellian plasmas", to be submitted
7. V. Maquet et al, "Implementation of a fast 2D wave solver using the Budé method with NGsolve", 25th Topical Conference on *Radio-Frequency Power in Plasmas* (2025)

ICRH modelling of the Baseline D-T scenario in JET

D. Van Eester[1], E.A. Lerche[1], D. Frigione[2], L. Garzotti[3], F. Rimini[3], V. Zotta[4]
and JET contributors* & the EUROfusion Tokamak Exploitation Team**

[1]Laboratory for Plasma Physics, LPP-ERM/KMS, 1000 Brussels, Belgium
[2]Università di Roma Tor Vergata, Via del Politecnico 1, Roma, Italy
[3] United Kingdom Atomic Energy Authority, Culham Campus, Abingdon, Oxon, OX14 3DB, United Kingdom of Great Britain and Northern Ireland
[4] Dipartimento di Ingegneria Astronautica, Elettrica ed Energetica, SAPIENZA Università di Roma, Via Eudossiana 18, 00184 Roma, Italy
d.van.eester@fz-juelich.de

In the 2021 and 2023 D-T campaigns in JET various scenarios with potential for application in fusion reactors have been studied. The mandate of the "Baseline" experiments was to explore the possibility to operate at high density, magnetic field and current. Although extremely promising results were obtained in D plasmas in the running-up to the actual D-T campaign and up to 8MW of fusion power was produced when adopting this scenario in D-T [1,2], it was – in contrast to the record T-rich scenario - not possible to sustain D-T shots for the envisaged 5 seconds. The underlying reasons are still being explored, offering perspectives for possible cures. The present contribution concentrates on the detailed modelling of ICRH aspects and on the synergy between ICRH and NBI, allowing a better understanding of the key role of the auxiliary heating in these high-performance shots. One aspect setting the scenarios apart and which has several repercussions is that the density – purposely - is higher, which changes the beam penetration, modifies the collisionality as well as the beam power deposition profiles, and necessitates the auxiliary power level to be higher to sustain fusion-relevant temperatures.

1. L. Garzotti et al., "Development of high-current baseline scenario for high deuterium-tritium fusion performance at JET", submitted to Plasma Phys. Contr. Fusion
2. D. Van Eester et al., "RF power as key contributor to high performance Baseline experiments in JET DD and DT plasmas in preparation of ITER", *AIP Conf. Proc.* 2984, 030004 (2023) https://doi.org/10.1063/5.0162425

* See the author list of C. F. Maggi et al. 2024 Nucl. Fusion 64 112012
** See the author list of E. Joffrin et al. 2024 Nucl. Fusion 64 112019

Integral dielectric kernel implementation to model RF heating in toroidal plasmas

B.C.G. Reman[1], J. Zaleski[3], P.U. Lamalle[1], C. Slaby[2], C. Geuzaine[3], P. Helander[2], E. Lerche[1], F. Louche[1], V. Maquet[1] and D. Van Eester[1]

[1]*Laboratory for Plasma Physics, Royal Military Academy, Brussels, Belgium*
[2]*Max-Planck-Institut für Plasmaphysik, 17491 Greifswald, Germany*
[3]*Dept. of Electrical Engineering and Computer Science, University of Liège, Belgium*

As discussed in Ref. [1], recent theoretical and numerical treatments [2, 3] have sought to express the plasma radiofrequency (RF) response as a nonlocal integral operator formulated in configuration space. Analytical expressions of the integral kernels are available for Maxwellian particle species. This approach enables *(i)* direct use of the finite element method (FEM) to model wave propagation and absorption in hot inhomogeneous fusion plasmas, *(ii)* local mesh-refinement, *(iii)* provides RF field representations suited to address tokamak geometry, and *(iv)* allows to connect plasma model with antenna models. The present contribution focuses on the concrete application of this method. We are exploring physical and numerical aspects through the development of a new "in- house" FEM code. It solves Maxwell's equations in the frequency domain in the presence of the nonlocal kernel in 2.5D slab to lowest order in finite Larmor radius as a first step, i.e. with focus on wave dispersion effects along the equilibrium magnetic field and the associated fundamental cyclotron and Landau dampings. This integro-differential formulation is untypical of FEM [4]. While the present efforts are dedicated to enrich the description of the parallel dynamics, they may at a later stage be complemented by ongoing efforts focusing on the perpendicular one, as with NGSolve [5, 6]. We present preliminary results and describe the future developments using extension of advanced FEM libraries such as Psydac [7], GetDP [8] and GmshFEM [9] to incorporate our new treatment.

[1] Lamalle, P. U., *et al.* "Integral dielectric kernel approach to modelling radiofrequency heating in toroidal plasmas." *Joint Varenna-Lausanne International Workshop on Theory of Fusion Plasmas*. 2024.

[2] P. U. Lamalle, *AIP Conference Proceedings*, **2254 1**, 100001 (2020).

[3] M. Machielsen *et al.*, *Fundamental Plasma Physics*, **3**, 100008 (2023).

[4] Shiraiwa, S., *et al.*, *Phys. Plasmas* **17**, 056119 (2010).

[5] D. Van Eester, *et al.* "Almost-off-the-shelf tools for ICRH modelling", *25th Topical Conference on Radio-Frequency Power in Plasmas* (2025).

[6] V. Maquet, *et al.* "Implementation of a fast 2D wave-solver using the BUDE method with NGSolve", *25th Topical Conference on Radio-Frequency Power in Plasmas* (2025).

[7] Güçlü, Y. *et al.*, *Numerical Methods for the Kinetic Equations of Plasma Physics (NumKin2019)* (2019).

[8] Geuzaine, C., *PAMM: Proceedings in Applied Mathematics and Mechanics.* Vol. **7**. No. 1. Berlin: WILEY-VCH Verlag, 2007.

[9] Royer, A. *et al. 14th World Congress on Computational Mechanics (WCCM), ECCOMAS Congress 2020.* Scipedia, 2021.

Predicting Wall Conditioning

A. Adriaens[1,2], D. Lopez[1,2], S. Deshpande[2], J. Buermans[2], K. Crombé[1,2], A. Goraiev[2]

[1]*KMS/ERM, Laboratory for plasma physics, Brussels, 1000, Belgium*
[2]*Ghent University, department of applied physics, Ghent, 9000,Belgium*

When a fusion reactor material has been subjected to impurities through experimental campains, these impurities will be stored in interstitial lattice sites (LS). The base material atoms are bound by a certain energy $E_b + E_s$ (lattice binding energy+surface binding energy) whilst the trapped impurity is bound by E_t, as most often $\mid E_t \mid < \mid E_b + E_s \mid$, wall conditioning, a technique of bombarding the wall with the gas we'd like to use in the future to get rid of current impurities, is effective. We will investigate 2 wall conditioning types, GDC (Glow Discharge wall Conditioning) and ICWC. GDC creates low energy ions which propagate to the wall as no magnetic field is present, whilst ICWC creates neutrals which may escape the magnetic field and thus bombard the wall.
In an experiment we may measure this kind of behaviour using a QMS (Quadrupole Mass Spectrometer) whereby we first load the wall with e.g helium (by subjecting it to Helium GDC) and then after pumping down subject the wall to either GDC or ICWC, tracking the outflux of helium, an example of such outgassing for H GDC is shown on figure 1.

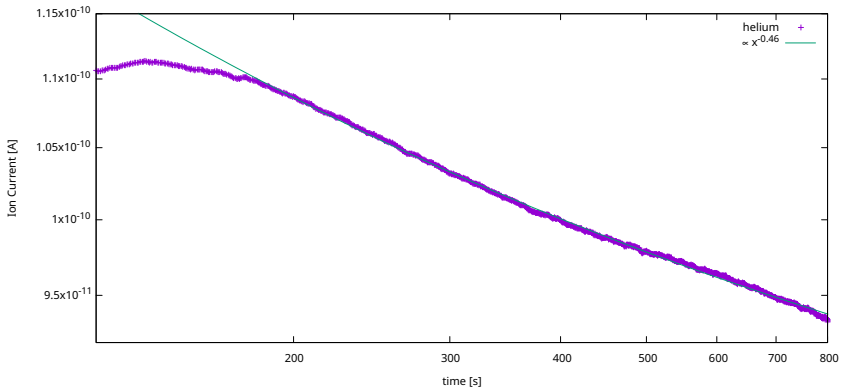

Figure 1: experimental outgassing observed using the QMS

The developed model may simulate such a H GDC phase using BCA, by first measuring the ion distribution of the incoming particles (using a RFEA) and then using that as input for iterative BCA, more particularly we define a layered material with an initial impurity concentration and evolve the system according to

$$\frac{dn_i^j}{dt} = -\frac{\mathcal{I}^j[\mathbf{D}, \mathbf{n_i}, \mathbf{n_p}]}{D^j} \tag{1}$$

$$\frac{dn_p^j}{dt} = -\frac{\mathcal{P}^j[\mathbf{D}, \mathbf{n_i}, \mathbf{n_p}]}{D^j} \tag{2}$$

$$\frac{dD^j}{dt} = -\frac{\mathcal{B}^j[\mathbf{D}, \mathbf{n_i}, \mathbf{n_p}]}{\rho} \tag{3}$$

whereby D^j is the thickness of layer j, n_i^j is the impurity concentration in layer j and n_p^j is the projectile concentration in layer j. Experimentally GDC evolves according to a power law with an exponent of 0.46, the model predicts 0.44656 ± 0.03497 in which the experiment lies.

Characterization of a microwave reflectometer for edge density profile measurements at the ICRH antenna on Wendelstein 7-X

D. López-Rodríguez[1,2], A. Krämer-Flecken[3], H.M. Xiang[4], K. Crombé[1,2], J. Ongena[1], A. Adriaens[1,2], D.A. Castaño-Bardawil[1], B. Schweer[1], M. Vervier[1], M. Verstraeten[1], P. Dumortier[1], I. Stepanov[1], X. Han[5], D. Hartmann[6], J.P. Kallmeyer[6], and the W7-X team

[1]*Laboratory for Plasma Physics, Royal Military Academy (LPP-ERM/KMS), TEC Partner, Brussels, 1000, Belgium*
[2]*Department of Applied Physics, Ghent University, Ghent, 9000, Belgium*
[3]*Institute of Fusion Energy and Nuclear Waste Management (IFN-1), Forschungszentrum Jülich GmbH, TEC Partner, Jülich, 52425, Germany*
[4]*Shenzhen Institute of Research and Innovation, University of Hong Kong, Shenzhen, Guangdong, 518063, China*
[5]*University of Wisconsin-Madison, Madison, Wisconsin, WI 53706, United States*
[6]*Max-Planck Institute for Plasma Physics, Greifswald, 17491, Germany*

An Ion Cyclotron Resonance Heating (ICRH) system has been designed for the stellarator Wendelstein 7-X (W7-X) [1]. The two-strap antenna works at frequencies of 25 MHz and 38 MHz, with a pulse length of up to 10 seconds, and can deliver radiofrequency (RF) power levels up to 1.5 MW [2]. The main objective of the ICRH antenna is the generation of fast ions, to demonstrate the fast ion confinement capabilities of W7-X. Additionally, the system can be used for Ion Cyclotron Wall Conditioning (ICWC) studies, for target plasma generation, and heating in future experimental campaigns [3].

To better understand the wave-particle coupling for plasma heating, the ICRH antenna is equipped with a microwave reflectometer, capable of measuring the electron density profiles in front of the antenna. This diagnostic utilizes a frequency modulated continuous wave (FMCW) scheme with a heterodyne detection method. The reflectometer has two frequency bands that cover a frequency range of 67.2 GHz to 110 GHz in the extraordinary polarization (X mode) regime, corresponding to a measurable density of $n_e \leq 6.0 \times 10^{19}$ m^3 at the central magnetic field of $B_0 = 2.5$ T [4, 5].

During the latest W7-X experimental campaigns, the ICRH antenna was commissioned, and the first results have been obtained using up to 800 kW of ICRH power. The microwave reflectometer was installed and calibrated successfully; the diagnostic was routinely operated to measure the electron density profiles during the experiments. The objective of this work is to describe the microwave reflectometer for edge density profile measurements, show the calibration procedure used to ensure a linear frequency sweep and estimate the delay time in the waveguides, and present a summary of the results that have been obtained during the first experiments, focusing on exploring the effect of the ICRH antenna on the edge density profiles.

[1] J. Ongena et al., "Study and design of the ion cyclotron resonance heating system for the stellarator Wendelstein 7-X", *Physics of Plasmas*, **21**, 061514 (2014).
[2] J. Ongena et al., "Physics design, construction and commissioning of the ICRH system for the stellarator Wendelstein 7-X", *Fusion Engineering and Design*, **192**, 113627 (2023).
[3] M. Endler et al., "Wendelstein 7-X on the path to long-pulse high-performance operation", *Fusion Engineering and Design*, **167**, 112381 (2021).
[4] X. Han et al., "Development of a dual-band X-mode reflectometer for the density profile measurement at ICRH antenna in W7-X", *14th International Reflectometry Workshop*, (2019).
[5] H.M. Xiang et al., "Statues of microwave reflectometry for density profile and density fluctuation measurements in Wendelstein 7-X for OP. 2", *15th International Reflectometry Workshop*, (2022).

Suprathermal ion transport and toroidal helicon wave studies in the low-temperature plasma device TORPEX

C. Sepulchre, S. P. H. Vincent, M. Baquero-Ruiz and I. Furno

École Polytechnique Fédérale de Lausanne (EPFL), Swiss Plasma Center (SPC)
CH-1015 Lausanne, Switzerland

Basic plasma devices are essential to understand fundamental plasma physics challenges in the quest of nuclear fusion power [1]. TORPEX, a toroidal low temperature plasma experiment located at the Swiss Plasma Center (EPFL, Switzerland), has significantly contributed to the study of instabilities, turbulent transport and suprathermal ion transport in the last decades [2-3]. Plasmas in TORPEX can be generated either with microwaves in the electron-cyclotron frequency range or with a recently installed birdcage resonant helicon antenna [4]. An extensive number of *in situ* diagnostics are used to characterize plasmas of various gases (mainly H and Ar) in several magnetic configurations being of direct relevance for fusion, such as the simple magnetized torus (SMT) and the X-point configurations.

The understanding of plasma dynamics and cross-field turbulent transport around the X-point is crucial for the mitigation of heat fluxes in tokamaks. In this work, we present the general characteristics of hydrogen plasmas generated close to an X-point in TORPEX [5]. The magnetic shear s, defined as the sharpness of the change in the pitch angle of a magnetic field line, is varied and is shown to significantly affect relevant plasma properties.

The transport of suprathermal ions in the plasma close to the X-point is experimentally studied and is observed to have non-diffusive properties. These experiments are conducted by injecting $^6Li^+$ ions in the area of the plasma where dominant plasma modes are propagating. 3D suprathermal ion beam profiles are reconstructed by scanning the poloidal plane with a gridded energy analyzer (GEA) and by moving the emitter in the toroidal direction from one discharge to the other. The transport of suprathermal ions is quantified by fitting $\sigma^2 \propto t^\gamma$, where σ^2 is the horizontal variance of the FI beam and γ is the transport exponent. We show that γ depends on E_{ion} and that the transport is generally non-diffusive (i.e. $\gamma \neq 1$). The results are compared with previous studies conducted in TORPEX in the SMT configuration [6].

Finally, the new birdcage antenna is presented. The toroidal helicon wave is characterized with two magnetic probes and the impact of helicon waves on plasma parameters (density, floating potential and spectra) is shown. The impact of helicon waves on plasma parameters paves the way for new diagnostic development and for the extension of suprathermal ion studies.

[1] Fasoli A., *et al* 2019 *Nat. Phys.* **15** 872-875
[2] Fasoli A., *et al* 2013 *Nucl. Fusion* **53** 063013
[3] Furno I., *et al* 2015 *J. Plasma Physics* **81** 345810301
[4] Vincent S.P.H., *et al* 2024 *Rev. Sci. Instrum.* **95** 093505
[5] Sepulchre C., *et al* 2025 *submitted to Physics of Plasmas*
[6] Bovet A., *et al* 2015 *Phys. Rev. E* **91** 04110

Programming twist angle and strain gradient in two-dimensional materials

M. Kapfer[1], B.S. Jessen[1], M.E. Eisele[1], D.R. Danielsen[2,3], N.R. Finney[4], A. Marchese[4], V. Hsieh[1], K. Watanabe[5], T. Taniguchi[5], P. Bøggild[2,3], J. Hone[4] and C.R. Dean[1]

[1]*Department of Physics, Columbia University, New York, NY, USA*
[2]*Center for Nanostructure Graphene, Technical University of Denmark, DK-2800, Denmark*
[3]*DTU Physics, Technical University of Denmark, DK-2800, Denmark*
[4]*Department of Mechanical Engineering Columbia University, New York, NY, USA*
[5]*National Institute for Materials Science, 1-1 Namiki, Tsukuba, 305-0044, Japan*

The possibility to isolate atom-thick layer of material from a bulk crystal allows the design of structures with a wide range of properties [1]. In particular, by twisting those single layer sheets, a periodic potential, called moiré potential, is superimposed over the lattice modifying the properties of the parent material [2,3]. Twisted two-dimensional materials have generated tremendous excitement as a platform for achieving quantum properties on demand. However, the moiré pattern is highly sensitive to the interlayer atomic registry, and current assembly techniques suffer from imprecise control of the average twist angle, spatial inhomogeneity in the local twist angle, and distortions due to random strain [4].

Here, we demonstrate a new way to manipulate the moiré patterns in hetero- and homo-bilayers through in-plane bending of monolayer ribbons, using the tip of an atomic force microscope [5]. This technique achieves continuous variation of twist angles with improved twist-angle homogeneity and reduced random strain, resulting in moiré patterns with highly tunable wavelength and ultra-low disorder. Our results pave the way for detailed studies of ultra-low disorder moiré systems and the realization of precise strain-engineered devices.

[1] K. S. Novoselov *et al.*, *Science*, **353**, aac9439 (2016)

[2] Y. Cao *et al.*, *Nature*, **556**, 43–50 (2018)

[3] M. Yankowitz *et al.*, *Science*, **363**, 1059–1064, (2019)

[4] C. N. Lau *et al.*, *Nature*, **602**, 41–50, (2022)

[5] M. Kapfer, B.S. Jessen *et al.*, *Science*, **381**,. 677–681, (2023)

Charge transport in 2D flakes networks: the case of $Ti_3C_2T_x$

O. de Leuze[1], M. Berthe[2], S. Hermans[1], and B. Hackens[1]

[1]*IMCN, UCLouvain, Louvain-La-Neuve, Belgium*
[2]*IEMN, CNRS, Université de Lille, Villeneuve d'Ascq, France*

In recent years, 2D materials have garnered significant attention notably for electronic applications. Among them, energy storage and sensors. In the latter case, the 2D materials are used as a layer made of several micro or nano-sized flakes, randomly stacked on top of each other. This layer can be represented as a "2D network" whose electronic transport can be modeled. In the recent work of Gabbett *et al*. [1], the 2D network is modeled by a conductive path involving several flakes with decoupling of the flake resistance, R_F and the junction resistance between two flakes, R_J. These values are challenging to access at the flake-level given the morphology of the flakes considered, requiring scanning probe microscopy techniques or microfabrication processes.

Here, we focus on $Ti_3C_2T_x$, which is part of the MXene family, for which the "T_x" notation indicates the surface terminations. These surface groups can be tuned depending on the synthesis method, making MXenes very versatile materials. Despite their attractiveness for electronic applications, more fundamental characterization of charge transport in MXenes is required [2]. The present work uses a multi-technique approach to study charge transport in few-layer $Ti_3C_2T_x$ flakes, combining microfabricated devices and scanning probe techniques such as Conductive Atomic Force Microscopy (C-AFM) and Scanning Tunneling Microscopy (STM). Both techniques are represented on Figure 1. In particular, C-AFM measurements were used to decouple in-plane and out-of-plane transport and assess the resistivity anisotropy of $Ti_3C_2T_x$. Then, 4-probe STM experiments and measurements on fabricated devices show that the junction resistance R_J between the flakes is the dominant contribution to the total resistance in a conductive path. Such findings provide key elements necessary to understand charge transport in a 2D conductive path and then in 2D networks.

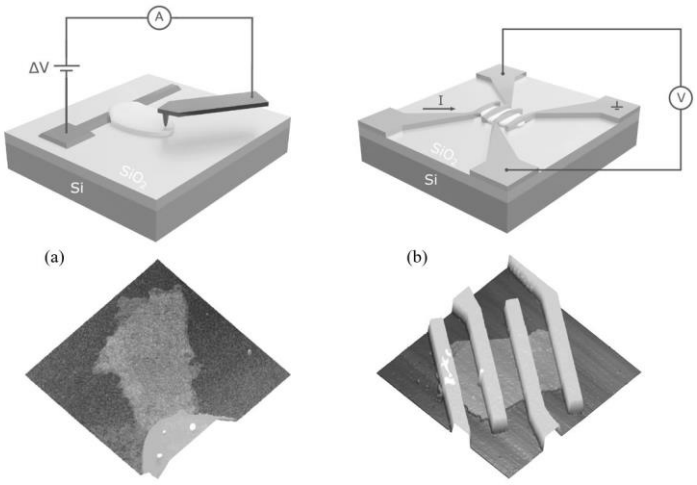

Figure 1: (a) C-AFM and (b) microfabricated device on 2D flakes illustrations and 3-D topography images of the $Ti_3C_2T_x$ samples, obtained with atomic force microscopy.

[1] Gabbett C *et al* 2024 *Nature Communications* ***15*** 4517
[2] Barsoum M and Gogotsi Y 2022 *Ceramics International* ***49*** 24112

Superconductivity of Kagome materials

Yaojia Wang[1], Heng Wu[1,2], Mazhar N. Ali[2]

[1]Quantum Solid-State Physics, Department of Physics and Astronomy, KU Leuven, Celestijnenlaan 200D, Leuven, B-3001, Belgium
[2]1Department of Quantum Nanoscience, Faculty of Applied Sciences, Delft University of Technology, Lorentzweg 1, 2628 CJ, Delft, The Netherlands

yaojia.wang@kuleuven.be

Materials with a Kagome lattice, composed of corner-sharing triangles, are of great interest due to their potential to host strong electronic correlations, exotic magnetism, and nontrivial topology. The AV_3Sb_5 family (A = K, Cs, Rb) has attracted significant research attention for its diverse physical properties, including cascade charge orders, superconductivity, and topological states, as well as the intricate interplay between these phenomena[1]. Despite extensive studies, the nature of superconductivity in these materials remains not fully understood. In this presentation, I will introduce the key physical properties of Kagome materials and discuss our recent study on the superconductivity of KV_3Sb_5. We observed critical current oscillations in the intrinsic KV_3Sb_5 superconductor, providing evidence of supercurrent interference in this system. Furthermore, we discovered that the critical current oscillations propagate between a superconductor and a superconducting ring along the applied current trajectory. This finding suggests the presence of a global critical current effect[2], meaning that the superconducting properties of a given region can be influenced by adjacent parts.

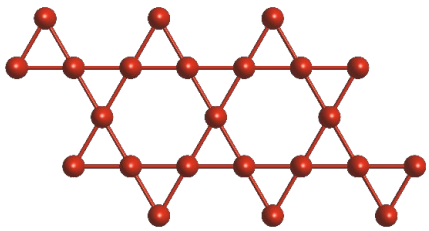

Figure 1. A schematic of Kagome lattice

REFERENCES

[1] Wang, Y. Quantum states and intertwining phases in kagome materials. Nat. Rev. Phys 5, 635-658 (2023).
[2] Wu, H *et al*. The global critical current effect of superconductivity. arXiv:2412.20896 (2025)

Inverse design of plasmonic metasurface using machine learning

Amirmostafa Amirjani[1] and Ewald Janssens[1]

[1] *Quantum Solid-State Physics, Department of Physics and Astronomy, KU Leuven, Celestijnenlaan 200D, Leuven, 3001 Belgium*

Metamaterials have gained significant attention in recent years for their unique ability to manipulate light in the visible spectrum. Metamaterials can be defined as artificial materials, for which their electromagnetic (EM) response is dependent on periodic subwavelength structures as opposed to intrinsic material properties. Notable applications of optical metamaterials include photonic waveguides, next-generation displays, bio-sensors, invisibility cloaking, anti-counterfeit, and information storage. For designing these metasurfaces, traditionally, multiple full wave electrodynamics simulations are carried out to optimize for the desired optical response or functionality. This process includes searching for either new non-intuitive nanostructure designs or optimizing the geometrical parameters of a candidate nanostructure with a simple design. Various EM Maxwell's equations solver-based brute force simulation methods are used to design and optimize nanostructures. However, these forward design methodologies either suffer from the significant expense of computational resources and time because of the iterative solving strategy, or they simply fall short of capturing the functionalities with different-unique nanoantenna designs due to the high non-linearity of the nanophotonic design problem.

The inverse design of nanophotonic structures means the design of an optimal metamaterial given a desired spectral response using numerous iterations of these computational simulations in conjunction with an optimization algorithm. Deep learning (DL) is a sub-category of machine learning (ML) where multi-layer neural networks (NNs) are used for feature extraction and learning of large quantities of data with multiple layers of abstraction. In this study, we have assessed the suitability of deep neural networks (DNNs) models for the forward mapping relationship between the metamaterial structure and EM response. The obtained results show that these deep neural networks with encoder and decoder-like models (Fig. 1) can replace numerical simulations for tightly restrained structures, significantly reducing the computational burden. The final output of the model can be higher modes of resonances or maximum EM field enhancement, both beneficial for sensing and holography applications.

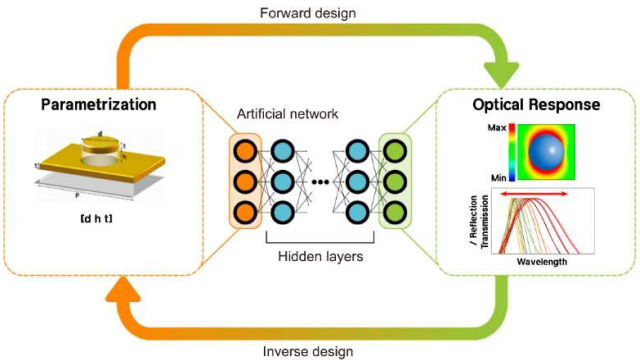

Figure 1: Schematic representation of the NN approach for the inverse design of the metasurface parameters.

Electromechanical coupling at the nanoscale: The ubiquitous case of flexoelectricity

Vincent Meunier[1]

[1] *Department of Engineering Science and Mechanics, Pennsylvania State University, USA*

Electromechanical coupling at the nanoscale involves the direct conversion between mechanical and electrical energy in structures with dimensions of 1-100 nanometers. This phenomenon enables critical functionality in nanotechnology applications such as energy harvesters, nanoresonators, and nanoscale sensors where piezoelectric, electrostrictive, and flexoelectric effects become particularly significant due to increased surface-to-volume ratios.

Flexoelectricity—the polarization induced by strain gradients—manifests with remarkable intensity in two-dimensional materials due to their extraordinary mechanical flexibility and structural sensitivity. This phenomenon reaches peak expression in highly curved nanostructures, where extreme charge redistribution creates measurable electrostatic effects.

My presentation will begin with an introduction to flexoelectricity's fundamental principles in 2D materials. [1] I will then explore its microscopic origins in graphene nanowrinkles (NW) through density functional theory (DFT), demonstrating how intense curvature at the top of the NWs generates significant local Gaussian curvature values, producing observable macroscopic effects.

This research establishes graphene NWs as an ideal system for investigating strong flexoelectric effects. The findings highlight significant potential applications in strain-engineered nanoscale electronic and electromechanical devices, opening new avenues for harnessing this phenomenon in future technologies. This work bridges theoretical predictions with experimental validation, advancing our understanding of how nanoscale structural deformations in 2D materials can be leveraged for novel electronic properties and functionalities. [2]

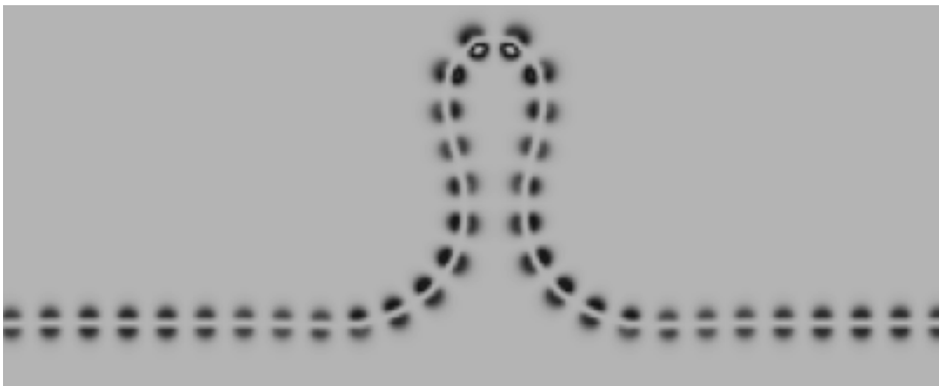

Figure 1: Low-energy charge distribution in a section of NW, as calculated by DFT.

[1] S. Kalinin and V. Meunier, Phys. Rev. B, **77**(3), 033403 (2008)
[2] Sathvik Ajay Iyengar et al, manuscript under review (2025)

Straining group-IV color centers in diamond: Using density functional theory to model the Zero-Phonon-Line shift

T.G.I. van Wijk[1,3], E.A. Melan[1,3,4], R. Mary Joy[2,3], E.Y. Guillaume[1,3,4], P. Pobedinskas[2,3], K. Haenen[2,3], and **D.E.P. Vanpoucke[1,3]**

[1]*Hasselt University, imo-imomec, QuATOMs group, Hasselt, 3500, Belgium*
[2] *Hasselt University, imo-imomec, WBGM group, Hasselt, 3500, Belgium*
[3]*imec, imo-imomec, Diepenbeek, 3590, Belgium*
[3]*University of Namur, NISM, Namur, 5000, Belgium*

Since the dawn of time, color centers in diamond have attracted great interest. Where initial interest focused on gemstone quality, recent years saw a growing interest in their application for quantum information technology and nano-sensing.[1] For the latter, group-IV color centers gained interest due to their excellent Debeye-Waller factor, making them suitable for optically based quantum applications.[2]

In this work, we present a Density Functional Theory (DFT) study of the group-IV color centers in diamond. We investigate the impact of strain and defect concentration on the zero-phonon-line (ZPL), and use our theoretical results to shed light on the experimental observation of these ZPL in nanocrystalline diamond (NCD) films.

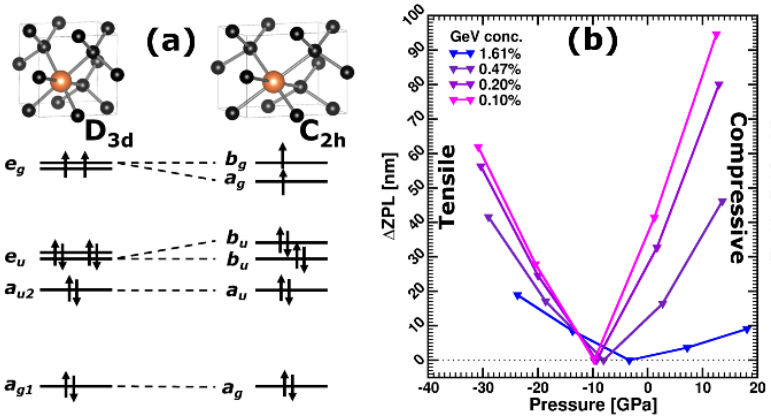

Figure 1: (a) GeV^0 level-splitting under linear strain, and (b) calculated resulting ZPL shift.

Although the atomic configuration of these centers is well established as a split-vacancy geometry, the impact of strain and concentration is less clear. Neutral and negatively charged color centers with concentrations of 1.5% down to 0.1% (64-to 1000-atom conventional cells) are modeled using DFT.[3] The supercells are strained both isotropic and anisotropic to mimic possible conditions in reality experienced in the NCD films. The evolution of the color center related bands is traced as function of strain, while the impact of concentration on the ZPL-shift is established.[3] The resulting ZPL-shift versus strain relationships are used to interpret the experimentally observed distribution of ZPL lines for the GeV and SnV systems. In the case of the GeV center, both blue-and red-shifted ZPL are explained, as well as the asymmetry in the experimentally observed ZPL distribution.[3]

[1] V. Damle, *et al* 2020 *Carbon* **162** 1-12
[2] E.Y. Guillaume, *et al* 2025 in *Nanophotonics with Diamond and Silicon Carbide for Quantum Technologies* **Chap. 5** ISBN: 978-0-443-13717-4
[3] T.G.I. van Wijk, *et al* 2025 *Carbon* **234** 119928

First principles theory of nonlinear long-range electron-phonon interaction

M. Houtput[1,2], L. Ranalli[2], C. Verdi[3], S. Klimin[1], S. Ragni[2], C. Franchini[2,4], and J. Tempere[1]

[1]*Theory of Quantum Systems and Complex Systems, Universiteit Antwerpen, B-2000 Antwerpen, Belgium*
[2]*Faculty of Physics, Computational Materials Physics, University of Vienna, Kolingasse 14-16, Vienna A-1090, Austria*
[3]*School of Mathematics and Physics, University of Queensland, 4072 Brisbane, Queensland, Australia*
[4]*Department of Physics and Astronomy, Alma Mater Studiorum - Università di Bologna, Bologna, 40127 Italy*

Electron-phonon interactions in a solid are crucial for understanding many interesting material properties, such as transport properties and the temperature dependence of the electronic band gap. For harmonic materials, the linear interaction process where one electron interacts with one phonon is sufficient to quantitatively describe these properties. However, this is no longer true in anharmonic materials with significant electron-phonon interaction, such as quantum paraelectrics and halide perovskites. Currently, the only available models for nonlinear electron-phonon interaction are model Hamiltonians, written in terms of phenomenological parameters. Here, we provide a microscopic semi-analytical expression for the long-range part of the 1-electron-2-phonon matrix element, which can be interfaced with first principles techniques. We show that unlike for the long-range 1-electron-1-phonon interaction, the continuum approximation is not sufficient and that the entire phonon dispersion must be taken into account. We calculate an expression for the quasiparticle energies and show that they can be written in terms of a 1-electron-2-phonon spectral function. To demonstrate the method in practice, we calculate the 1-electron-2-phonon spectral function for LiF and KTaO3 from first principles. The framework in this article bridges the gap between model Hamiltonians and first-principles calculations for the 1-electron-2-phonon interaction.

Inference based model Hamiltonians balancing accuracy, interpretability and data efficiency.

Simon M.-M. Dubois

[1]*Institute of Condensed Matter and Nanosciences, Modelling division, UCLouvain, Louvain-La-Neuve, 1348, Belgium*

Predicting electronic structure efficiently and accurately remains a major challenge for large and complex systems. While deep learning has made significant strides in this area, it often requires vast datasets and sacrifices interpretability. This work introduces an inference-based approach that balances accuracy, interpretability and data efficiency. An approach we refer to as shallow learning.

Our method establishes an equivariant analytic mapping of first-principles Hamiltonians. It relies on two key components: the expansion of the electronic manifold in terms of quasi-atomic orbitals, and the factorization of operators into products of parametric two-center integrals. This framework enables a seamless progression from plain two-center tight-binding models to more accurate representations aiming at first-principles precision. Additionally, we investigate the application of soft orthogonality and localization constraints to improve computational efficiency.

Analytic Methods for Polarons in a Non-Parabolic Conduction Band

S. N. Klimin, M. Houtput, J. Tempere

Theorie van Kwantumsystemen en Complexe Systemen (TQC), Universiteit Antwerpen, B-2610 Antwerpen, Belgium

The talk focuses on analytic methods for polarons in a nonparabolic finite-width conduction band. First, we incorporate quadratic interaction into the method of squeezed phonon states, which has proven effective for analytically calculating the polaron parameters. Additionally, we extend this method to nonparabolic finite-width conduction bands while maintaining the periodic translation symmetry of the system [1]. Our results are compared with those obtained from Diagrammatic Monte Carlo, partially reported in a recent study [2], covering a wide range of coupling strengths for nonlinear interaction. Remarkably, our analytic method predicts the same features as the Diagrammatic Monte Carlo simulation.

The method described in [1] is applied to the polaron with the Holstein electron-phonon interaction for all coupling strengths, resulting in exact analytic expressions for the polaron self-energy in several limiting cases and showing a good agreement with Diagrammatic Monte Carlo data.

Second, we have extended the all-coupling Feynman variational method for a polaron in a nonparabolic finite-band conduction band. The obtained polaron self-energy shows an excellent agreement with the results of Diagrammatic Monte Carlo calculations. The developed analytic technique is straightforwardly extended to a polaron with the Rashba spin-orbit coupling.

References

1. S. N. Klimin, J. Tempere, M. Houtput, S. Ragni, T. Hahn, C. Franchini, A. S. Mishchenko, Phys. Rev. B **110**, 075107 (2024).
2. S. Ragni, T. Hahn, Z. Zhang, N. Prokof'ev, A. Kuklov, S. Klimin, M. Houtput, B. Svistunov, J. Tempere, N. Nagaosa, C. Franchini, A. S. Mishchenko, Phys. Rev. B **107**, L121109 (2023).
3. S. N. Klimin, J. Tempere *et al*. (*to be published*)

The global critical current effect of superconductivity

Heng Wu[1,2,3], Yaojia Wang[1,2,3], and Mazhar N. Ali [1,2]

[1]*Department of Quantum Nanoscience, Faculty of Applied Sciences, Delft University of Technology, Lorentzweg 1, 2628 CJ, Delft, The Netherlands*
[2]*Kavli Institute of Nanoscience, Delft University of Technology, Lorentzweg 1, 2628 CJ, Delft, The Netherlands*
[3]*Quantum Solid-State Physics, Department of Physics and Astronomy, KU Leuven, Celestijnenlaan 200D, Leuven, B-3001, Belgium*

Superconductivity has been investigated for over a century, but there are still open questions about what determines the critical current; the maximum current a superconductor can carry before switching to its normal state. For a given superconductor, the zero-field critical current is widely believed to be determined by its inherent properties and be related to its critical magnetic field. Here, by studying superconducting polycrystalline films, single crystal flakes, and layered heterostructures, we find that the critical current of a superconductor can vary with measurement configuration. It can be influenced, or even determined, by adjacent superconducting segments along the applied current trajectory, whereas the critical magnetic field and critical temperature remain unaffected. This "global critical current effect" both reveals the need to revisit fundamental theory describing superconductivity, as well as implies that superconductors can transfer critical current related phenomena to each other. We demonstrate this by designing and fabricating a simple superconducting structure that transferred a superconducting diode effect from one segment to another segment which could not manifest the effect on its own. This observation merits a reconsideration of contemporary superconducting circuit design, and developing a full understanding will lead to a new paradigm of superconducting electronics.

Properties of Kondo cloud modulations in quantum dots coupled to cavities

D. Fossion[1], B. Brun-Barrière[2], V. Champain[2], U. Genser[3], D. Mailly[3], X. Jehl[2], S. De Franceschi[2], L. Janssen[2], H. Sellier[1]

[1]Univ. Grenoble Alpes, CNRS, Institut Néel, 25 avenue des Martyrs, 38000 Grenoble, France
[2]Univ. Grenoble Alpes, CEA, Grenoble INP, IRIG-Pheliqs, 38000 Grenoble, France
[3]CNRS, C2N, 10 Boulevard Thomas Gobert, 91120 Palaiseau, France

The Kondo effect is a many-body effect, initially observed in metals containing magnetic impurities. The localized spin of the impurity is gradually screened by the spin of the conduction electrons, forming, at temperatures below the Kondo temperature (T_K), a many-body singlet. This phenomenon is also observed in quantum dots [1,2], with an odd number of electrons, leading to the presence of a localized spin that mimics that of a single magnetic impurity. Theory predicts that the many-body singlet is not limited to the quantum dot but extends over a characteristic length (ξ_K) [3], forming a so-called Kondo cloud of correlated electrons.

In this work, we investigate a GaAs/AlGaAs quantum dot in the Kondo regime using RF reflectometry (Fig. 1a). The Kondo cloud is probed by embedding the dot next to an electronic Fabry-Pérot cavity of comparable length to affect the Kondo temperature by finite-size effects. We demonstrate how the cavity allows for modulating the Kondo temperature via density-of-state modulations at the Fermi level [4,5]. We also study the effect of symmetry of the coupling to the reservoirs on the amplitude of the modulations, as well as on the subtle relationship between the Kondo temperature and the Kondo conductance (Fig. 1b and c). These results provide insight into the properties of the strongly correlated electron cloud that forms around degenerate localized states via the Kondo screening mechanism.

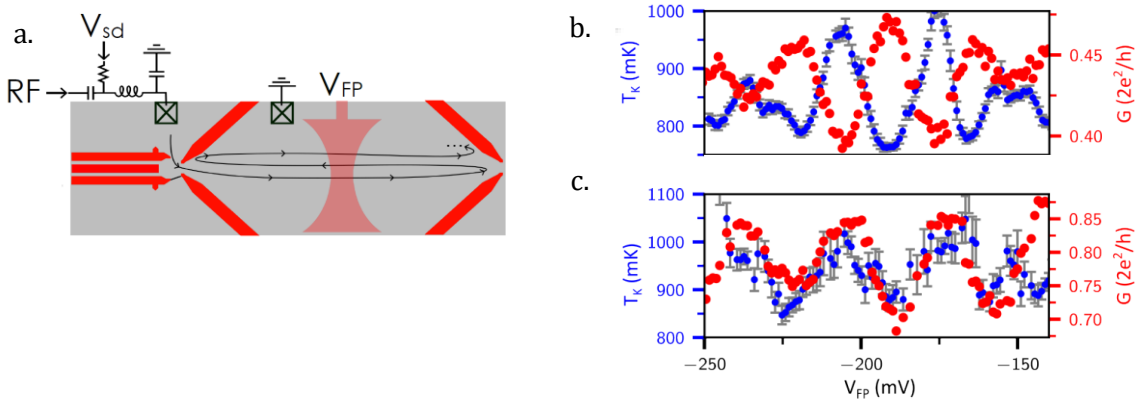

Figure 1: (a) Schematic of a quantum dot coupled to a Fabry-Pérot cavity in a 2DEG. A middle gate (V_{FP}) tunes the interference pattern by locally modifying the electron wavelength without depleting the 2DEG (b) In the strong coupling regime, resonance tuned via V_{FP} induces conductance (red) and Kondo temperature (T_K) (blue) oscillations that are out of phase. (c) In the weak coupling regime, conductance and T_K oscillations are in phase.

[1] D. Goldhaber-Gordon et al., Nature (1998)
[2] S.M. Cronenwett et al., Science (1998)
[3] I. Affleck et al., PRL (1996)
[4] J. Park et al., PRL (2013)
[5] I.V. Borzenets et al., Nature (2019)

Identification and characterisation of the reaction path of β-O-4 dimerisation of monolignols by means of first-principles calculations

P. Castenetto[1,2,3], E. Guillaume[1,2,3,4], M.-T. Bui[1,2,3] and D. E. P. Vanpoucke[1,2,3]

[1]*Hasselt University, Institute for Materials Research (IMO-IMOMEC), Diepenbeek, 3590, Belgium*
[2]*Hasselt University, Quantum and Artificial inTelligence design Of Materials (QuATOMs), Diepenbeek, 3590, Belgium*
[3]*IMOMEC, IMEC vzw, Diepenbeek, 3590, Belgium*
[4]*University of Namur, Namur Institute of Structured Matter (NISM), Namur, 5000, Belgium*

Lignin is a naturally occurring substance found in plant cells, which confer their rigidity and therefore, their structural support. It is primarily composed of three monolignol units: p-coumaryl alcohol (H), coniferol alcohol (G) and sinapyl alcohol (S). In the paper industry, lignin is a by-product often regarded as low-value and incinerated for energy production. However, with increasing interest in sustainable materials, this by-product has emerged as a promising candidate for the development of bio-based plastics due to its potential to form durable and robust products [1].

Although early industrial processes have been established, the molecular details of lignin polymerisation remain unclear. This study uses first principles methods to investigate the dimerisation of monolignols. Focusing on the formation of the β-O-4 linkage, the most prevalent in native lignin, the energy profile of the reaction is investigated in detail to gain fundamental understanding of the physics behind the dimerformation.

Contrary to earlier studies [2, 3, 4], we find that monolignol dimerization is not a straightforward process but possess a small barrier. Additionally, the role of solvents, both including and excluding van der Waals interactions, is examined. These results shed new light on the dimerisation of monolignols, thus unravelling part of the (de)polymerisation process of lignin.

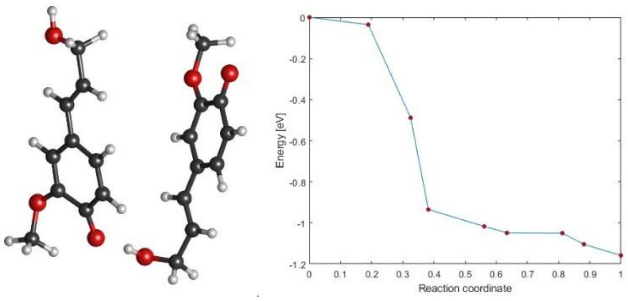

Figure 1: Representation of two G monolignols forming a β-O-4 linkage and energy profile along the reaction pathway.

[1] M. N. Collins M. N. *et al* 2019 *International Journal of Biological Macro-molecules* **131**, 828
[2] Gani T. Z. H. *et al* 2019 *ACS Sustainable Chem. Eng.* **7**, 15, 13270–13277
[3] Bickelhaupt F. M. and Houk K. N. 2017 *Angewandte Chemie International Edition* **56**, 10070
[4] C. H. Lee, J. Kim, J. Ryu, W. Won, C. G. Yoo, and J. S.-I. Kwon 2024 *Chemical Engineering Journal* **487**, 150680

From DFT to GW: Benchmarking the Electronic Structure of Diamond

E. A. Melan[1,2,3], L. Henrard[3] and D. E. P. Vanpoucke[1,2]

[1]*Hasselt University, Institute for Materials Research (imo-imomec), Quantum Artificial intelligence design Of Materials (QuATOMs), Martelarenlaan 42, B-3500 Hasselt, Belgium*
[2]*imec, imo-imomec, Wetenschapspark 1, B-3590 Diepenbeek, Belgium*
[3]*University of Namur, Namur Institute of Structured Matter (NISM), Rue de Bruxelles 61, 5000 Namur, Belgium*

Diamond color centers have piqued the interest of many researchers because of their unique properties, which make them suitable as single photon emitters and magnetic sensors. Although over 500 color centers have been identified, only a limited number have a well-described atomic scale structure [1]. Furthermore, distortions such as strains commonly found in (nano)diamonds have an effect on the optical properties, leading to even more defect possibilities in diamond [2].

This project set out to study the band structure of diamond and its different color centers. While Density Functional Theory (DFT) is the most common method for band structure calculations, the GW approximation takes quasiparticle energies into account, resulting in more accurate band structures. However, the computational cost that comes with GW calculations limits the system size that can be studied. Especially for defects in solids, such as diamond color centers, large-scale calculations are a must to obtain experimentally comparable results [2].

One approach to solve the scalability issue of GW calculations is Delta Machine Learning (ΔML) as a means to predict the material's GW band structure from a DFT band structure [3]. While the training data is to be created, they are simultaneously studied. The current study provides insight into GW calculations of the GeV center and as well forms the first set of data needed to build up a database directed at the ΔML of the electronic structures.

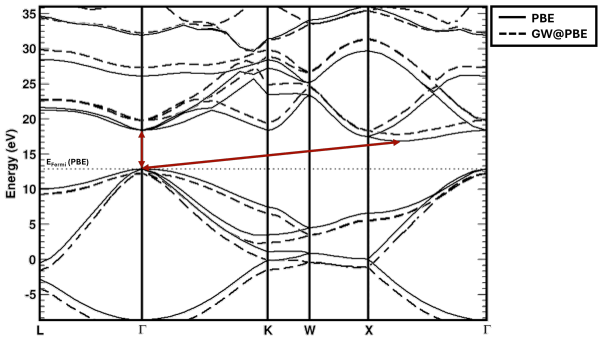

Figure 1: Band structure of diamond calculated using DFT and GW. The direct band gap is calculated to be 5.6 eV and 7.5 eV using PBE and GW respectively. The indirect band gap is 4.1 eV for PBE and 5.7 eV for GW. For reference, the experimental band gap of diamond is indirect and 5.5 eV.

[1] E.Y. Guillaume, *et al* 2025 in *Nanophotonics with Diamond and Silicon Carbide for Quantum Technologies* **Chap. 5** ISBN: 978-0-443-13717-4

[2] T.G.I. van Wijk, *et al* 2025 *Carbon* **234** 119928

[3] N.R. Knøsgaard, K.S. Thygesen, 2022 *Nature Communications* **13** 468

Physicochemical characterisation of iron oxides and hydroxides applied as food additive E 172

L. Siciliani[1,5], F. Fumagalli[2], E. Verleysen[1], J. Ponti[2], F. Cubadda[3], A. Haase[4], S. Bals[2] and J. Mast[1]

[1] Electron microscopy unit (EM unit), Trace Elements and Nanomaterials, Sciensano, 1180 Uccle, Belgium
[2] European Commission, Joint Research Centre (JRC), 21027 Ispra, Italy
[3] Istituto Superiore di Sanità - National Institute of Health (ISS), 00161 Rome, Italy
[4] Bundesinstitut für Risikobewertung - German Federal Institute for Risk Assessment (BfR), 10589 Berlin
[5] Electron Microscopy for Materials Science (EMAT), University of Antwerp, 2020 Antwerp, Belgium

Iron oxides and hydroxides are a group of inorganic substances allowed for use as food additive E 172 in the European Union. They were re-evaluated by EFSA as food additive in 2015 [1], following the classification of the EU specifications [2], namely iron oxide yellow ($FeO(OH)\cdot H_2O$), iron oxide red (Fe_2O_3), and iron oxide black ($FeO\cdot Fe_2O_3$). After the publication of the 2015 re-evaluation, ensemble methods and counting methods, including electron microscopy, reported particle sizes in the nano- and micrometre size range, and showed high amounts of iron oxide nanoparticles (NP) in commercially available E 172 [3].

In this context, a detailed physicochemical characterisation of six different E 172 materials (2 yellow, 3 red and 1 black) available on the European market was performed. For qualitative and quantitative (scanning) transmission electron microscopy ((S)TEM) analysis, the materials were dispersed following an adapted Nanogenotox protocol ensuring electrosteric stabilisation [4]. This resulted in stable dispersions, with maximal de-agglomeration, except for black iron oxide. Based on their particle morphology, at least 4 different forms of E 172 were identified. The manually measured particle size distributions of the constituent particles showed that all materials contained a fraction of nanoparticles. In addition, tomography showed pores at the surface of the rod-like hematite materials. The diffraction patterns of the yellow, red and black E 172 materials measured by both electron diffraction and X-ray diffraction matched with goethite, hematite and magnetite, respectively. Surface chemistry of E 172 materials was analysed via X ray photoelectron spectroscopy (XPS) and Time-of-flight Secondary Ions Mass Spectrometry (ToF-SIMS). Analysis of high-resolution Fe 2p (3/2) allowed to determine the iron chemical species present on the samples surface. Experimental peak shapes were modelled, considering multiplets splitting, and an estimation of valence states mix composition was obtained following an approach by Biesenger et al. [5] multi-variate analysis of ToF-SIMS spectra allowed to group materials based on correlations between their surface chemistry and revealed the presence of organic and inorganic contaminants.

Several types of iron oxides and hydroxides with differences in particle size, shape, crystal structure, elemental composition and surface properties were shown to be used as food additive E 172.

This research is performed under the NAMS4NANO action via funding from the European Union through a grant of the European Food Safety Authority (agreement GP/EFSA/MESE/2022/01). This communication reflects only the author's view and EFSA is not responsible for any use that may be made of the information it contains.

[1] EFSA Panel on Food Additives and Nutrient Sources added to Food (ANS), *Scientific Opinion on the re-evaluation of iron oxides and hydroxides (E 172) as food additives*, EFSA Journal **13**(12), 4317 (2015).
[2] European Commission, *Commission Regulation (EU) No. 231/2012 of 9 March 2012 Laying down Specifications for Food Additives Listed in Annexes II and III to Regulation (EC) No. 1333/2008 of the European Parliament and of the Council*, Off J Eur Union **83**, 1 (2012).
[3] L. Voss et al., *The Presence of Iron Oxide Nanoparticles in the Food Pigment E172*, Food Chemistry **327**, 127000 (2020).
[4] K. A. Jensen et al., *The Generic NANOGENOTOX Dispersion Protocol,* Standard operating procedure (SOP) (2011).
[5] M. C. Biesenger et al., *Resolving surface chemical states in XPS analysis of first row transition metals, oxides and hydroxides: Cr, Mn, Fe, Co and Ni*, Applied Surface Science **257**, 2717–2730 (2011).

Multiscale modelling of LTO PVD growth

E. Y. Guillaume[1,2], A. G. El Hachimi[1], P. Moskovkin[1,3], J. Müller[1,3], and S. Lucas[1,3]

[1]*Département de Physique, Namur Institute of Structured Matter (NISM), Université de Namur, 5000 Namur, Belgium*
[2]*QuATOMs, Universiteit Hasselt, 3590 Diepenbeek, Belgium*
[3]*Innovative Coating Solutions (ICS), 5032 Isnes, Belgium*

In an ever-increasingly electrified society, investigation, characterisation and improvement of the production methods of battery-related material are becoming central to pave the way for the development of new technologies. Within the framework of the BatFactory consortium, our group focuses on lithium-titanate oxide (LTO) materials, which are generally regarded as an alternative to carbon-based anodes in batteries: LTO has been shown to significantly improve the charging time and lifespan of the batteries, yet at a cost of a lower energy density [1].

We aim at delivering the most complete description of the plasma vapor deposition (PVD) growth of LTO crystals, from first-principles calculations to kinetic Monte-Carlo (kMC) simulations.

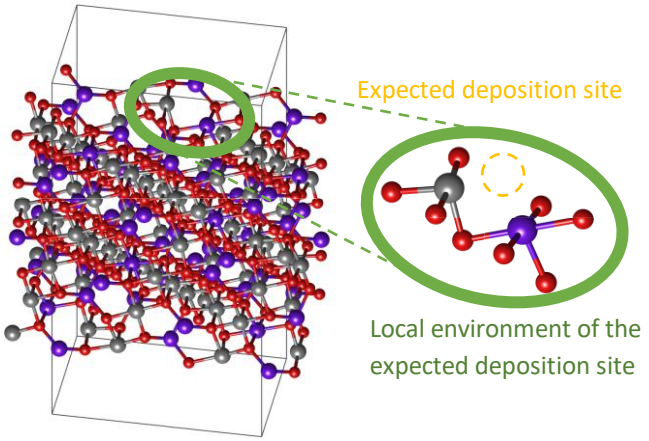

Figure 1: LTO slab in the (100)-crystallographic orientation. A specific reactive surface site is highlighted, along with the expected position of the deposition site.

To bridge the gap between the microscopic and macroscopic realms, we first model surfaces as slabs, on which several reactive sites will be characterised through the absorption energy of different species (Li, Ti, O). Calculations are carried out using the Vienna ab-initio simulation package (VASP) implementation of the density functional theory (DFT).

Upon completion of the first-principles investigation, absorption energies are translated into sticking coefficients providing relative probabilities for each species to stick on a LTO substrate. Using Virtual Coater [2], we perform kMC simulation of the growth according to several macroscopic parameters such as temperature, pressure, plasma compositions, …

Our results will provide our partners with indications on how to optimise production methods depending on their specific needs. We propose this workflow as a versatile approach to describe PVD growth in various crystalline materials.

[1] Yang, X.-G. et al., 2018. Proc. of the Nat. Ac. of Sciences. 115 (28): 7266–7271.
[2] Tonneau, R. et al., 2021. J. Phys. D: Appl. Phys. 54 155203

Real-time gas sensing with lead-sulfide quantum-dots

F. M. Fernandes[1] and B. Hackens[1]

[1]*IMCN-NAPS UCLouvain, Louvain-La-Neuve, 1348, Belgium*

In resistive type gas sensors, the variable electrical resistance depends on the concentration of a specific gas in the environment. The application of a sensing layer based on nanoparticles (NPs) (i.e. with diameters close to the Debye-length of the material) is particularly advantageous to achieve high sensitivity [1]. In addition, the electron Bohr-radius in the case of lead-sulfide (PbS) is considered big and crystalline NPs with diameter smaller than 18 nm will exhibit quantum-confinement effect leading to quantum dots (PbS-QDs) [2]. We verified that PbS-QDs can form a core-shell structure with tunable sensitivity to different gases, depending on how oxidized lead and sulfur species are distributed on the superficial layer. These findings are supported by DFT simulations and surface characterization techniques. By combining charge-transport and gas-sensing measurements, we first propose a physical model for PbS-QDs gas-sensors that considers the out-of-equilibrium dynamic response. Thanks to this model, a new strategy was derived for real-time gas monitoring that eliminates the main drawback related to slow response and recovery times for resistive-sensors when operated at ambient-temperature. The new sensing strategy was validated for low concentration of NO_2, suitable for applications in environmental monitoring and indoor air-quality control.

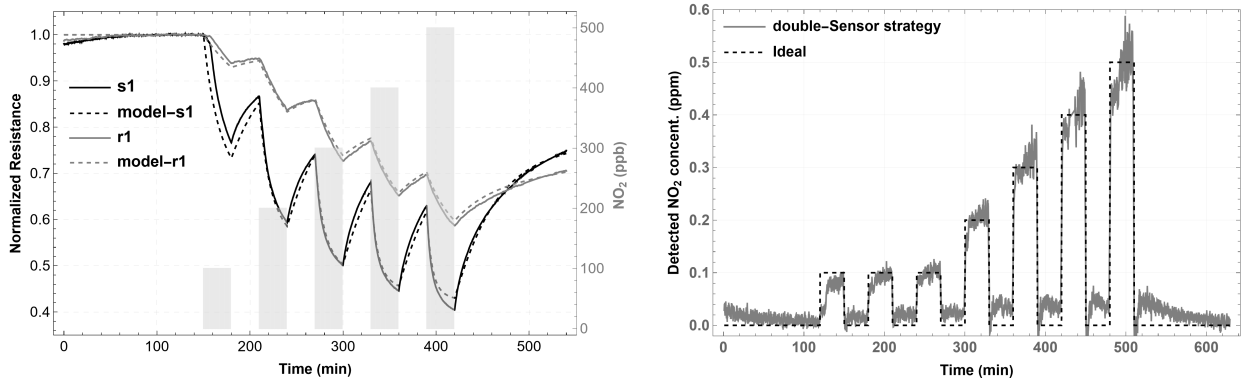

a b

Figure 1: (a) Normalized resistance variation when different concentrations of NO2-gas are mixed in a constant flow of synthetic-air with 44% relative humidity. The continuous lines corresponds to the experimental data, and the dashed lines are fittings to the device model. (b) Concentration of NO_2 as detected using samples s1 and r1 in the double-sensor strategy.

[1] Jian, Y. et al. Gas sensors based on chemi-resistive hybrid functional nanomaterials. *Nano-Micro Letters 12, 71* (2020). URL https://doi.org/10.1007/s40820-020-0407-5.

[2] Mirzaei, A. et al. Resistive-based gas sensors using quantum dots: A review. *Sensors* 22 (2022). URL https://www.mdpi.com/1424-8220/22/12/4369.

Calculating the vibrational spectrum of the GeV defect in Diamond.

Thijs G.I. van Wijk[1,2], Danny E.P. Vanpoucke[1,2]

[1]*Institute for Materials Research (IMO), Quantum and Artificial inTelligence design Of Materials (QuATOMS), Hasselt University, Agoralaan Gebouw D, 3590 Diepenbeek, Belgium*
[2]*IMOMEC, IMEC vzw, Wetenschapspark 1, 3590 Diepenbeek, Belgium*
thijs.vanwijk@uhasselt.be

As quantum information science advances, the demand for novel devices and materials capable of manifesting quantum effects becomes increasingly important. Diamond color centers are considered excellent candidates as single photon emitters. The interest in the GeV center and other group-IV color centers arises mainly from their intense zero-phonon line and small phonon sideband. [1,2] However, further research is needed to characterize the GeV center under experimental conditions, such as strain, which commonly arises during diamond growth and is known to alter the ZPL wavelength significantly. [3] To better understand these influences, a thorough examination of the phonon sideband is needed to characterise defects and zero-phonon line (ZPL) properties. Density Functional Theory (DFT) calculations provide valuable insights into the vibrational structure of the color center and serve as a powerful complement to experimental studies. [4,5] However, achieving precise vibrational calculations requires tremendous computational resources, often beyond what is available.

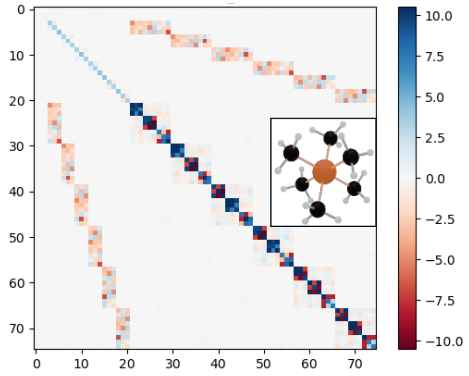

Figure 1: Dynamical matrix of GeC_6H_{18} cluster

In this work, we aim to predict vibrational spectra with Density Functional Theory (DFT) enhanced Machine Learning (ML). By combining these methodologies, we aim to address the critical need for accurate vibrational calculations in a computationally efficient manner. As a first step, we focus on the QM9 dataset, which consists of small organic molecules, to develop and benchmark a machine learning framework that can later be extended to solid-state systems. This test set with small molecules is used to develop a machine learning protocol that can be transferred to solids. Our approach relies on redundant internal coordinates (RICs) [6], which describe molecular or solid structures through bond lengths, bond angles, and dihedral angles. The Hessian matrix, initially calculated in Cartesian coordinates, is transformed into the RIC representation. The elements of this transformed Hessian matrix serve as the prediction targets. For each matrix element, we construct a feature vector that incorporates geometric information—such as bond lengths, angles, and dihedrals—along with descriptors of the local chemical environment. Using this setup, we train several machine learning models, including linear regression, random forest, and support vector machines, to learn the relationship between structural features and vibrational properties. The ultimate goal is to transfer this protocol to solids, enabling accurate and efficient vibrational spectra predictions for complex systems like color centers in diamond.

References

1. E. Neu, *et al*., New Journal of Physics 2011, 13, 025012.
2. Y. N. Palyanov, *et al*.,, Scientific Reports 2015, 5, 14789.
3. T. G. I. Van Wijk, *et al*.,, Carbon 2024, 119928.
4. K. N. Boldyrev, V *et al*.,, Diamond and Related Materials 2022, 126, 109049.
5. D. E. P. Vanpoucke, Computational Materials Science 2020, 181, 109736.
6. H. B. Schlegel, Journal of Computational Chemistry 1982, 3, 214.

Creating *NOON* states with ultracold atoms using time crystals

C. Delaive[1] and P. Schlagheck[1]

[1]*CESAM, research unit, University of Liège, Belgium*

We propose two protocols for the creation of *NOON* states involving N ultracold bosonic atoms distributed over multiple modes in the framework of time crystals. For two modes, such a state is defined by the coherent superposition $|N,0\rangle + e^{i\varphi}|0,N\rangle$. By applying an appropriate periodic driving to our system, we induce the formation of resonance islands that confine the condensate dynamics to specific regions of the phase space. The first protocol relies on the collective tunneling of the condensate atoms between islands of the same resonance. The *NOON* state naturally emerges at half the tunneling time. The second protocol is based on the adiabatic transition of the condensate when prepared in an additional mode symmetrically coupled to the modes of a resonance. By slowly tuning the energy of this extra mode across the levels of the resonance, the system evolves adiabatically toward a *NOON* state. However, both of these methods are intrinsically slow. We will manage to boost them respectively through chaos-assisted tunneling and through counterdiabatic driving.

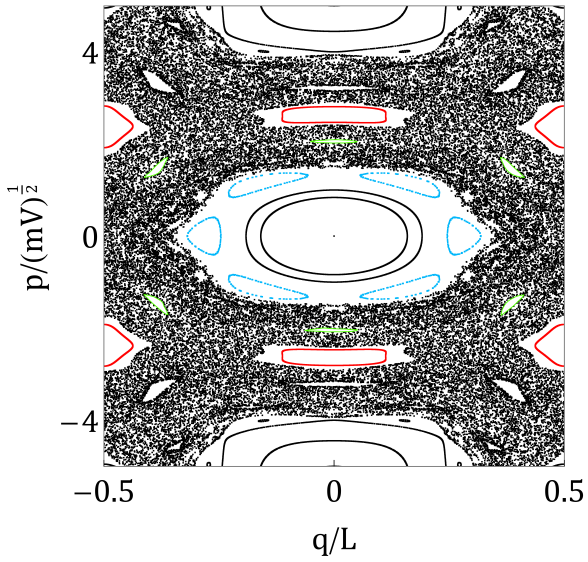

Figure 1 : Example of a Poincaré section of the system for $\omega_0 t = 0 + 2\pi n$ of the classical single-particle dynamics corresponding to the Hamiltonian $H = p^2/2m + V[1+\delta\cos(\omega_0 t)]\cos(2\pi/L)$ with $\omega_0 = 5$ and $\delta = 2$. We see in red the islands of the 2:1 resonance that are separated by a chaotic sea, making them a good candidate for the chaos-assisted tunneling protocol. In green we have the islands of the 6:1 resonance, they are not separated by a chaotic see but they are good candidate, in addition to the center well, for the counterdiabatic driving protocol.

Study of out-of-plane electronic transport in multilayer graphene films by C-AFM

Michael TZVETKOV, Oriane DE LEUZE, Viet-Hung NGUYEN, Jean-Christophe CHARLIER, Benoit HACKENS

IMCN (NAPS et MODL), UCLouvain, Louvain-La-Neuve, Belgique

The discovery of graphene in 2004 sparked scientific interest in electronic devices based on 2D materials, which continues to this day. While most studies of electronic transport in graphene focus on in-plane transport properties, relatively little is known about out-of-plane transport. Despite two decades of work on graphene, measuring plane-perpendicular transport in multilayer graphene (MLG) remains a significant challenge. Indeed, conventional transport techniques are not suitable for measuring transport in this direction, due to the nanometric thickness of these materials and the difficulty of fabricating distinct metal contacts on both sides of crystals of a few layers using standard deposition methods.

This work consists of an experimental study of the electronic behavior of MLG in the out-of-plane direction, which will focus its efforts on isolating the intrinsic electronic properties of MLG by combining different methods. The main method we employ to induce an out-of-plane current in the MLG is the 'Conductive AFM' (C-AFM) technique [1] (Fig. 1 a), based on the measurement of an electric current between the tip and the sample, in 'contact' mode. Typically, it enables the effects of MLG thickness on its transport properties to be studied effectively.

The experimental results collected to date (Fig. 1 b and c) on MLG sheets of increasing thickness deposited on gold, show an increase in the C-AFM current with the number of layers. These intriguing results call for further study to gain a better understanding of the physical origin of this phenomenon, for example by means of other local probe microscopy techniques and ab initio simulation results taking into account graphene-metal coupling.

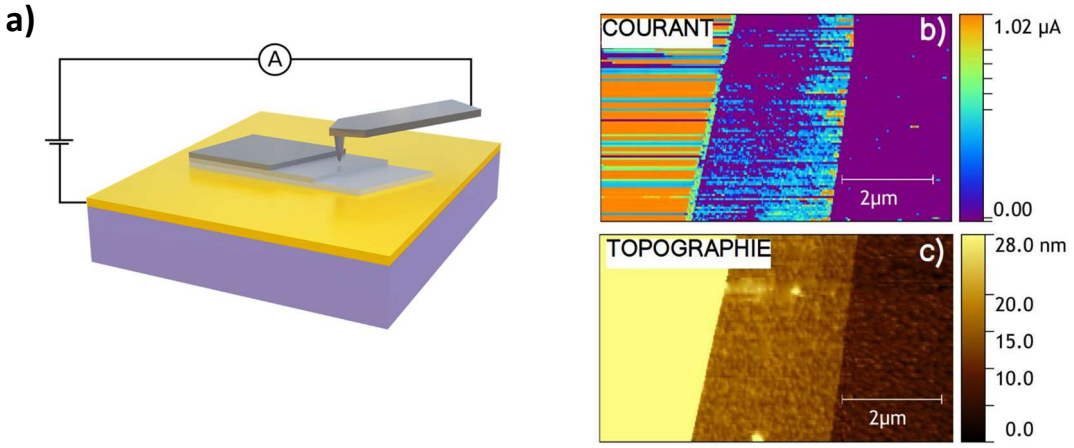

Figure 1 : a) Schematic representation of the analysis of a sample by the C-AFM method, showing a 'staircase' of MLG deposited on a gold substrate serving as electrode. b) and c) Current and topographic images respectively of the area of interest, showing that out-of-plane current tends to increase with graphene thickness.

[1] Lim, S.; Park, H.; Yamamoto, G.; Lee, C.; Suk 2021 J.W. *Nanomaterials*, ***11***, 2575

[2] Melitz, W.; Shen, J.; C.Kummel, A.; Lee, S. 2011 *Surface Science Reports*, ***66***, 1

ESTIMATION OF ELECTRICAL CONDUCTIVITY ANISOTROPY IN MXENES BY CAFM MODELING

S. Arib[1], B. Hackens[1]
[1]*IMCN/NAPS, Université catholique de Louvain, Louvain-la-Neuve, 1348, Belgium*

It is inherent in 2D crystals to exhibit anisotropic properties due to their planar geometry. One important property of these materials, electrical conductivity, is no exception to the rule, and is of particular interest as it opens up a multitude of applications. For example, MXenes, a family of 2D materials, can typically be used to protect against electromagnetic interference [1]. The study of charge transport in these 2D crystals is therefore a natural step. A 4-contact electrical measurement is the conventional choice, enabling the in-plane electrical conductivity of the measured sample to be determined. For this study, we opted for conductive atomic force microscopy (CAFM) [2], which not only allows current to flow in-plane, but also out-of-plane, which is not possible with conventional 4-contact measurements.

However, the study of transport properties with CAFM is complicated by the fact that it is difficult to avoid contact resistance between the tip and the conductive electrode on which the sample is placed (Figure a). What's more, this contact resistance can vary according to several parameters, such as the indentation of the tip in the sample [3]. Here, we combine experimental data and simulations to extract a quantitative value for electrical conductivity anisotropy in metallic MXenes. Figures b and c illustrate, for example, the distribution of electrical potential across the thickness of a 2D crystal for an isotropic (b) and anisotropic (c) sample. Figures (d) and (e) highlight the fact that the equivalent radius of the same tip will not be identical for samples with different anisotropies.

This work shows the value of combining experimental data with simulation results in the extraction of quantitative data in 2D crystals such as MXenes.

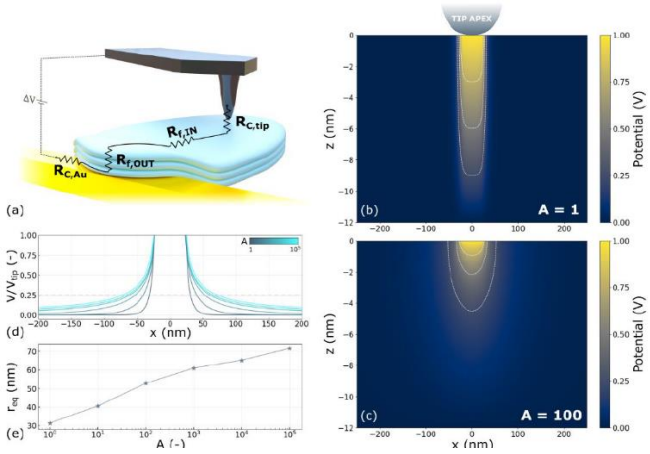

Figure 1: (a) Equivalent circuit of the C-AFM. (b-c) Simulated potential distribution within the flake. (d) Simulated potential distribution at the flake surface. (e) Simulation of the equivalent radius r_{eq} as a function of the anisotropy. r_{eq} is defined as the radius corresponding to the area where 75% of the potential drop occurs at the flake surface.

[1] F. Shahzad; M. Alhabeb; C. B. Hatter, *Science* **2016**, *353*, 1140.
[2] O. G. Reid; K. Munechika; D. S. Ginger, *Nano Letters* **2008**, *8*, 1602.
[3] D. Moerman; N. Sebaihi; S. E. Kaviyil, *Nanoscale* **2014**, *6*, 10596.

Observation of fast atom diffraction through suspended graphene

A. Dochain[1], P. Guichard[2], R. Marion[1,3], P. de Crombrugghe de Picquendaele[1], N. Lejeune[1,4], B. Hackens[1], P.-A. Hervieux[2] and X. Urbain [1]

[1]*Institute of Condensed Matter and Nanosciences, Université Catholique de Louvain, Louvain-la-Neuve, 1348, Belgium*
[2] *Université de Strasbourg, CNRS, Institut de Physique et Chimie des Matériaux de Strasbourg, UMR 7504, Strasbourg, 67000, France*
[3]*Royal Observatory of Belgium (ROB-ORB), Brussels, 1180, Belgium*
[4]*EPHEC, Louvain-la-Neuve, 1348, Belgium*

We report the observation of fast atom diffraction through single-layer graphene. High resolution images have been recorded with hydrogen atoms at kinetic energies ranging from 150 eV to 1200 eV, following the experimental protocol suggested by Brand et al. [1]. Commercial suspended graphene samples were characterized using micro-Raman spectroscopy, prior to and after beam exposure for the quantification of defects. Monocrystalline domains within the illuminated area produced characteristic hexagonal diffraction patterns, making such an experimental approach suitable for matter-wave interferometry.
Density functional theory calculations with pseudopotentials [2] have been performed to determine the H-graphene interaction potential over the whole unit cell. Nice agreement with the calculations of Ehemann *et al.* [3] is found, who used the Self-Consistent Charge-Density Functional Tight Binding method. In order to simulate diffraction images, we generate a phase mask by integrating the three-dimensional potential along the coordinate normal to the graphene plane and performing an eikonal treatment of the scattering events. Our computed diffraction patterns fall in better agreement with experiment than those generated with an interaction potential derived from electron density [1] or by summing up pair-wise interactions between H and C atoms.

[1] Brand C, Debiossac M, Susi T, Aguillon F, Kotakoski J, Roncin P, and Arndt M 2019 *New J. Phys.* **21** 03004
[2] Giannozzi P, Baroni S, Bonini N *et al.* 2009 *J. Phys.: Condens. Matter* **21** 395502
[3] Ehemann R C, Krstić P S, Dadras J, Kent P R C, and Jakowski J, 2012 *Nanoscale Res. Lett.* **7** 198

A Scanning Thermal Microscope at cryogenic temperatures

V. Fonck[1], M. Rohde[1], and P. Gehring[1]

[1]1*Institute of Condensed Matter and Nanosciences, Université Catholique de Louvain, Louvain-la-Neuve, 1348, Belgium*

The characterization of the thermal properties of nanoscopic materials has become a flourishing field of research since the first realization of a micrometric thermometer probe using a partially exposed Pt/Rh wire in 1994. Scanning Thermal Microscopy has enabled the local characterization, excitation and lithography of materials at the nanometric scale. A variety of thermometry mechanisms have been implemented on AFM probes based on their different performances for given applications. [1] Most of these commercial probes are not suited for operations below 50K as their sensitivity will drastically drop. An exception remains in the superconducting quantum interference device (SQUID) on probe approach, but they lack in versatility as their use is limited to liquid helium temperatures and moderate magnetic fields. [2] Furthermore, implementing a contact feedback mechanism in a cryostat, where tuning forks are usually favored, is by itself a challenge. These hurdles have long impeded the local investigation of thermal and thermoelectric properties of materials at cryogenic temperatures.

We report here early results in the fabrication of a scanning thermal microscope capable of operating from room temperature to 1.4K. Interferometry-based feedback was chosen for its superior sensitivity for contact modes. [3] The dipstick presented at Figure 1b is designed for an ultra-low vibration cryostat, see Figure 1e. An AC modulation scheme is used to take advantage of the natural noise rejection of lock-in amplifiers, see Figure 1a.

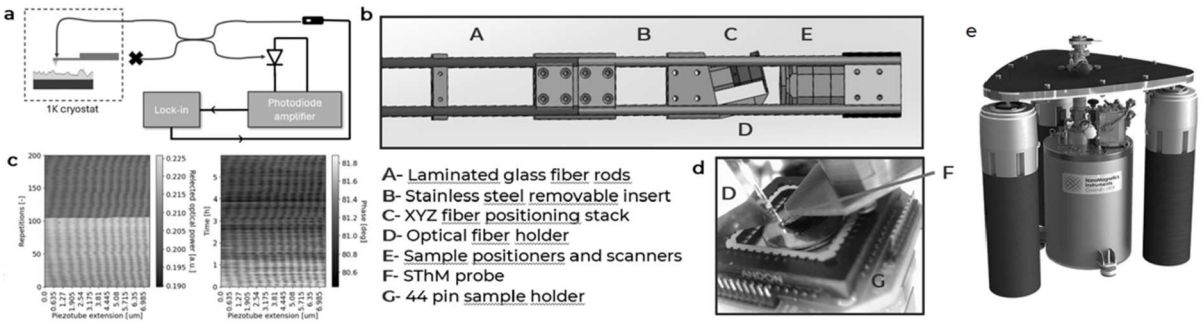

Figure 1: a Measurement scheme for the AC-modulated interferometric feedback **b** 3D model of the scanning insert **c** Stability along time benchmark graphs using the piezoelement supporting the AFM probe **d** Microscope image of the sample space and the scanning head **e** Photography of the ultra-low vibration cryostat

[1] Zhang, Y. *et al.* 2020 *Advanced Functional Materials* **30** 1900892
[2] Völkl, T. *et al*. 2024 *Nat. Phys*. **20** 976–983
[2] Rugar, D. *et al.* 1989 *Applied Physics Letters* **55** 2588–2590

Observation of the first ultra-high energy cosmic neutrino

Aart Heijboer[1]

[1]*Nikhef and University of Amsterdam, Amsterdam, 1098XG, The Netherlands*

The KM3NeT collaboration is building a neutrino observatory on the bottom of the Mediterranean Sea. At a depth of 3.5 km, thousands of optical sensors, located on 700m long vertical lines are detecting the faint flashes of Cherenkov light that occur when a neutrino interacts and produces charged particles. While only a fraction of the instrument is currently complete, the first results on neutrino oscillations and astronomy have already been obtained.

On February 13, 2023, the detector registered an extremely bright neutrino event (Figure 1). After analysis the energy of the neutrino was measured to exceed 100 PeV, making this the highest-energy neutrino ever observed [1].

In the talk, I will discuss the status of KM3NeT, some of the engineering challenges involved in building an instrument at the bottom of the Sea, and the first results, including the ultra-high-energy neutrino, and its possible origin.

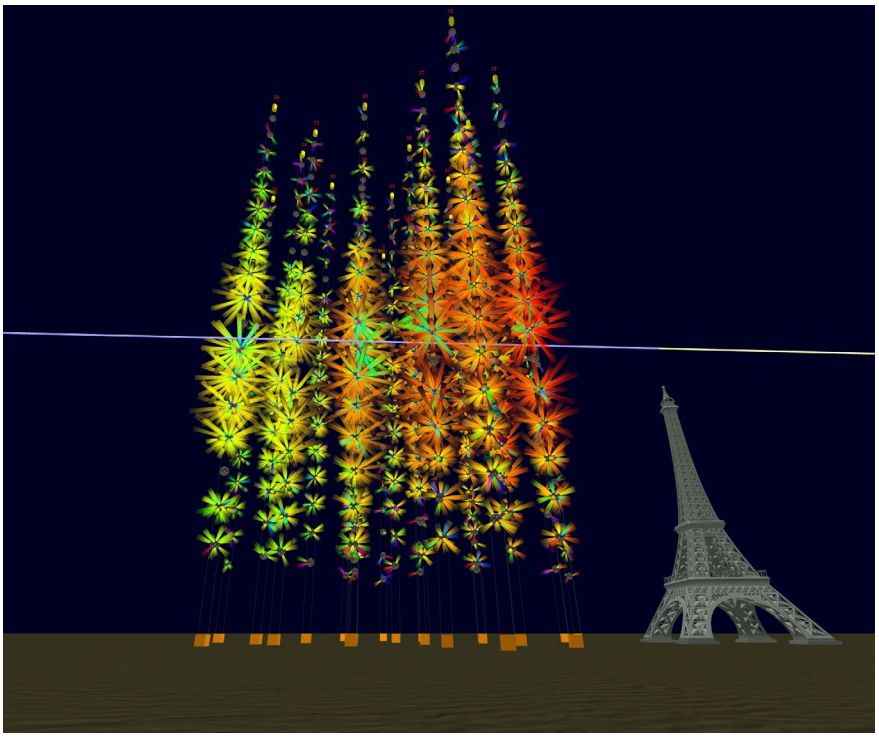

Figure 1: Event display of KM3NeT's Ultra-high-energy cosmic neutrino. The image shows the 21 detection lines that make up the detector; The Eifel tower is shown for scale. The colorful cones indicate the detection of light by the sensors. From the arrival times and intensity of the light, the direction and energy of a muon (blue line) are reconstructed. The muon must have been produced by a neutrino, which is shown as the yellow line, somewhere prior to entering the detector.

[1] The KM3NeT Collaboration. Observation of an ultra-high-energy cosmic neutrino with KM3NeT. *Nature* **638**, 376–382 (2025)

Parametrized test of general relativity with gravitational waves including higher harmonics and precession

S. Roy[1,2], M. Haney[3], G. Pratten[4], P. T. H. Pang[3,5], C. V. D. Broeck[3,5]

[1]*Centre for Cosmology, Particle Physics and Phenomenology - CP3, Université Catholique de Louvain, Louvain-La-Neuve, B-1348, Belgium*
[2]*Royal Observatory of Belgium, Avenue Circulaire, 3, 1180 Uccle, Belgium*
[3]*Nikhef – National Institute for Subatomic Physics, Science Park 105, 1098 XG Amsterdam, The Netherlands*
[4]*School of Physics and Astronomy and Institute for Gravitational Wave Astronomy, University of Birmingham, Edgbaston, Birmingham, B15 2TT, United Kingdom*
[5]*Institute for Gravitational and Subatomic Physics (GRASP), Utrecht University, Princetonplein 1, 3584 CC Utrecht, The Netherlands*

When testing general relativity (GR) with gravitational wave observations, parametrized tests of deviations from the expected strong-field source dynamics are one of the most widely used techniques. We present an updated version of the parametrized framework with the state-of-the-art IMRPhenomX waveform family [1, 2]. Our new framework incorporates deviations in the dominant mode as well as in the higher-order modes of the waveform. We show that the missing physics of either higher-order modes or precession in the parametrized model can lead to a biased conclusion of false deviation from GR. Our new implementation alleviates this issue and enables us to perform the tests for highly asymmetric and precessing binaries without being subject to systematic biases due to missing physics. Finally, we use the improved test to analyze events observed during the third observing run of LIGO and Virgo, and combine our results with those from previous observation runs. Our findings show no evidence of violations of GR. In particular, our recent analysis of the GW230529 event places an upper bound on the Gauss-Bonnet (GB) coupling of $\sqrt{\alpha_{\rm GB}} \leq 0.28\,\text{km}$, which is the most stringent bound on Einstein-scalar-Gauss-Bonnet theories of gravity reported to date [3].

[1] G. Pratten et al., 2020 *Phys. Rev. D* **102**, 064001
[2] G. Pratten et al., 2021 *Phys. Rev. D* **103**, 104056
[3] E. M. Sänger, S. Roy et al., 2024 *arXiv:* 2406.03568 [gr-qc]

Multi-Messenger Search for Neutrino and Gravitational-Wave Emissions from Binary Black Holes Near Active Galactic Nuclei

L. Ricca[1], M. Vereecken[2], G. Bruno[3] and G. de Wasseige[4]

[1,2,3,4] *Centre for Cosmology, Particle Physics and Phenomenology – CP3, Université Catholique de Louvain, Louvain-La-Neuve, Belgium*

Binary black holes (BBHs) in the vicinity of Active Galactic Nuclei (AGNs) are particularly interesting systems from both a cosmological and astrophysical point of view. Matter and radiation fields within the dense AGN environment could produce electromagnetic and neutrino emission in addition to gravitational waves (GWs) [1,2,3]. Moreover, interactions between BBHs and AGN accretion disks are expected to influence BBH formation channels and merger rates. Understanding these sources could help explain the unexpectedly high BBH masses observed through GWs by the LIGO-Virgo-KAGRA collaborations.

We present a search for coincident gravitational-wave and neutrino emission from AGNs. Our new innovative approach combines information from gravitational-wave data, neutrino observations, and AGN optical catalogs to increase the chances of identifying potential sources and studying their properties.

We assess the sensitivity of the search using subthreshold gravitational-wave candidates from LIGO-Virgo-KAGRA data and neutrino event candidates from public IceCube Neutrino Observatory data. A confident detection of such an event would mark a breakthrough in multi-messenger astronomy.

[1] McKernan B. *et al* 2019 *Astrophys. J. Lett.* **884** 2, L50
[2] Kimura S., Murase K., Bartos I. 2021 *Astrophys.J.* **916** 2, 111
[3] Bruno G. *et al* 2023 *PoS ICRC2023 1514*

Using the null stream to detect strongly lensed gravitational waves

J. Heynen[1], S. Roy[2], and J. Janquart[3]

[1,2,3]*UC Louvain, Louvain-La-Neuve, 1348, Belgium*
2,3 Royal Observatory of Belgium, Uccle, 1180, Belgium

Gravitational lensing of gravitational waves is expected to be observed in current and future detectors' data. In view of the growing numbers of gravitational wave detections, a false alarm probability is required to claim a confident detection and for this, a background needs to be constructed. Current detection pipelines are expensive which makes constructing a large background unfeasible. We present a novel strong lensing detection method, whose detection statistic can be constructed using the null stream of a detector network. By considering the null stream of the total network of two gravitational wave events, one obtains measurements of the null energy, which helps us identifying lensed pairs. We show the method's validity by applying it on noiseless injected waveforms. We also give an outlook on how to apply this method on noisy data.

Neutrino energy distributions of astrophysical sources: the GRB example

E. Moyaux[1], E. O'Sullivan[2] and G. de Wasseige[1]

[1]*Centre for Cosmology, Particle Physics and Phenomenology, Université catholique de Louvain, Louvain-la-Neuve, 1348, Belgium*
[2]*Department of Physics and Astronomy, Uppsala University, Box 516, S-75120 Uppsala, Sweden*

Currently, the identification of neutrino sources relies on joint observations with electromagnetic telescopes. This method has led to some successes, but is constrained by the field of view, availability, and observational limitations of traditional telescopes. The ongoing development of neutrino detectors around the world suggests that future datasets will allow for precise source analysis based solely on neutrino observations. Our objective is to provide the scientific community with theoretical predictions of neutrino emissions that can be compared with observational data from neutrino detectors, and eventually, to develop an identification method using only neutrino observations.

Our work focuses on the example of GRBs. We aim to construct the neutrino energy distribution of such events by combining several theoretical neutrino emission models spanning different energy ranges, which are sensitive to key GRB parameters such as the Lorentz factor and baryonic loading. Then, we use the effective area, angular response and energy response of the IceCube Neutrino Observatory to convert this theoretical energy spectrum to a set of simulated neutrino events that we could expect from a given GRB. Our prospect is to use these results to train machine learning models to search for signature emissions of GRBs in both archival and future data.

Dark matter search in the Galactic Center with IceCube Upgrade

N. Chau[1] and J. A. Aguilar[1]

[1] *Université Libre de Bruxelles, Science Faculty CP230, B-1050 Brussels, Belgium*

The nature of dark matter remains one of the most profound open questions in fundamental physics [1]. Indirect detection seeks for anomalous excesses in standard model particles - such as neutrinos - produced by dark matter annihilation or decay. These searches typically focus on astrophysical regions with high concentrations of dark matter [2]. Among these, the Galactic Center stands out as a particularly promising target due to its substantial dark matter density and relative proximity to Earth.

In this talk, we present sensitivity projections for dark matter searches in the Galactic Center using the IceCube Upgrade - an upcoming extension of the IceCube Neutrino Observatory designed to enhance detection capabilities in the GeV energy range [3, 4]. This study suggests that the IceCube Upgrade could improve current limits set by IceCube [5] by up to an order of magnitude and potentially deliver world-leading constraints for certain dark matter model configurations.

[1] G. Bertone and D. Hooper, “History of dark matter,” Rev. Mod. Phys. 90, 045002 (2018).
[2] C. Pérez de los Heros, “Status, Challenges and Directions in Indirect Dark Matter Searches,” Symmetry 12, 1648 (2020).
[3] IceCube Collaboration, “The IceCube Neutrino Observatory: Instrumentation and Online Systems”, JINST 12, P03012 (2017).
[4] IceCube Collaboration, “The IceCube Upgrade – Design and Science Goals”, PoS ICRC2019, 1031 (2019)
[5] N.Chau for the IceCube Collaboration, “Indirect dark matter search in the Galactic Centre with IceCube”, PoS ICRC2023 1394 (2023).

Searching for GeV neutrinos from Gamma-Ray Burst sub-populations with IceCube

K. Kruiswijk[1] and G. de wasseige[1]

[1] *UCLouvain, Louvain-La-Neuve, 1348, Belgium*

Astrophysical transients like Gamma-Ray Bursts (GRBs) have been promising candidates of neutrino source since their discovery. While neutrinos associated with these events are yet to be observed, it is possible that a sub-population of GRBs are neutrino emitters. GRBs are famous for their variability, with two different precursors generally accepted and several sub-populations suspected, based on kilo- or supernova association, luminosity, duration, and spectra, among other properties [1]. This can also indicate a differing neutrino flux over sup-populations, and this neutrino flux can be detected by IceCube. While IceCube is built for TeV and higher neutrino energies, GeV neutrinos are detectable as well, allowing for transient searches [2]. Using unsupervised machine learning, the sub-populations of GRBs can be separated from each other [3]. We discuss the methods to find these sub-populations of GRBs, how to test their predicted flux with a generic neutrino emission model, and how to perform the individual as well as stacking searches with IceCube to search for GeV neutrinos.

[1] B. Zhang 2018 *Cambridge University Press*

[2] IceCube Collaboration, K. Kruiswijk, and G. de Wasseige 2023 *PoS: ICRC2023* **1513**

[3] K. Kruiswijk, and G. de Wasseige 2023 *PoS: ICRC2023* **1508**

Late inspiral of eccentric asymmetric binaries

G. Lhost[1] and G. Compère[2]

[1] *Physique de l'univers, champs et gravitation, Université de Mons, Mons, 7000, Belgium*
[2]*Service de physique théorique et mathématique, Université libre de Bruxelles, Bruxelles, 1050, Belgium*

Eccentric binary compact mergers are key targets for current and future gravitational wave observatories. In particular, extreme mass ratio inspirals (EMRIs) will be prime sources for both space-based (LISA) and next-generation ground-based (Einstein Telescope) detectors. While quasi-circular asymmetric binaries are now well understood in the self-force framework [1], significant progress is still required to successfully solve the problem of modelling eccentric binaries. In the small mass ratio expansion, post-adiabatic inspirals have been described up to the last stable orbit, where first-principles methods remain inapplicable [2]. However, constructing a complete waveform model for eccentric asymmetric binaries requires an accurate treatment of the plunge and the transition from the inspiral to the plunge. This latter phase of the motion must be consistently matched to the late inspiral.

In this presentation, I will discuss the challenges of waveform modelling for EMRIs within the self-force framework and focus on an analytical solution to the post-adiabatic equations governing the inspiral of an eccentric binary in the extreme mass ratio regime [3].
Unlike the quasi-circular case, these solutions feature Lambert W functions. These asymptotic adiabatic equations and their solutions pave the way towards a full description of the transition to the plunge.

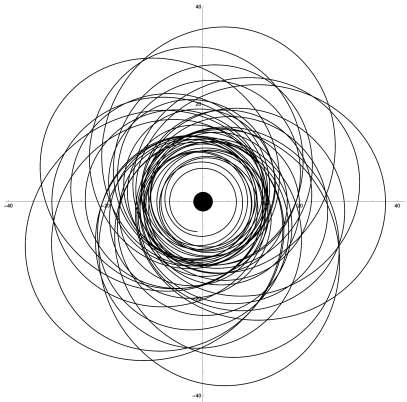

Figure 1: Eccentric EMRI at adiabatic order in a Schwarzschild background. The initial eccentricity and semi-latus rectum are $e_0 = 0.5$ and $p_0 = 20$ respectively. This trajectory was computed using the Black Hole Perturbation Toolkit. As shown, the adiabatic inspiral ends at some specific values of e and p corresponding to the last stable orbit, where the plunge occurs.

[1] Wardell B. *et al* 2023 *Phys. Rev. Lett.* **130** 241402
[2] Flanagan E. and Hinderer T. 2012 *Phys. Rev. Lett.* **109** 071102
[3] Lhost G. and Compère G. 2024 2412.04249

Sensitivity to Solar Dark Matter using the IceCube Upgrade

E. Genton[1,2], J. Lazar[1], G. de Wasseige[1], C.Argüelles[2]

[1]*Université Catholique de Louvain, Louvain-la-neuve, 1348, Belgium*
[2]*Harvard University, Cambridge, MA 02138, U.S.A*

While astrophysical observations imply that 85% of the matter content is unaccounted for, the nature of this dark matter (DM) component remains unknown. Weakly Interacting Massive Particles (WIMPs)—DM particles that interact at or below the weak interaction scale—could naturally explain this missing matter. These interactions with the Standard Model (SM) allow them to be gravitationally captured in celestial bodies like the Sun. Trapped DM in the solar core could subsequently annihilate, producing stable SM particles, of which only neutrinos can escape the Sun's dense interior. Therefore, an excess of neutrinos originating from the direction of the Sun would serve as evidence of DM. The IceCube Upgrade, a dense infill of the IceCube Neutrino Observatory, will lower the energy threshold and improve sensitivity in the range from 1 to 500 GeV, thereby enhancing IceCube's ability to detect GeV-scale DM. In this contribution, I present projections of the IceCube Upgrade's sensitivity to the DM-proton scattering cross section for DM masses between 3 GeV and 500 GeV. These sensitivities position IceCube as the most sensitive indirect detection experiment for DM in the mass range from 3 GeV to 10 TeV.

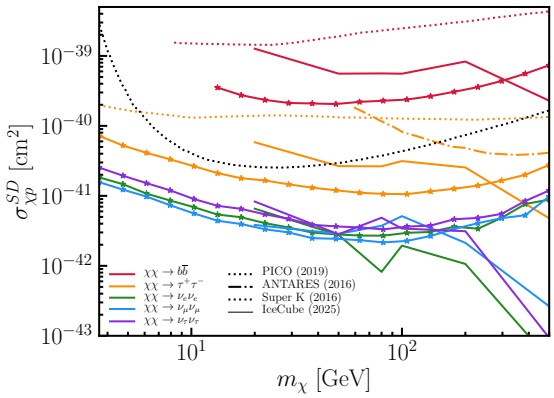

Figure 1:These projected limits that the IceCube Upgrade can deliver would extend IceCube's limits to 3 GeV, offering complementarity to the lowest masses probed by direct detection experiments. Furthermore, the IceCube Upgrade would produce world-leading limits on DM-proton scattering cross sections below $\mathcal{O}(100)$ GeV. The prospective limits from the IceCube Upgrade are compared to limits from [1,2,3].

[1] S. Adrián-Martínez et al. *Physics Letters B: Limits on dark matter annihilation in the sun using the antares neutrino telescope* **759** 69-74

[2] Kamiokande Collaboration *et al Search for neutrinos from annihilation of captured low-mass dark matter particles in the sun by super-kamiokande, 2015*

[3] C. Amole *et al* 2019 *Physical Review D: Dark matter search results from the complete exposure of the pico-60 C3F8 bubble chamber, 2015* **100(2):** 022001

Low-latency neutrino follow-up combining diverse IceCube selections

C. Raab[1], S. Hori[2], S. Sclafani[3], and J. Thwaites[2]

[1]*CP3 – UCLouvain, Louvain-la-Neuve, 1348, Belgium*
[2]*WIPAC – UW Madison, Madison, WI 53703, USA*
[3]*University of Maryland, College Park, MD 20742-4111, USA*

Neutrino observations are a crucial component of multi-messenger astronomy, but are currently limited by effective area and high atmospheric background. However, while other telescopes with limited field of view must be pointed in order to capture observations, IceCube's full-sky field of view and high uptime make it an excellent instrument for realtime follow-up of astrophysical transient sources.

IceCube searches for neutrino transients using an unbinned maximum likelihood method with parameters for the source's emission time period, extension, and energy spectrum. This Fast Response Analysis can provide analysis results within tens of minutes of an astrophysical transient. Besides the follow-up of astrophysical transients manually selected as candidates, it also routinely scans areas of the sky compatible with gravitational wave alerts from LIGO/Virgo/KAGRA and IceCube event singlets which have a high probability of originating from an astrophysical source. Currently the analysis uses TeV muon neutrino candidate events whose track signature is especially suited for a precise angular reconstruction, selected and reconstructed at the South Pole and transmitted with low-latency over a satellite connection.

Recently, IceCube and the neutrino astronomy community are evolving to use event samples constructed with different selections. These efforts include the follow-up of gravitational wave events with GeV neutrinos detected by IceCube-DeepCore and the observation of the Galactic plane with cascade events produced by all neutrino flavors. With plans to make IceCube-DeepCore GeV neutrino candidates and cascade events available on a day-scale latency, they can also be used in Fast Response Analyses. Moreso, multiple event samples can be combined in a Fast Response Analysis that is sensitive to a broader energy range of a neutrino transient spectrum and ensures the inclusion of all neutrino flavours.

We present the analysis method and technical aspects of such an extension of the existing framework. This includes a proposed new pipeline allowing the inclusion of the more computationally-intensive reconstruction methods used by the aforementioned event selections. The extension is validated using example analyses implemented in this framework.

Multi-messenger astrophysics with the ACME consortium

M. Lamoureux[1], G. De Wasseige[1]

[1] *UCLouvain, Centre for Cosmology, Particle Physics and Phenomenology, Chemin du Cyclotron, 2, Louvain-la-Neuve, 1348 Belgium*

In the coming years, the coordination and accessibility of telescopes and observatories across the globe will be essential towards the success of multi-messenger astrophysics researches. The ACME project, funded by the European Union, aims to facilitate and improve the access to multi-messenger data and services. It brings together about forty institutes across Europe, covering all domains in multi-wavelength astronomy, gravitational waves, neutrinos, and cosmic rays.

ACME will provide transnational access to infrastructures, virtual access to tools and archives, as well as training and guidance for researchers in the field or in other disciplines, and citizen scientists. The presentation will cover the scope of the project, the ongoing actions, and the expected results.

Probing neutrino yield from different gamma-ray burst populations using the entire ANTARES data set

A. Kouchner[1,2], M. Lamoureux[3], **M. Scarnera[3]** and G. de Wasseige[3]

[1]Université Paris Cité, CNRS, Astroparticule et Cosmologie, F-75013 Paris, France
[2]Institut Universitaire de France, 1 rue Descartes, Paris, 75005 France
[3]UCLouvain, Centre for Cosmology, Particle Physics and Phenomenology, Chemin du Cyclotron, 2 Louvain-la-Neuve, 1348 Belgium

While the evidence of high-energy neutrinos was established a decade ago and confirmed independently by the observation of an ultra-high-energy neutrino recently announced, the origin of these neutrinos is not yet fully identified. Gamma-ray bursts (GRBs) have long been one of the most promising candidate emitters of such neutrinos. Despite not having led to a significant detection in neutrinos so far, the observations were focusing on GRBs that were bright in gamma rays. Dividing the GRBs detected so far in various subpopulations based on their signal in gamma rays and searching for neutrinos from each of the subpopulations separately may lead to more relevant constraints of the sources. The ANTARES telescope offers a great opportunity to test this assumption because of the more than 15 years of data that were collected. In this contribution, we present the sensitivity to different subpopulations of GRBs and describe the various efforts that will lead to the first catalogue of neutrino constraints from GRBs.

Studying Muon Bundles for Improved EHE Neutrino Identification in IceCube

T. Delmeulle[1]

[1]*Université Libre de Bruxelles, Bruxelles, 1050, Belgium*

The IceCube Neutrino Observatory is a cubic-kilometer Cherenkov detector located at the South Pole. It was originally built to detect astrophysical neutrinos, with a best sensitivity in the energy range of 1 TeV to 1 PeV. [1] Over the years, however, the IceCube Collaboration has expanded its research focus to cover even higher energies. Detecting extremely high-energy (EHE) neutrinos in such a large dataset, where background signals are strong, requires reliable, precise, and efficient analysis methods.

The main goal of this research project is to develop a new analysis method to improve the identification of EHE events in IceCube. The first step focuses on studying muon bundles, i.e. groups of atmospheric muons that pass through the detector. These events, which are the main part of the background, can imitate EHE neutrino signatures and are therefore important to understand in detail. By investigating properties such as bundle multiplicity, energy losses, lateral spread, and other characteristics, it should become possible to better distinguish these events from true EHE neutrino signals. The next stage of the project involves training a deep learning model and designing a new analysis specifically tailored to EHE neutrino detection. This presentation shows the first set of studied features of muon bundles, extracted from Corsika simulations in the energy range of 1 PeV to 10 EeV. These results are compared to the features of single muons obtained from NuGen simulations in the same energy range, with the aim of identifying discriminating variables for background rejection.

[1] Aartsen M *et al* 2017 *J. Instrum.* **12** P03012

Cosmic Ray Simulation for Background Rate Estimation in the ARA Detector using the FAERIE Framework

M. Vilarino

Université Libre de Bruxelles, Bruxelles, 1050, Belgique

Ultra-high-energy (UHE) neutrinos, with $E > 10^{17}$ eV, have not been detected so far but are key particles to unveiling the most energetic cosmic accelerators in the Universe. The Askaryan Radio Array (ARA) is a radio detector deployed at the South Pole that aims to detect the first UHE neutrinos via the Askaryan radiation they emit when cascading in the ice.

Cosmic rays are a major background since they also produce radio signals through geomagnetic and Askaryan effects when interacting in the ice or in the atmosphere. These signals must therefore be carefully modeled to distinguish neutrinos from cosmic rays.

We simulate cosmic-ray emission, as seen by in-ice observers, using the FAERIE Monte-Carlo framework. Based on these simulations we present cosmic-ray radio signatures and preliminary results towards a background estimate for the Askaryan Radio Array.

Laser spectroscopy of radioactive probes: study of the nuclear force and searches for new physics

Á. Koszorús[1,2]

[1]*KU Leuven, Instituut voor Kern- en Stralingsfysica, 3001 Leuven, Belgium*
[2] *Belgian Nuclear Research Centre, SCK CEN, Mol, Belgium*

The study of radioactive isotopes plays a crucial role in advancing our understanding of the nuclear force and its evolution in systems with extreme proton-to-neutron ratios. The quest to uncover how collective phenomena emerge from complex many-body interactions continues to drive innovation across multiple fields, including nuclear and atomic theory, as well as the development of methods for producing and measuring radioactive ions. Laser spectroscopy techniques, in particular, have proven to be powerful tools for determining fundamental nuclear properties such as spin, shape, and size [1], significantly enhancing our knowledge of nuclear interactions. Moreover, recent advances have demonstrated that laser spectroscopy of radioactive isotopes—and molecules containing radioactive isotopes—can serve as sensitive probes for exploring physics beyond the Standard Model [2]. This has opened a new frontier in radioactive ion beam laboratories, with a growing focus on high-precision measurements.

In this talk, I will present an overview of recent breakthroughs in nuclear structure research, along with emerging plans to search for new physics through precision laser spectroscopy.

[1] Koszorús Á. *et al. The European Physics Journal A* **60** 20 (2024)
[2] Garcia Ruiz R. *et al. Nature* **581** 396-400 (2020)

How Belgium is ensuring the CMS tracker data performance

Martin Delcourt[1], on behalf of the CMS Tracker group

[1]*Vrije Universiteit Brussel, Ixelles, 1050, Belgique*

The Compact Muon Solenoid silicon tracker is the biggest detector of its kind, with a total detector surface of 200 m² and over 75 million read-out channels [1]. Located at the center of the CMS experiment, its task is to reconstruct the position of charged particles emanating from high energy collisions provided by the Large Hadron Collider.

The outstanding performance of the accelerator is leading to unprecedented levels of both instantaneous and integrated luminosity, with last year alone representing about half of the complete proton-proton dataset recorded before hand. The amount of data recorded, paired with increasingly challenging data-taking conditions due to both pile-up and radiation damage puts significant pressure on the detector calibration and data-reconstruction.

The CMS Tracker Detector Performance Group is undertaking the challenging task of ensuring that the data recorded and the corresponding position estimates is of the highest quality, thus allowing the overall performance of high-level object reconstruction and maintaining the physics reach of the experiment.

This contribution aims at showcasing the central role that the Belgian community has in this respect, from silicon strip calibration and monitoring to detector alignment, through pixel local reconstruction developments and preparations for the high-luminosity LHC.

[1] CMS Collaboration, Operation and performance of the CMS tracker, arXiv:1402.0675v1 [physics.ins-det] 4 Feb 2014

The Belgian contribution to the CMS Silicon Strip Tracker Upgrade

A. Das[1], on behalf of the CMS Tracker group

[1]*Inter-University Institute For High Energies, ULB, Brussels, 1050, Belgium*

The CMS Silicon Strip Tracker, the largest detector of its kind, is undergoing a comprehensive upgrade as part of the High-Luminosity LHC (HL-LHC) program. This next-generation system, known as the Phase-2 Tracker, is being entirely re-designed to withstand the significantly increased radiation levels and data throughput expected at the HL-LHC. Belgium is playing a leading role in the Outer Tracker upgrade, particularly in module assembly and system integration, with a target of producing over 1,500 modules and assembling a complete detector endcap through its participating institutes.

In this presentation, I will outline the role of the Phase-2 Outer Tracker modules in enhancing the performance of the CMS detector, with a focus on Belgium's contributions to their assembly. Special attention will be given to the work carried out at the Inter-University Institute for High Energies (IIHE) by researchers from IIHE and its partner institutions. To date, Belgium has successfully assembled multiple fully operational modules, which have been delivered to the MuonE experiment at CERN for evaluation and integration studies. The setups and procedures are being developed since 2016. An exercice consisting of a pipeline production of seven modules, at a sustained rate of one new module started each day, was run to assess the readiness of the assembly site. The talk will emphasize the key technological developments and engineering solutions established over the past eight years to enable module design, assembly procedures, and testing protocols. The success and lessons learned from the pipeline exercise will be reported milestone in ramping up the production capacity. The presentation will conclude with an outlook on the upcoming production phases and Belgium's continued involvement in this critical component of the CMS Phase-2 upgrade.

Developement of a portable particle detector for imaging with cosmic ray muons

S. Ikram[1], E. Cortina Gil[1], P. Demin[1], A. Giammanco[1]

[1]*Centre for Cosmology, Particle Physics and Phenomenology (CP3), Université catholique de Louvain, Louvain-la-Neuve, Belgium*

Muography, also known as muon radiography, is an imaging method that relies on naturally occurring cosmic muons as a safe and freely available radiation source [1]. To achieve high-resolution muography of compact targets in scenarios with complex logistical constraints, we are developing a portable muon detector system utilizing glass Resistive Plate Chambers (RPCs). Although RPCs are well understood and widely used, our work focuses on developing a gas-tight variant specifically tailored for a broad range of muography applications, with key design goals including portability, robustness, autonomy, versatility, safety, and cost-effectiveness. In this talk, after reviewing the basics of muography and motivating the guiding principles of our project, we provide a snapshot of its status as documented in [2, 3, 4, 5, 6].

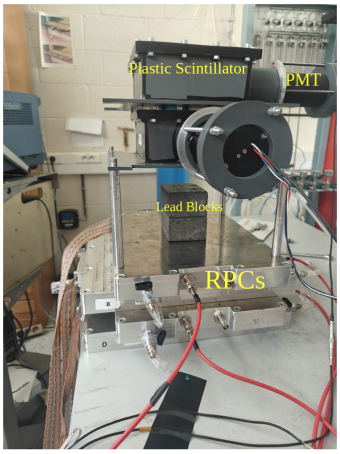

Figure 1: Experimental setup for muon absorption tomography with current prototype.

References

[1] Bonechi L, D'Alessandro R and Giammanco A 2020 *Rev. Phys.* **5** 100038

[2] Ikram S *et al* arXiv:2504.08146 [physics.ins-det]

[3] Kumar V *et al* 2024 *Nucl. Inst. Met. A* **1070** 170025

[4] Gamage R M I D *et al* 2022 *JINST* **17** C01051

[5] Basnet S *et al* 2020 *JINST* **15** C10032

[6] Wuyckens S *et al* 2018 *Phil. Trans. R. Soc. A* **377** 20180139

Dual Models revisited: A bootstrap perspective

Felipe Figueroa Vilar del Valle

Abstract for Belgian Physical Society's Young Speaker Contest

March 2025

Scattering amplitudes are fundamental quantities in quantum theory, determining the probability of specific outcomes in scattering experiments. While perturbative techniques often allow explicit computation of these amplitudes to a given precision, such methods fail in strongly coupled regimes or when the underlying microscopic theory remains unknown.

To address these challenges, the S-matrix bootstrap provides a powerful alternative, constraining—or even fully determining—scattering amplitudes based solely on fundamental physical principles: unitarity, ensuring total probability conservation in a quantum theory; causality, enforcing that events only influence their future light cone; and crossing symmetry, which relates amplitudes of different processes related by exchanging incoming and outgoing particles.

In this talk, I will present key results from my PhD research, where I developed a novel framework to apply the S-matrix bootstrap to a special class of amplitudes known as Dual Model Amplitudes. These describe weakly coupled scattering processes involving the exchange of infinitely many massive higher-spin states. They are central to tree-level string theory, with the Veneziano and Virasoro-Shapiro amplitudes as iconic examples, and also emerge in the large-N limit of gauge theories. Notably, in this limit, Quantum Chromodynamics (QCD) transforms into a theory of an infinite spectrum of weakly coupled mesons, baryons, and glueballs, yet the precise dual model describing large-N QCD remains unknown.

Despite their rich structure, Dual Model Amplitudes have only recently attracted significant interest within the S-matrix bootstrap community, largely because standard bootstrap techniques are ill-suited to their study. In this talk, I will outline recent progress in this direction, leveraging Regge theory and the complex angular momentum formalism to analyze these amplitudes. After a brief introduction to dual model amplitudes and the essentials of Regge theory, I will showcase two key results:

- A proof that the consistency of dual model amplitudes requires an infinite set of Regge trajectories.
- A novel numerical method to construct consistent dual amplitudes with customizable spectrum and high-energy behavior.

These findings open new avenues for exploring dual amplitudes within the bootstrap framework and bring us a step closer to uncovering the elusive dual model for large-N QCD.

Tau $g-2$ at future colliders

ZeQiang Wang[1]

[1]*Centre for Cosmology, Particle Physics and Phenomenology (CP3), Université catholique de Louvain, 1348 Louvain-la-Neuve, Belgium*

The anomalous magnetic moments of leptons are powerful windows into the Standard Model and potential new physics. Motivated by the persistent hint of beyond–Standard-Model effects in the muon $g-2$ [1, 2], the presentation give the brief introduction of the currents state of art in the research of tau g–2 as well as how well we could measure the tau g–2 at a future high-energy collider [3]. In particular, in the future muon collider, we look at Drell–Yan processes such as

$$\mu^+\mu^- \;\to\; \tau^+\tau^-\,(h),$$

and vector-boson-fusion channels like

$$\mu^+\mu^- \;\to\; \tau^+\tau^-\,\mu^+\mu^-, \quad \mu^+\mu^- \;\to\; \tau^+\tau^-\,\nu_\mu\bar{\nu}_\mu.$$

We also find that we can probe the sensitivity of tau anomalous magnetic moment down to $\mathcal{O}(10^{-5}-10^{-4})$, which is orders of magnitude better than today's limits. Moreover, at a high-luminosity FCC-ee using the equivalent-photon approximation (EPA), we can reach the same level of sensitivity, offering an additional promising avenue to nail down the tau $g-2$.

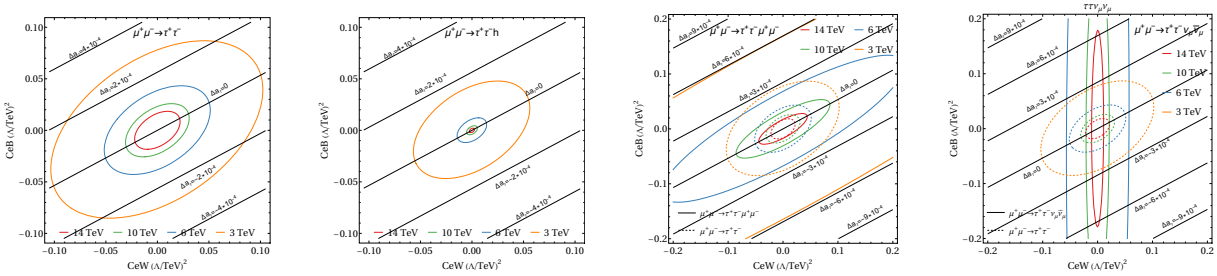

Figure 1 95% CL limits on the Wilson coefficients C_{eW} and C_{eB} from the Drell-Yan processes $\mu^+\mu^- \to \tau^+\tau^-(h)$, or vector-boson-fusion processes such as $\mu^+\mu^- \to \tau^+\tau^-\mu^+\mu^-$ and $\mu^+\mu^- \to \tau^+\tau^-\nu_\mu\bar{\nu}_\mu$ at muon colliders of different energies; the black isolines indicate the corresponding value of Δa_τ.

[1] T. Aoyama *et al.* 2020 *Phys. Rept.* **887** 1
[2] D. P. Aguillard *et al.* (Muon g-2) 2023 *Phys. Rev. Lett.* **131** 161802
[3] A. Hayrapetyan *et al.* (CMS) 2024 *Rept. Prog. Phys.* **87** 107801

Glueballs with two and three constituent gluons within the helicity formalism

C. Chevalier[1]

[1]*Nuclear and Subnuclear Physics, Mons, 7000, Belgium*

One of the earliest predictions of Quantum Chromodynamics (QCD) is the existence of color singlet pure-gauge states, known as glueballs. Nevertheless, achieveing consensus on their properties and identifying experimental evidence remain significant challenges. While two-gluon glueball states have been extensively studied both theoretically and experimentally, three-gluon glueballs have received comparatively less attention due to the technical complexities involved.

We use the helicity formalism to describe two- and three-gluon systems within constituent models. The formalism for two-body systems is presented and applied to the study of two-gluon glueballs. By incorporating symmetries, selection rules consistent with lattice QCD results are derived. Additionally, the inclusion of dynamical considerations enables the quantitative reproduction of the lattice QCD spectrum.

The helicity formalism is further extended to three-body systems to model three-gluon glueballs. The implementation of symmetries involves the use of two distinct definitions of three-body helicity states. By following a procedure analogous to the two-gluon case, the three-gluon glueball spectrum is calculated and compared with lattice QCD data. As a prospect, the odderon trajectory will be investigated using the aforementioned three-gluon glueball calculations within constituent approaches.

High precision automated metrology of the 2S modules for the CMS phase-II tracker upgrade

A. Chaliyath[1] on behalf of the CMS Tracker group

[1]*Inter-University Institute For High Energies, VUB, Brussels, 1050, Belgium*

The High-Luminosity upgrade of the Large Hadron Collider (HL-LHC) at CERN will provide the experiments with higher collision rates and overall increased luminosity, which will significantly enhance the precision of Standard Model measurements and the sensitivity to new physics processes. To handle the resulting demanding conditions like intense radiation and particle rates, the Compact Muon Solenoid (CMS) experiment is upgrading its detector and trigger systems with radiation-hard sensors, extended coverage, fast timing layers, and improved real-time data processing. This contribution focuses on the construction of the new CMS Tracker for the HL-LHC phase and specifically describes the metrology method used during the assembly of the 2S silicon sensor modules for the outer strip tracker part. A significant fraction of the latter modules is currently being assembled and qualified at the Inter-University Institute for High Energies in Brussels.

The precise alignment of the two sensors of the 2S module enables real-time reconstruction of high-momentum particle stubs (two-hit track segments) at 40 MHz while filtering out signals from low-momentum particles. Without this capability, CMS would be unable to identify the relevant collisions during the LHC's high-luminosity phase.

The method involves automated optical metrology using a three-axis motion system and high magnification imaging to precisely measure and evaluate the alignment of double-sided 2S modules. The technique leverages pattern recognition algorithms to accurately identify fiducial markers (circular patterns) present on both sides of a module, as well as corresponding reference markers (ultra-fine needle tips, 5 μm) attached to a fixed surface.

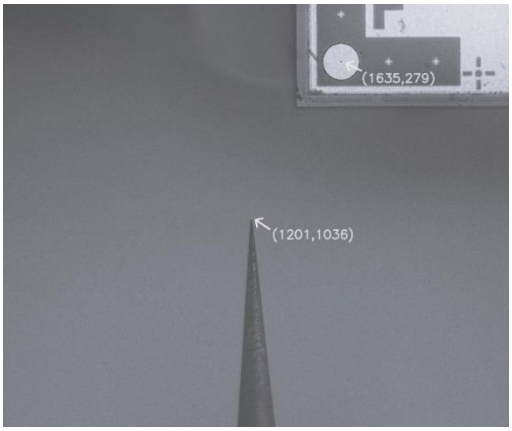

Figure 1: figure showing pixel coordinates of the needle tip and a module fiducial marker (center of the circle), both identified by the algorithm

Initially, fiducial positions on one side are automatically recorded to establish a baseline. The module is then flipped along its y-axis, and the procedure is repeated for the opposite side. By comparing positions of eight fiducial markers from both module surfaces to their reference positions, the system determines relative alignment between the two sides, specifically shifts (dx, dy) along x and y axes and rotation (α). Measurement uncertainties are systematically evaluated using noise distribution analysis and error propagation assessments. This method significantly improves precision and efficiency compared to previous techniques.

The ScIDEP Muon Radiography Project at the Egyptian Pyramid of Khafre

D. Geeraerts[1], S. Aly[2], M. Gamal[2], A. Hecht[5], R.T. Kouzes[6], A. Mahrouss[2], I. Mostafanezhad[4], A. Aftoiu[3], D. Stanca[3], M. Tytgat[1], C. Vancea[3], J. Valencia[5], Z. Wang[1]

[1]*Inter-University Institute for High Energies, Vrije Universiteit Brussel, Brussels, Belgium.*
[2]*Institute of Basic and Applied Science, Egypt-Japan University of Science and Technology, Alexandria, Egypt.*
[3]*Horia Hulubei National Institute for Physics and Nuclear Engineering, Magurele, Romania.*
[4]*Nalu Scientific, Honolulu, Hawaii, USA.*
[5]*Department of Nuclear Engineering, University of New Mexico, Albuquerque, New Mexico, USA.*
[6]*Pacific Northwest National Laboratory, Richland, Washington, USA.*

Despite centuries of study, the Egyptian pyramids at Giza still hold many mysteries, especially regarding their interior layouts and methods of construction. While the Great Pyramid at the Giza plateau near Cairo has a complex internal structure, the second largest one, the Pyramid of Khafre, appears to have a much simpler inner layout. This could have been done on purpose by the pyramid builders, or it could point to the fact that we have yet to discover the full interior structure of the latter monument.

Muon radiography (muography in short) [1] is an imaging technique that uses cosmic-ray muons to detect density variations and hence structures inside large objects, such as buildings, nuclear reactors, geological sites and more. High-energy muons generated in collisions of primary cosmic rays with the Earth's atmosphere, can penetrate large amounts of material and will undergo attenuation proportional to the density of the matter they cross. Hence, detecting cosmic muons passing through a target object and comparing to free-sky measurements allows to determine a density map of the internal structure of the object.

The ScIDEP (Scintillator Imaging Detector for the Egyptian Pyramids) Collaboration is developing muon telescopes based on scintillator technology to investigate the internal structure of the Pyramid of Khafre at Giza using cosmic-ray muons [2]. The collaboration aims to image the pyramid from multiple viewpoints, i.e. both from the inside with a detector placed in the King's burial chamber that is centrally located at the base of the pyramid, and from the outside of the pyramid. This should in principle allow a 3D reconstruction of potentially unknown internal structures. An overview of the project is presented, including details of the detector setups and the Geant4-based simulation framework, along with initial results of the tracking algorithm and image reconstruction.

References

[1] L. Cimmino, *Principles and perspectives of radiographic imaging with muons*, Journal of Imaging 7 (2021) 253.

[2] M. Gamal *et al.*, *The ScIDEP Muon Radiography Project at the Egyptian Pyramid of Khafre*, e-Print: 2503.21959 [physics.ins-det]

Differentiable Optimization of Muon Scattering Tomography Detector Designs

Z. Zaher[1], A. Giammanco[1], M. Lagrange[1]

[1]*Centre for Cosmology, Particle Physics and Phenomenology, Université catholique de Louvain, Ottignies-Louvain-la-Neuve, 1348, Belgium*

Muon tomography, or muography [1], is a non-invasive imaging technique that leverages the natural flux of cosmic-ray muons to explore the internal structure of large and otherwise inaccessible objects. These high-energy muons are generated in the upper atmosphere through interactions between primary cosmic rays and atmospheric nuclei, providing a continuous and passive source of radiation for probing dense volumes.

Muon scattering tomography (MST), in particular, utilizes the deflection of muon trajectories as they undergo multiple Coulomb scattering within a target. Since the degree of scattering correlates with the atomic number (Z) of the material, MST enables the identification and localization of high-Z substances such as uranium and lead—distinguishing them from low-Z backgrounds like plastic or aluminum. This makes MST especially valuable in applications requiring the detection of concealed high-density materials, including border security screening, nuclear waste monitoring, and archaeological site mapping [2]. Although MST does not rely on active radiation sources, one of its key challenges remains the relatively long data acquisition times required to achieve high-resolution imaging. Nevertheless, its passive nature and sensitivity to dense materials make it an attractive option for inspection systems where safety and material selectivity are critical.

In this poster, we present the current status of ongoing work with TomOpt [3], a fully differentiable simulation and optimization framework tailored to MST detector design. TomOpt provides a physics-informed, end-to-end differentiable model that spans muon generation, transport through the scanned volume, and image reconstruction. This enables the use of gradient-based optimization techniques to iteratively refine detector parameters for improved detection performance. Our ongoing study focuses on applying TomOpt to optimize MST systems for realistic border control scenarios, highlighting its potential to guide the automated design of future MST scanners.

[1] Bonechi L, D'Alessandro R and Giammanco A 2020 *Rev. Phys.* **5** 100038
[2] International Atomic Energy Agency 2022 *IAEA TECDOC*
[3] Strong, G. C. *et al* 2023 *Mach. Learn. Sci. Tech.* **5** 035002

Is visible light the way forward for cutting-edge nanolithography?

John T. Fourkas[1,2,3], N. C. Fisher[2], S. Yamaguchi[1,4], M. Cohen[1], N. Liaros[1,5], J. S. Petersen[1,6], A. S. Mullin[1] and D. E. Falvey[1]

[1]*Department of Chemistry & Biochemistry, University of Maryland, College Park, MD 20742, USA*
[2]*Institute for Physical Science & Technology, University of Maryland, College Park, MD 20742, USA*
[3]*Maryland Quantum Materials Center, University of Maryland, College Park, MD 20742, USA*
[4]*Sony Semiconductor Solutions Corporation, Research Division 3, 4-14-1 Asahi-cho Atsugi-shi, Kanagawa 243-0014, Japan*
[5]*Department of Physics, University of Patras, 26504 Rio Achaea, Greece*
[6]*imec, Kapeldreef 75, Leuven, BE 3001, Belgium*

Moore's Law had a remarkable run for decades, but the density of transistors on an integrated circuit not longer follows this trend. At the same time, generative artificial intelligence is fueling a renewed push to create denser and less power-hungry integrated circuits. A crucial part of the approach to tackling these problems is the use of ever shorter wavelengths of light in photolithography. Extreme ultraviolet (EUV) lithography has overcome a remarkable number of challenges in meeting fabrication nodes with ever finer pitches. Still, given its cost, EUV lithography will only ever be practical for high-volume applications. There are almost countless low-to-mid-volume applications, such as application-specific integrated circuits, that would benefit from the resolution that can be attained by EUV lithography. Additionally, new direct-write tools with higher performance are sorely needed in many areas of the semiconductor industry, such as advanced packaging and mask writing, and will also find many applications in the research laboratory. Electron-beam lithography offers one path towards addressing these needs, but this technique is slow and scale-up is limited by space-charge effects.

We and others have drawn inspiration from advances in optical microscopy to develop techniques for using near-infrared, visible, and/or near-UV light to perform photolithography far beyond the diffraction limit. Unlike EUV, light at these wavelengths is inexpensive to generate, does not need to travel in high vacuum, and is compatible with reflective optics. These multicolor lithography methods have reached the point that we believe that they will soon be attractive alternatives to current direct-write techniques that offer higher throughput and higher resolution at substantially lower cost. The first generation of multicolor techniques, 2-color lithography, employed one beam to activate a negative-tone photoresist and a second, phase-shaped beam to counteract cross-linking and improve resolution. Notable improvements in resolution have been achieved with 2-color techniques, but the fact that deactivation and crosslinking both proceed from the same state ultimately limits the resolution enhancement that can be achieved. In recent years we have pursued a class of 3-color lithographic techniques that involve preactivation to a metastable state that is chemically inactive using one color of light, deactivation to the ground state by a second color of light, and activation of remaining preactivated species using a third color of light. This scheme decouples the processes of deactivation and crosslinking, greatly improving the theoretical resolution attainable.

I will discuss the current state of 3-color lithography, including the search for materials with ideal photophysics, the development of optical techniques to characterize the complex photophysical pathways in these system, and our state-of-the-art resolution achieved.

Propagation of space-time optical beams in multimode fibers

Spencer W. Jolly, Julien Dechanxhe, and Pascal Kockaert
Service OPERA-Photonique, Université libre de Bruxelles (ULB), Brussels, Belgium

Ultrashort pulses and nonlinear optics in multimode fibers [1] and space-time shaping in free-space beams [2] have recently been experiencing a renaissance based on increasing fundamental understanding, more powerful simulation codes, and better availability of multi-mode fibers and pulse shaping apparatuses. Building on recent work [3], we have proposed studying the combination of these two burgeoning fields [4,5], namely complex space-time pulses coupled to and propagating within multimode fibers.

We show one example in Figure 1a, a space-time optical vortex that has a space-time singularity, with the phase circulating around it. Such special beams are thought to have transverse orbital angular momentum – in contrast to circularly polarized light or standard optical vortices that have longitudinal angular momentum. When such a beam couples to the spatial modes (Figure 1b) of a multimode fiber (by focusing onto the input facet of the fiber), interesting things happen. In fact, each spatial mode will have a different temporal envelope (Figure 1c), with the complexity and total number of modes excited increasing with the number of times the phase winds around the space-time singularity ("topological charge" l).

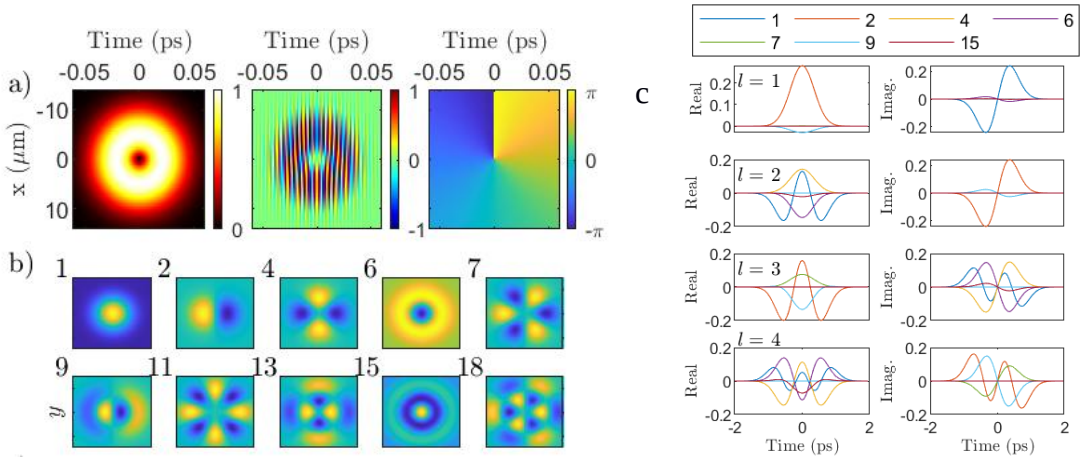

Figure 1: A space-time optical vortex (a), is a unique space-time laser beam. Interesting effects occur when such a pulse couples to the spatial modes (b) of a multi-mode fiber. Each mode will acquire a different temporal phase and envelope (c), different modes are different colors, with complexity increasing with the topological charge l.

We have studied the linear and nonlinear propagation of such pulses in multimode fibers [5], showing interesting fundamental effects. For example, we see the orbital angular momentum changing along propagation, and the creation of multimode soliton pulses. In conclusion, we expect that the combination of unique space-time beams and multimode fibers provides a rich platform for studying fundamentals of ultrafast and nonlinear guided-wave interactions, and a road towards enabled multimode devices or technologies.

[1] K. Krupa, et al., "Multimode nonlinear fiber optics, a spatiotemporal avenue," APL Photonics **4**, 110901 (2019).
[2] Y. Shen, et al., "Roadmap on spatiotemporal light fields," Journal of optics **25**, 093001 (2023).
[3] Q. Cao, et al., "Propagation of transverse photonic orbital angular momentum through few-mode fiber," Advanced Photonics **5**, 036002 (2023).
[4] J. Dechanxhe, S. W. Jolly, and P. Kockaert, "Accessing different higher-order modes with beam self-cleaning under simple realistic tuning of initial conditions," https://arxiv.org/abs/2502.04932
[5] S. W. Jolly, J. Dechanxhe, and P. Kockaert, "Propagation of space-time optical vortices in multimode fibers," https://arxiv.org/abs/2504.01643

Going to 2.1 µm for Space Quantum Key Distribution

S. Chaabani[1,2], A. Groulard[1], M. Zajnulina[2], J.-B. Lecourt[2], S. Habraken[1], and Y. Hernandez[2]

[1]*Centre Spatial de Liège, Université de Liège, Angleur, 4031, Belgium*
[2]*Multitel Innovation Centre, Mons, 7000, Belgium*

Quantum key distribution (QKD) is a secure communication method that relies on the laws of quantum mechanics. Despite the success of the Micius satellite in 2016 [1], and Europe's will to develop the IRIS^2 QKD satellite network [2], the operating wavelength is not yet determined.

We developed a comprehensive model to simulate a link between a ground station and a satellite at an arbitrary location on its orbit. This broadband model incorporates effects such as beam divergence, atmospheric absorption, solar noise, and more, to find the optimal wavelength regarding the signal-to-noise ratio (SNR) at the receiver telescope for given losses (Fig. 1(a)). For both uplink and downlink scenarios, we found the ∼2 to ∼2.5 µm atmospheric window to be by far the most promising, with the lowest atmospheric losses near 2.1 µm.

To validate our model, we present a tunable heralded single-photon source (Fig. 1(b)). An amplified mode-locked pulsed fibre laser (1064 nm, 32.45 MHz, 7.9 ps) is frequency doubled in a periodically poled lithium niobate (PPLN) crystal C1. Subsequently, the output of C1 is exploited for Type-0 spontaneous parametric down-conversion (SPDC) in the seven-grating PPLN crystal C2. When light is launched into the first and fifth gratings, idler photons are centred at 713 and 804 nm, with signal photons at 2.1 µm and 1570 nm respectively (Fig. 1(c)).

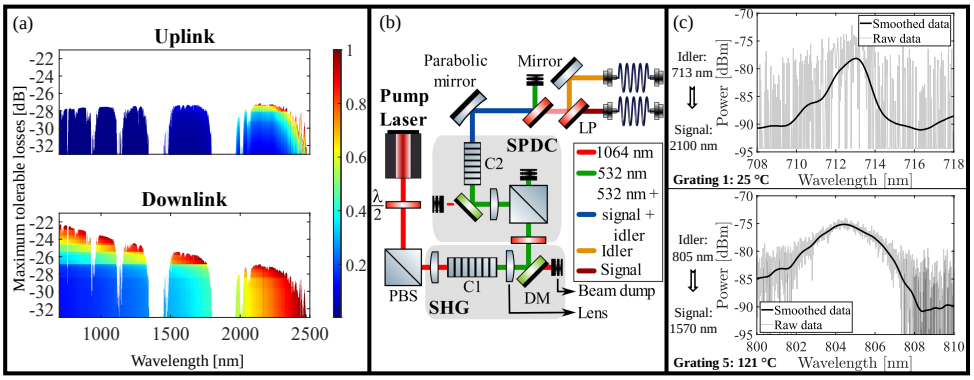

Figure 1: (a): Normalized SNR for each wavelength assuming any tolerable losses for a satellite at zenith at 500 km, (b): Schematic representation of the experimental set-up. PBS: polarisation beamsplitter, SHG: second-harmonic generation, C1: PPLN crystal, DM: dichroic mirror, C2: multi-grating PPLN crystal, SPDC: spontaneous parametric down-conversion, LP: longpass filter. (c): output spectra of idler photons in two different positions of the crystal C2.

As a next step, we will refine the model by incorporating a computation of the Quantum Bit Error Rate (QBER) to assess the interest of longer wavelengths in a quantum communication context. In parallel, our source will allow to study the propagation of the correlated photon pairs with signal photons from 1064 to 2300 nm in free-space. We will first characterise and optimise our source in the range accessible by the detectors available in the lab ($<$ 1700 nm) and expand to further wavelengths later.

[1] J. Yin *et al* 2017 *Science* **356**, 1140-1144.
[2] O. Johnson, A. Kürsteiner 2023 *International Telecommunications Society (ITS)*, 277981.

Construction and Characterization of a Ca Magneto-Optical Trap for Rydberg Physics

J.A.L. Grondin[*1,2], E. Marin-Bujedo[1], A. Bouillon[1], Thomas Schiltz[1], Thomas Corbo[1], and M. Génévriez[1]

[1]*Institute of Condensed Matter and Nanosciences, Université catholique de Louvain, BE-1348 Louvain-la-Neuve, Belgium*
[2]*Instituut voor Kern en Stralingsfysica, Katholieke Universiteit Leuven, BE-3001, Heverlee, Belgium*

Ultracold gases of divalent atoms excited to high Rydberg states are an exciting tool to explore subjects from fundamental Rydberg physics to quantum simulation [1]. While calcium has received little attention compared to other divalent species such as strontium or ytterbium, its unique features, including low autoionization rates or the smallest electronic affinity of all atomic species, are expected to open up new possibilities to control, manipulate and study Rydberg gases. We will report on the development of an experimental setup for ultracold calcium Rydberg atoms.

Our experimental setup features a custom-made oven combined to a 3D-printed permanent-magnet Zeeman slower, for first stage cooling of calcium atomic beam. Atoms exiting the Zeeman slower at velocities near 30 m/s are then trapped in a magneto-optical trap whose magnetic-field gradient is generated with a pair of home-built coils than can withstand large currents ($>$ 220 A). This approach allows us to prepare a trapped ensemble of Ca atoms at a temperature of a few mK. We then employ a resonant three-photon scheme to excite ground-state atoms to 4snp ^{1}P and 4snf ^{1}F Rydberg states. The measurement of the detailed properties of our calcium magneto-optical trap, together with the modelling and characterization of the Rydberg excitation, is currently under way and will be reported in our communication. With the present setup, we will be in a position to investigate the direct cooling of Rydberg atoms with an isolated core transition [2] or high lying doubly excited "planetary" states of the Ca atom.

[1] Dunning et al., *J. Phys. B.* **49**, 112003 (2016).
[2] Bouillon, A. and Marin-Bujedo, E. and Génévriez, M., *Phys. Rev. Lett.***132**, 193402 (2024).

High precision optical spectroscopy using trapped Sr ions

R. Van Duyse[1], P. Lassègues[1], and R. de Groote[1]

[1]*Instituut voor Kern- en Stralingsfysica, KU Leuven, B-3001 Leuven, Belgium*

Since the invention of ion and atom traps, they have been a widely used tool for high precision optical measurements. Despite extensive development, an ion trap for short-lived radioactive isotopes at online Radioactive Ion Beam (RIB) facilities has not yet been achieved. This motivated the creation of two ion trapping setups at KU Leuven within the group of Prof. dr. de Groote aimed at high precision optical spectroscopy of trapped ions. Currently, both ion traps, BICEPS (Bespoke Ion Cooling Experiment for Precision Spectroscopy) and STRIPE (Stopping and Trapping of Radioactive Isotopes for Precision Experiments).

One application of high precision optical spectroscopy is isotope shift (IS) spectroscopy. To first order, the IS of two transitions in an isotopic chain lie on a straight line, which can be fit using a King plot method. Probing the nonlinearities of this King plot allows probing higher-order nuclear effects (e.g. quartic nuclear charge moment), as well as searching for intermediate mass range dark-matter candidates.[1] To probe these nonlinearities, it is advantageous to have as many IS as possible. Currently, the results are limited by the number of stable isotopes of one element. Combining both ion traps, we will perform the first high precision IS spectroscopy on trapped radioactive ions (Sr^+), significantly improving the ability to probe higher-order nuclear effects using King plots and expanding high precision optical spectroscopy to radioactive ions.

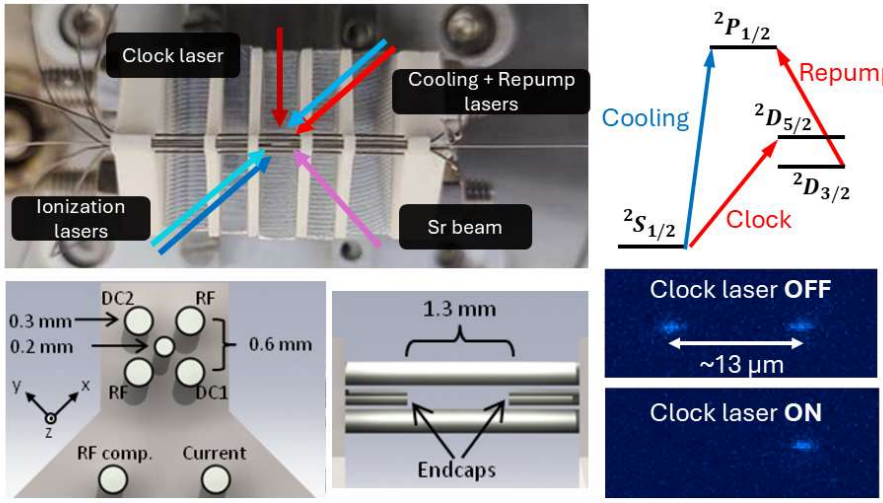

Figure 1: Schematic overview of the linear Paul trap with dimensions, laser configuration and level scheme.[2] (Bottom right) A two ion crystal, both ions fluorescing. Once the clock laser is turned on, the ions can be shelved to the $^2D_{5/2}$ state outside of the laser cooling cycle and therefore appear dark at times.

I will discuss our developments in building an ion trapping setup fit for high precision optical spectroscopy. Further, I will show our current and future efforts towards high precision IS spectroscopy of radioactive ions, the first of which was our recent success in directly probing the clock transition in Sr^+, shown in Figure 1 along with a schematic of the BICEPS setup.

[1] Door, M., et al., Phys. Rev. Lett., 134, 063002 (2025).

[2] Akerman, N. & Ozeri, R., Thesis for the Degree Doctor of Philosophy, Trapped Ions and Free Photons (2012).

High resolution spectrum of D_2O-CO_2 van der Waals complex around the 3OD vibrational excitation

A. Bogomolov[1], R. Glorieux[1], M. Herman[2], N. Moazzen-Ahmadi[3] and C. Lauzin[1]

[1]*Université catholique de Louvain, Louvain-la-Neuve, 1348, Belgium*
[2]*Université libre de Bruxelles, Brussels, B-1050, Belgium*
[3]*University of Calgary, Calgary, T2N 1N4, Canada*

Water and CO_2 are the most important greenhouse gases of our atmosphere. The solvation of CO_2 is a decisive process in the chemistry of clouds and oceans. A precise characterization of the interaction of these two molecules is thus of prime importance. In the present work, we recorded the rotationally resolved spectrum associated to the triple excitation of the OD stretch in the D_2O-CO_2 molecular complex. This represents a further step in our longstanding effort to characterize better the dynamics of interaction of CO_2 and H_2O notably through a systematic increase of the vibrational excitation [1–3]. All the measurements were performed using the FANTASIO experimental setup [4,5]. The complexes were formed from 8 cm long pulsed slit supersonic jet and probed using CRDS technique in the spectral range of the second OD overtone of D_2O. The recorded spectrum was vibrationally assigned to the $(v_1,v_2,v_3) \leftarrow (v_1',v_2',v_3') = (2,0,1) \leftarrow (0,0,0)$ and $(1,1,1) \leftarrow (0,0,0)$ where v_1,v_2,v_3 are the vibrational quantum numbers of the isolated D_2O molecule. In this talk, I will present the experimental spectrum and the improvements of the experimental set-up which allowed the recording of this spectral signature. I am going to present our progress in the analysis of this spectrum using group theory and effective Hamiltonian.

[1] C. Lauzin, A.C. Imbreckx, T. Foldes, T. Vanfleteren, N. Moazzen-Ahmadi, and M. Herman, Mol. Phys. 118, e1706776 (2020).
[2] A.S. Bogomolov, A. Roucou, R. Bejjani, M. Herman, N. Moazzen-Ahmadi, and C. Lauzin, Chem. Phys. Lett. 774, 138606 (2021).
[3] T. Gartner, C. Lauzin, A.R.W. McKellar, and N. Moazzen-Ahmadi, J. Phys. Chem. A 127, 3668 (2023).
[4] M. Herman, K. Didriche, D. Hurtmans, B. Kizil, P. Macko, A. Rizopoulos, and P.V. Poucke, Mol. Phys. 105, 815 (2007).
[5] A.S. Bogomolov, R. Glorieux, M. Herman, T. Corbo, S. Collignon, B.M. Hays, D. Lederer, N. Moazzen-Ahmadi, A. Libert, B. Tomasetti, J. Fréreux, and C. Lauzin, Mol.Phys., doi: 10.1080/00268976.2024.2413417.

Impact of Higher Order Effects in the Far-field for Dipole-Forbidden Transitions near Plasmonic Structures

M. Hantro[1], B. Maes[2], G. Rosolen[2] and C. Van Dyck[1]

[1]1*Theoretical Chemical Physics Group, Research Institute for Materials Science and Engineering, University of Mons, 20 Place du Parc, 7000 Mons, Belgium*
[2]*Micro- and Nanophotonic Materials Group, Research Institute for Materials Science and Engineering, University of Mons, 20 Place du Parc, 7000 Mons, Belgium*

Understanding spontaneous emission at the nanoscale is key to advancing photonic technologies. Traditionally, emission is modeled using a point-dipole approximation (PDA), which truncates the multipolar expansion at the dipolar term. However, near sharp metallic structures supporting strong field gradients, PDA fails, and higher-order contributions become critical [1]. In earlier work, we adopted an eigenpermittivity mode expansion framework [2] that fully accounted for all multipolar contributions and interferences. While this method provided valuable insight into the modal decomposition of the enhancement, it featured a complex implementation and required significant expertise.

Here, we introduce MIRAGE, a black-box, user-friendly tool that predicts optical properties of molecular emitters near nanostructures while still capturing the full multipolar contribution. Additionally, beyond simply addressing the near-field modifications, MIRAGE grants us access to far-field radiative enhancements, and absorption pathways, wich is a key for applications where the observable brightness of the emitter is paramount.

We apply MIRAGE to dipole-allowed and dipole-forbidden molecules near an STM-tip. A notable result shows that a dipole-forbidden dimer achieves a radiative enhancement nearly 6000× that of a dipole emitter in vacuum [3], confirming that dark states can become bright through higher-order coupling. This result, shown below, illustrates how MIRAGE unlocks design strategies for plasmonic and quantum optical devices.

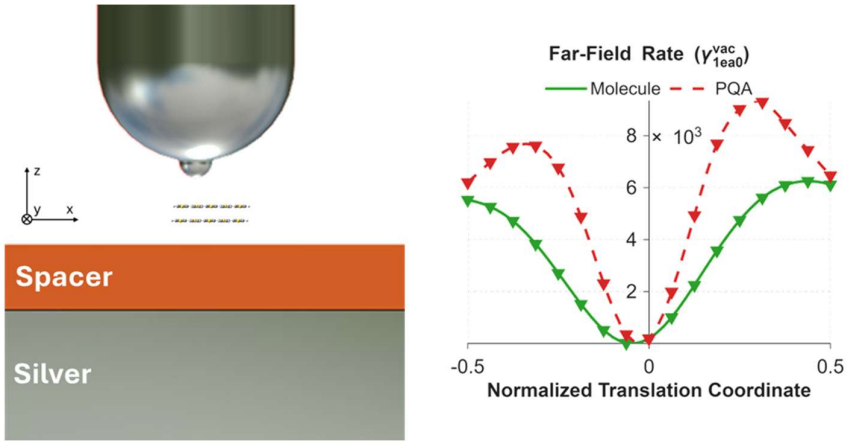

Figure 1: Left: Molecular dimer under STM tip. Right: Radiative rate vs. tip position. MIRAGE (green) shows strong molecular emission of the dipole-forbidden dimer.

[1] Rivera N, Kaminer I, Zhen B, Joannopoulos J D and Soljačić M 2016 *Science* **353** 263–269
[2] Hantro M, Maes B, Rosolen G and Van Dyck C 2025 *J. Chem. Phys.* **162** 035101
[3] Hantro M, Maes B, Rosolen G and Van Dyck C 2025 To be submitted

Finite-Difference Time-Domain Analysis of Stimulated Emission in NZI Materials

A. Debacq[1], E. Semenova[2], A. V. Laurynenka[2], O. Deparis[1] and M. Lobet[1]

[1]*University of Namur, Dept of Physics, Namur Institute of Structured Materials, Rue de Bruxelles 61, 5000 Namur, Belgium*
[2]*DTU Electro-Department of Electrical and Photonics Engineering, Technical University of Denmark, DK-2800 Kongens Lyngby, Denmark*

Near-zero index (NZI) media, characterized by a vanishing effective refractive index, exhibit unconventional electromagnetic properties such as uniform phase distribution and effectively infinite wavelengths. These features enable extreme light manipulation, with applications spanning nonlinear optics, sensing, and quantum technologies [1]. NZI media are typically classified into three categories: Epsilon-Near-Zero (ENZ), Mu-Near-Zero (MNZ), and Epsilon-and-Mu-Near-Zero (EMNZ), depending on whether the permittivity, permeability, or both approach zero. Despite sharing a near-zero phase index, these categories differ significantly in impedance and group index—key factors influencing light–matter interactions [1,2].

Recent studies have shown that the Einstein coefficient of stimulated emission is enhanced in 3D ENZ and suppressed in 3D MNZ media [2]. However, since the photonic density of states vanishes in both cases, stimulated emission remains intrinsically limited. Building on these observations, we investigate how NZI media affect laser dynamics using numerical modeling.

We develop a Finite-Difference Time-Domain (FDTD) [3] simulation framework to model laser emission in NZI media. Our approach captures the interaction between an electric field and quantum emitters embedded in a dispersive environment, allowing us to investigate how NZI dispersion affects stimulated emission. The implementation includes a four-level population dynamics model for carrier pumping and relaxation, the quantum polarization equation of motion to describe light–matter coupling, and a frequency-dependent material response incorporated via the Auxiliary Differential Equation (ADE) method [3]. Accurately accounting for dispersion is essential to reflect the intrinsic electromagnetic behavior of NZI media and its impact on amplification processes.

Altogether, our work offers tools to understand laser dynamics in NZI media, paving the way for the design of NZI-based lasers.

[1] Liberal I *et al* 2017 *Nat. Photonics* **11** 149–158
[2] Lobet M *et al* 2020 *ACS Photonics* **7** 1965–1970
[3] Taflove A *et al* 2005 Computational Electrodynamics: The Finite-Difference Time-Domain Method 3rd ed. (Boston: Artech House)

Nature-Inspired Strategies for Infrared Control and Thermal Insulation

K. Delmote[1], A. Marchand[2], O. Deparis[1], and **S. R. Mouchet**[1,2,3]

[1]*Department of Physics and Namur Institute of Structured Matter (NISM), University of Namur, Rue de Bruxelles 61, 5000 Namur, Belgium*
[2]*Micro- and Nanophotonic Materials Group, Research Institute for Materials Science and Engineering, University of Mons, Place du Parc, 20, Mons 700, Belgium*
[3]*Department of Physics and Astronomy, University of Exeter, Stocker Road, Exeter EX4 4QL, UK*

The ability to regulate thermal radiation is essential for the survival of many species, particularly those living in extreme environments or lacking internal thermoregulation. Nature offers a wide array of elegant solutions to infrared management, with evolution shaping organisms over millions of years to develop highly specialised structures that optimise the absorption, emission, or reflection of thermal radiation. From the nanostructured scales of butterfly wings to the fur of Arctic foxes and polar bears, biological systems demonstrate remarkable capabilities in modulating heat transfer [1].

This contribution investigates several case studies where thermal regulation has been refined to a high degree of efficiency. Particular attention is given to cold-blooded insects, which rely on precise control of infrared interactions due to their dependency on environmental temperatures, and to warm-blooded animals such as dromedaries that thrive in desert climates. The micro- and nanostructures found in these species often serve multiple functions, combining camouflage, signalling, and thermal control into a single morphological design [1].

Recent advances in the field of bioinspired materials science have allowed the mimicry of these natural solutions, translating biological strategies into synthetic systems that manage infrared radiation with enhanced precision and energy efficiency. By examining the photonic structures and thermoregulatory adaptations in biological systems [2], we can derive design principles for the development of multifunctional materials that exhibit both effective insulation and selective infrared absorption.

This presentation explores the interdisciplinary potential of such bioinspired approaches, bridging biology, physics, and materials engineering. Applications span a range of sectors where the demand for passive thermal control is ever increasing. Ultimately, the study underscores how nature's innovations, when carefully studied and adapted, can lead to sustainable and high-performance solutions for modern engineering challenges.

[1] Mouchet, SR 2025 *J. Roy. Soc. Interface* **22(223)** 20240284.
[2] Mouchet, SR, Deparis, O 2021 *Natural Photonics and Bioinspiration*, Artech House: Boston, MA, USA; London, UK.

Spectroscopy of methanol in the near-infrared at the 10^{-13} level

A. Altman[1], F.M.J. Cozijn[2], A. Bogomolov[1], A. Libert[1], W. Ubachs[2] and C. Lauzin[1]

[1]*Institute of Condensed Matter and Nanosciences, Université catholique de Louvain, Louvain-la-Neuve, 1348, Belgium*
[2]*Department of Physics and Astronomy, LaserLaB, Vrije Universiteit Amsterdam, De Boelelaan 1081, 1081 HV Amsterdam, The Netherlands*

This presentation showcases the application of Noise-Immune Cavity-Enhanced Optical Heterodyne Molecular Spectroscopy (NICE-OHMS) for precision spectroscopy of methanol. This approach, invented almost thirty years ago [1] and further developed as an optical precision tool [2], allows the measurement as Lamb-dips of extremely weak transitions [3], combining both sensitivity and accuracy.

We report sub-kHz precision measurements of three vibrational line pairs, corresponding to the $3_{-1}E$ - 2_0E combination difference in the vibrationless ground state. This allows the determination of this 12.2 GHz radio line frequency, highly sensitive to potential variations in the proton-electron mass ratios [4, 5], at kHz precision. Furthermore, having moved our NICE-OHMS setup, I will end this talk by presenting a comparison of results obtained in Amsterdam and Louvain-la-Neuve on these very accurate frequency determination of methanol resonances.

[1] J. Ye, L-S. Ma, and J.L. Hall, Opt. Lett. **21**, 1000–1002 (1996).

[2] A. Foltynowicz, F.M. Schmidt, W. Ma, and O. Axner, Appl. Phys. B **92**, 313–326 (2008).

[3] F. M. J. Cozijn, M. L. Diouf, and W. Ubachs, Phys. Rev. Lett. **131**, 073001 (2023).

[4] P. Jansen, L.-H. Xu, I. Kleiner, W. Ubachs, and H. L. Bethlem, Phys. Rev. Lett. **106**, 100801 (2011).

[5] S. A. Levshakov, M. G. Kozlov, and D. Reimers, Astroph. J. **738**, 26, 26 (2011).

Weak values as stereographic projections

Lorena Ballesteros Ferraz[1,3], Dominique L. Lambert[2], and **Yves Caudano**[1]

[1]*Department of Physics, Namur Institute for Complex Systems (naXys) and Namur Institute for Structured Matter (NISM), University of Namur, Rue de Bruxelles 61, 5000 Namur, Belgium*
[2]*Department of Sciences, Philosophies, and Societies, Philosophical Space of Namur Institute (ESPHIN), University of Namur, Rue de Bruxelles 61, 5000 Namur, Belgium*
[3]*Present address: Laboratoire de Physique Théorique et Modélisation, CNRS Unité 8089, CY Cergy Paris Université, 95302 Cergy-Pontoise cedex, France*

In a typical pre- and post-selected weak measurement configuration, the experimental deflection of the measuring device, also called the pointer, depends on the real part or on the imaginary part of a complex quantity known as the weak value. However, as a complex number, a weak value also possesses a polar representation in terms of its modulus and argument.

We show that arbitrary weak values correspond to a stereographic projection of the post-selected state, involving an appropriate Möbius transformation of the complex plane related to the geometry of a non-normal operator [1]. This construction provides a complete interpretation of the weak value in geometric terms, enabling a joint visualization the weak value's modulus, argument, and associated quantum states. In a weak measurement with a Gaussian meter, this stereographic projection provides the position of the meter coherent state in the quantum phase space after post-selection, enabling the visualization of the meter shifts as well, in terms of the real and imaginary part of the weak value.

Our results are based on an expression of the weak value that we developed to study weak measurements in open quantum systems [2], but also in terms of non-normal operators [1]. Our geometric construction is built from an effective Bloch sphere that involves three quantum states (the pre-selected state, the post-selected state, and an effective state linked to the observable [3]). We showed previously that the argument of weak values in N-level systems corresponds to a geometric phase [3, 4] related to the symplectic area of a geodesic triangle in the larger-dimensional quantum state manifold. However, our construction shows the argument both as an angle in the complex plane and as a solid angle on the effective Bloch sphere, thereby reducing the description of an arbitrary weak value within the space of a two-level system.

[1] L. Ballesteros Ferraz, R. Muolo, Y. Caudano, and T. Carletti 2023 *J. Phys. A: Math. Theor.* **56** 475303.
[2] L. Ballesteros Ferraz, J. Martin, and Y. Caudano 2024 *Quantum Sci. Technol.* **9** 035029
[3] Lorena Ballesteros Ferraz, Dominique L. Lambert, and Yves Caudano 2022 *Quantum Sci. Technol.* **7** 045028
[4] L. Ballesteros Ferraz, D. L. Lambert, and Y. Caudano 2022, arXiv:2211.05692 [quant-ph]

NOON states creation with ultracold atoms via geodesic counterdiabatic driving

S. Dengis,[1] S. Wimberger,[2,3] and P. Schlagheck[1]

[1] CESAM research unit, University of Liège, B-4000 Liège, Belgium
[2] Dipartimento di Scienze Matematiche, Fisiche e Informatiche, Università di Parma, Parco Area delle Scienze 7/A, 43124 Parma, Italy
[3] INFN, Sezione di Milano Bicocca, Gruppo Collegato di Parma, Parco Area delle Scienze 7/A, 43124 Parma, Italy

A quantum control protocol is proposed for the creation of NOON states with N ultracold bosonic atoms on two modes, corresponding to the coherent superposition $|N,0\rangle + |0,N\rangle$. This state can be prepared by using a third mode where all bosons are initially placed and which is symmetrically coupled to the two other modes. Tuning the energy of this third mode across the energy level of the other modes allows the adiabatic creation of the NOON state. While this process normally takes too much time to be of practical usefulness, due to the smallness of the involved spectral gap, it can be drastically boosted through counterdiabatic driving which allows for efficient gap engineering. We demonstrate that this process can be implemented in terms of static parameter adaptations that are experimentally feasible with ultracold quantum gases. Gain factors in the required protocol speed are obtained that increase exponentially with the number of involved atoms and thus counterbalance the exponentially slow collective tunneling process underlying this adiabatic transition. Besides optimizing the protocol speed, our NOON state preparation scheme achieves excellent fidelities that are competitive for practical applications.

Weak measurements and Goos-Hänchen effects in the case of uniaxial anisotropic media

J. Bouchat[1], Y.Caudano[1]

[1]Physics Department, Namur Institute for Complex Systems (naXys) and Namur Institute for Structured Matter (NISM), University of Namur, Rue de Bruxelles 61, 5000 Namur, Belgium

Since a laser beam has a finite transverse extent and can be described as a superposition of plane waves, deviations from the laws of geometrical optics are expected when considering an interface between two media. The most well-known manifestations of these deviations are the spatial and angular shifts of the beam's central axis, known as the Goos-Hänchen and Imbert-Fedorov effects. These phenomena correspond respectively to displacements within the plane of incidence and perpendicular to it [1].

More specifically, angular and spatial Goos-Hänchen shifts occur under partial and total reflection and are directly related to the analysis of the Fresnel coefficients evaluated for the central plane wave within the paraxial approximation. While the Goos-Hänchen effect has been thoroughly studied with isotropic media, we considered an analytical treatment in the case of uniaxial anisotropic media, where the electric field splits into two plane waves; one experiencing an isotropic refractive index and the other an anisotropic refractive index linked to the angle between the optical axis of the crystal and the main direction of propagation [2]. In this work, we considered the case of a paraxial Gaussian beam undergoing a total internal reflection from an isotropic medium to a uniaxial anisotropic medium, related to the ordinary and/or extraordinary beam to study the Goos-Hänchen spatial shift.

Although these deviations have been studied theoretically for isotropic media a long time ago, the measurements of these phenomena are challenging to realize by standard consideration. In fact, these shifts are typically on the order of the beam's wavelength, making them difficult to detect by the use of classical digital imaging. To overcome this limitation, we employ the weak measurement formalism (derived from quantum mechanics) to amplify the shifts at the expense of the reflected or transmitted beam's intensity by considering a large weak value [3]. In our case of interest, the weak value amplification considers a pre-selected state and a post-selected state of polarization that must be taken nearly orthogonal to each other.

Moreover, weak measurements rely on precise control over the beam's polarization state, requiring accurate pre- and post-selection using waveplates and birefringent polarizers. Given that a paraxial beam consists of plane waves with slightly varying incidence angles, the precise polarization structure of the beam has to be taken into account. To address this, we investigate the study of a thin uniaxial anisotropic film between isotropic media, and a thin isotropic film between uniaxial anisotropic media in order to modelize the waveplates as well as the birefringent polarizers behaviour as it could influence the beam propagation in the weak measurement experimental set-up.

[1] Bliokh, K. Y., & Aiello, A. (2013). Goos–Hänchen and Imbert–Fedorov beam shifts: an overview. *Journal of Optics*, *15*(1), 014001.
[2] Lekner, J. (1991). Reflection and refraction by uniaxial crystals. *Journal of Physics: Condensed Matter*, *3*(32), 6121.
[3] Prajapati, C., & Viswanathan, N. K. (2017). Simultaneous weak measurement of angular and spatial Goos–Hänchen and Imbert-Fedorov shifts. *Journal of Optics*, *19*(10), 105611.

Electron transfer between ultra-long range Rydberg molecules and heavy-Rydberg molecules

A. Bouillon[1] and M. Génévriez[1]

[1]*UCLouvain, Institute of Condensed Matter and Nanosciences, BE-1348, Belgium*

The scattering of a Rydberg atom's electron off a neutral perturbing atom gives rise to exotic molecules known as ultra-long-range Rydberg molecules (ULRRM). The typical bound length of such molecules reaches several hundred atomic units, which corresponds to the length of its constituting Rydberg atom. In the case of Ca, the potential energy curves (PECs) of the ULRRMs corresponding to principal quantum numbers n of the Rydberg electron up to 25, cross the Coulomb potential of the ion-pair molecular states Ca^+ $(4s)$ + Ca^- $(4s^2 4p_j)$. Such states are also called "heavy-Rydberg" (HR) states because their vibrational energies and wavefunctions can be described analogously to the energies and wavefunctions of the electron of a Rydberg atom, but in a molecular case, as the electron has been replaced with an anion. The rather wide range of ULRRMs involved in the crossing with the HR states is a result of the small and positive Ca electron affinity.

Starting with a cold calcium gas, HR states cannot be efficiently excited from the initial ground-state Ca-Ca pair because of the too small overlap between their respective vibrational wavefunctions. The ULRRMs can, on the other hand, be efficiently excited [1]. We propose that the crossing between the ULRRMs and HR states PECs, and the associated state mixing, gives the opportunity to study the photoassociation of HR molecules via the excitation of the Ca-Ca pair to an ULRRM intermediate state. Non-adiabatic couplings between these states and the HR ones could indeed lead to an electron transfer from the former to the latter.

To investigate this hypothesis we carry out theoretical calculations of the electronic and vibrational structure and dynamics in the region of the crossings. We start by describing the PECs of the ULRRMs, using the Fermi-Omont contact potential model. Some effort is put into calculating them with a more accurate description of these molecules, relying on multi-channel quantum defect theory and with the aid of generalized local-frame transformations (GLFT) [2]. We then re-use the GLFT method to calculate the non-adiabatic interaction between the ULRRMs and the HR ion-pair molecules. The dynamics is finally studied by means of a non-adiabatic model relying on exterior complex scaling to treat the dissociative channels. Calculation of the transition dipole moments and molecular-state lifetimes will help us to determine if an efficient excitation scheme can actually be found.

[1] Eiles M. T. and Greene C. H. 2015 *Phys. Rev. Lett.* **115** 193201

[2] Giannakeas P. *et al* 2020 *Phys. Rev. A* **102** 033315

Two-photon molecular emitters enhanced with nanoantennas

S. Smeets[1], B. Maes[1], G. Rosolen[1], and C. Van Dyck[2]

[1]*Micro- and Nanophotonic Materials Group, Research Institute for Materials Science and Engineering, University of Mons, 20 Place du Parc, Mons B-7000, Belgium.*
[2]*Theoretical Chemical Physics Group, Research Institute for Materials Science and Engineering, University of Mons, 20 Place du Parc, Mons B-7000, Belgium.*

In the two-photon spontaneous emission process (TPSE), two entangled photons are emitted quasi-simultaneously by a quantum emitter (e.g., an atom, molecule, or quantum dot). Although TPSE is the reverse process of two-photon absorption (TPA), the design rules for efficient molecules differ significantly. Indeed, in TPSE, the virtual intermediate states $|m\rangle$ that connect the excited state $|e\rangle$ and the ground state $|g\rangle$ lie above the excited state, whereas in TPA, they can lie below it [Fig. 1]. As a result, TPSE is inversely proportional to the square of the energy gaps between the excited state and the virtual intermediate states, while TPA is inversely proportional to the square of the detuning factor [Fig. 1a, b]. Both processes scale with the fourth power of the first-order transition moments.

We design efficient two-photon emitters by employing TD-DFT to compute vacuum TPSE rates through the computation of transition moments. We consider various molecules, such as diphenylhexatriene [Fig. 1c]. In parallel, we design a photonic structure to enhance two-photon radiative emission [Fig. 1d], with the enhancement factor calculated using our framework based on the numerical calculation of one-photon Purcell factors [2].

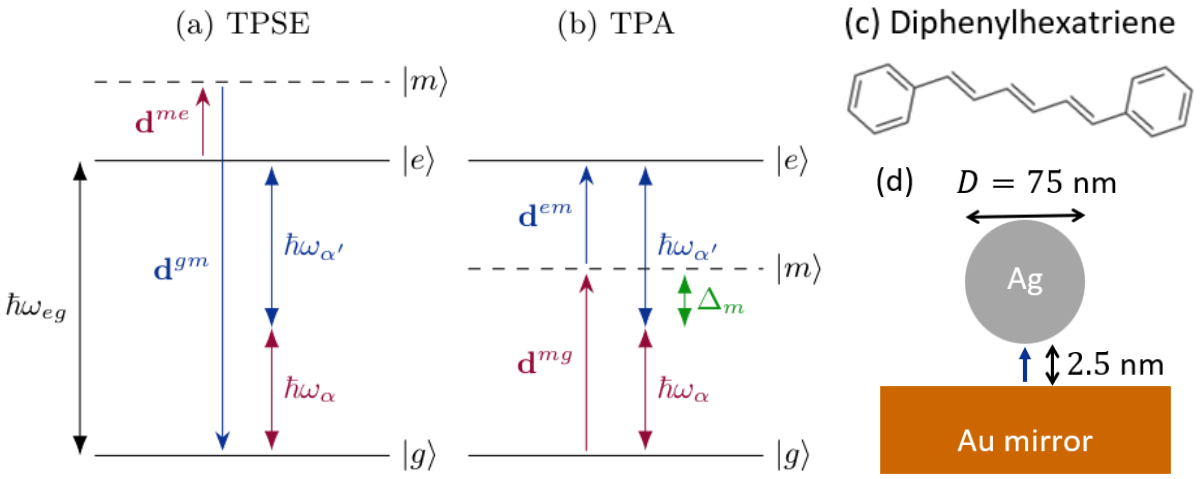

Figure 1: (a, b) Energy representation of second-order transitions. The emitter carries-out two transitions described by the first-order transition moments $\boldsymbol{d}^{me}$ and $\boldsymbol{d}^{gm}$, each emitting or absorbing a photon in the modes α or α'. The two photons have complementary frequencies: $\omega_\alpha + \omega_{\alpha'} = \omega_{eg}$. The detuning factor Δ_m corresponds to the energy mismatch between the energy of the absorbed photon and the energy gap between the ground and intermediate states. **(d)** Nanoparticle on mirror system to enhance radiative emission from an emitter (blue arrow).

Acknowledgements: we acknowledge support from Action de Recherche Concertée (project ARC-21/25 UMONS2).

[1] M. Pawlicki et al. *Angewandte Chemie International Edition* 48, 3244 (2009)
[2] S. Smeets et al. *Physical Review A* 107, 063516 (2023)

Study of the optical coupling between luminescent quantum dots and gold nanorods

H. Stassart[1], T. Noblet[1], L. Dreesen[1].

[1]GRASP-Biophotonics, CESAM, University of Liège, Liège, 4000, Belgium.

The accuracy of FRET-based biosensors is conditioned by (i) the efficiency of the optical coupling between the selected donor and acceptor fluorophores and (ii) the specificity of the molecular recognition between the fluorophores and the target molecule. To gain in sensitivity and selectivity, here we propose to study the optoelectronic interactions between luminescent quantum dots (as donor and acceptor fluorophores) and anisotropic gold nanoparticles (as plasmonic enhancers), benefiting from the exciton-plasmon coupling between the two kinds of nanostructures and the subsequent enhancement of the FRET process occurring between QDs (i.e. QD-QD FRET). This requires three steps. First, quantization of the QD-QD FRET efficiency according to the chemical functionalization of QDs and the QD-QD distance. Second, synthesis and chemical functionalization of gold nanorods (AuNRs). Third, study of the QD-QD FRET efficiency at QD-QD-AuNR interfaces.

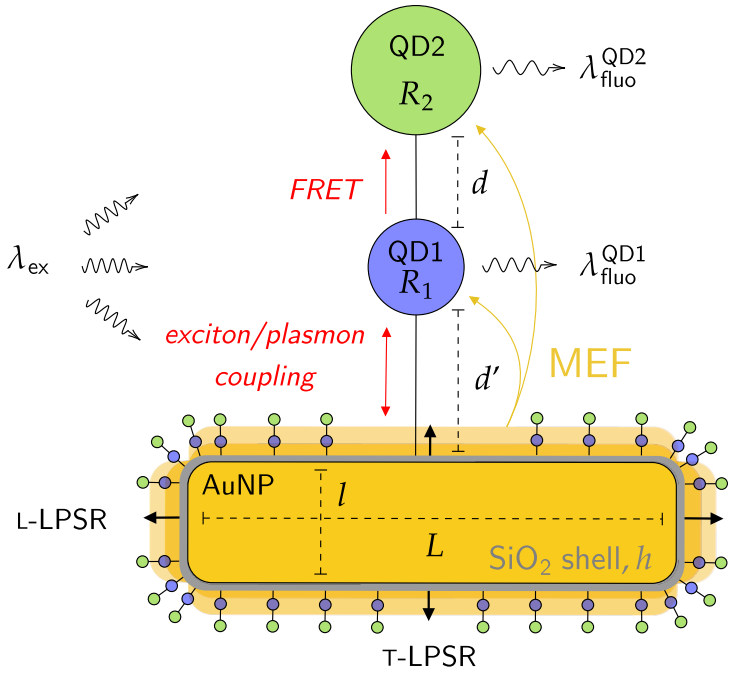

Figure 1 : Schematic representation of the final complex, illustrating the different physical processes under investigation, including exciton/plasmon coupling, Förster resonance energy transfer (FRET), and metal-enhanced fluorescence (MEF).

Achieving Optical Transparency: Simulations of Light Scattering in Biological Tissues

L. Cavenaile, C. Rousseau, G. Rosolen and B. Maes

Micro- and Nanophotonic Materials Group, Research Institute for Materials Science and Engineering, University of Mons, 20 Place du Parc, B-7000 Mons, Belgium

Enhancing optical transparency in biological tissues is a key challenge in the context of medical applications such as photothermal therapy, where deep light penetration is crucial for treatment efficiency. This work explores how refractive index matching can reduce scattering and increase light transmission through tissue-like media. Our approach was motivated by recent experimental results [1] showing that adding a visible dye (tartrazine, found in Doritos) to mouse skin reduces optical scattering by matching the refractive index of the interstitial fluid to that of cellular structures, enabling deeper optical access.

To reproduce the strong scattering behavior of human tissues, we use layers of 1 µm large SiO_2 spherical nanoparticles embedded in a homogeneous water background medium. To reproduce the complexity of tissue morphology while keeping the model computationally tractable, we randomly distribute 20 SiO_2 nanoparticles within a square periodic domain of 8 µm side length. The optical response is calculated at normal incidence using the T-matrix formalism, as implemented in the open-source Python package Treams [2]. S-matrices are computed for single layers of 8µm and stacked to mimic increasing tissue thickness. We evaluate the zero-order transmission while gradually increasing the refractive index of the host medium to simulate dopant-induced matching.

Our results, illustrated in Figure 1, demonstrate a clear increase in both specular and total transmission when comparing the undoped case (Figure 1a) with the doped configuration (Figure 1b). This supports the idea that biocompatible dopants can be used to tune the optical properties of tissues in order to enhance light delivery in therapeutic contexts.

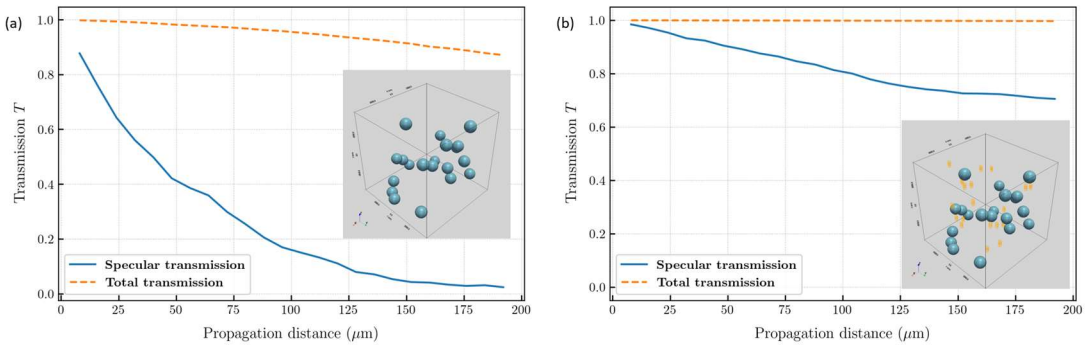

Figure 1: Specular and total transmission as a function of propagation distance through a simulated biological medium. (a) Undoped configuration: SiO_2 nanoparticles embedded in water. (b) Same configuration with the addition of dopant molecules (represented by orange helices in the inset), mimicking a refractive index matching strategy. Insets show the corresponding particle distributions in a unit cell.

Acknowledgment : Project ARC-23/27 UMONS3

[1] Z. Ou, *et al*. Achieving optical transparency in live animals with absorbing molecules. *Science* **385,** 2024
[2] D. Beutel *et al*, treams – A T-matrix scattering code for nanophotonic computations. *Computer Physics Communications,* **297,** 2023

Rest frequency determination of the 12.2 GHz methanol maser line with sub-kHz accuracy

S. Collignon[1], B. Hays[2], D. Lederer[3] and C. Lauzin[1]

[1]*Institute of Condensed Matter and Nanosciences, Université catholique de Louvain, Louvain-la-Neuve, B-1348, Belgium*
[2]*Physique des Lasers Atomes et Molécules, Université de Lille, CNRS, UMR8523, Lille, F-59000, France*
[3]*Institute of Information and Communication Technologies, Electronics and Applied Mathematics, Université catholique de Louvain, B-1348, Belgium*

The relative precision $\delta\nu/\nu$ achieved in the near-infrared region today reaches the 10^{-12} level [1, 2], whereas the state of the art in coherent-emission microwave spectroscopy remains several orders of magnitude lower, around 10^{-6}. Here, we aim to surpass this limit through time-domain analysis of the $2_0\ E \leftarrow 3_{-1}\ E$ torsion-rotation transition of methanol. Located at approximately 12.2 GHz, this transition is responsible for the second brightest class II maser emission observed in the universe [3]. Accurate laboratory determination of its rest frequency is critical for using this line to probe physical quantities near stellar objects, such as magnetic fields [4] or variations in the proton-to-electron mass ratio [5].

Measurements were performed using a new experimental setup combining a Ku-band waveguide cell with a Fourier-transform microwave spectrometer. Methanol molecules were maintained in the gas phase at pressures between 10^{-3} Pa and 10^{-2} Pa and probed within the waveguide cell. The spectrometer offers a high signal-to-noise ratio through the acquisition and averaging of large numbers of free induction decays (FIDs). The line center of the $2_0\ E \leftarrow 3_{-1}\ E$ transition is extracted via least-squares fitting of the FID using a time-domain, speed-dependent Voigt profile [5, 6]. Comparisons with alternative line-shape models are presented. Full automation of the setup enables statistical analysis of the line center and investigation of systematic experimental effects. In particular, we assess the impact of unresolved hyperfine structure on the measured rest frequency. The final value of the line center and its associated uncertainties are reported.

[1] R. Aiello *et al* 2022 *Nat. Commun.* **13** 7016
[2] S. Kassi *et al* 2022 *Phys. Chem. Chem. Phys.* **24** 23164-23172
[3] D. M. Cragg *et al* 2005 *Mon. Not. R. Astron. Soc.* **360**, 533-545
[4] P. Jansen *et al* 2011 *Phys. Rev. Lett.* **106** 100801
[5] F. Rohart *et al* 1994 *J. Chem. Phys.* **101** 6475-6486
[6] B. Hays *et al* 2020 *J. Quant. Spectrosc. Radiat. Transf.* **250** 107001

Rovibronic spectra of carbon monoxide dication CO^{2+}

X. Huet[1], A. Aerts[1], N. Vaeck[1], X. Urbain[2] and M. Génévriez[2]

[1]*Spectroscopy, Quantum Chemistry and Atmospheric Remote Sensing (SQUARES), Université libre de Bruxelles, Brussels, B-1050, Belgium*
[2]*Institute of Condensed Matter and Nanosciences, Université catholique de Louvain, Louvain-la-Neuve, B-1348, Belgium*

Diatomic dications are fascinating species whose relevance in atmospheric chemistry is well established [1]. However, experimental studies that have successfully characterized their rovibronic levels have rarely been reported. In this study, a rigorous theoretical framework based on advanced computational methods is supporting high-resolution experimental investigations on CO^{2+}. This integrated approach allows for the precise characterization of molecular energy levels, providing new insights into the rovibronic properties of this dication.

Carbon monoxide dication CO^{2+} belongs to a broad class of diatomic dications that share a common feature [2]: the potential energy curves (PECs) of some of their low-lying electronic states exhibit a well bounded by an inner potential wall and an outer potential barrier. This peculiar topology reveals the presence of metastable rovibronic states within the well of the curve, lying above the dissociation channel of the PEC. Predissociation of the molecule in such states is induced either by tunneling through the potential barrier or by spin-orbit (SO) and/or non-adiabatic couplings with other electronic states. Previous theoretical investigations on CO^{2+} [3,4] have pointed out the significant role of SO coupling in predissociation of the molecule. For instance, in the ground electronic state $X^3\Pi$ of CO^{2+}, all vibrational levels except for $v = 0, 1$ are short lived.

On the theoretical side, the potential energy curves of twelve low-lying electronic states of CO^{2+}, along with their spin-orbit couplings, were computed using the multi-reference configuration interaction method. The results allow us to determine the position of the rovibrational levels and compute their lifetimes with a complex-scaling-based method. Experimentally, CO^{2+} molecules, produced from a plasma ion source in the vibrational level $v = 0$ of the $X^3\Pi$ electronic ground state, are excited to the $A^3\Sigma^+$ electronic state by running the beam of an OPO laser almost collinearly to the ion beam. Predissociation occurs on a nanosecond timescale through a SO-coupled purely repulsive state. The resulting C^+ and O^+ fragments are detected using position-sensitive detectors, allowing us to reconstruct their kinetic energy distribution and, consequently, deduce the rovibronic levels of the parent ion.

The combination of theoretical and experimental approaches allowed us to assess the accuracy of each method. The experimental results are in good agreement with the theoretical predictions, confirming the accuracy of our computational approach while also allowing us to identify potential weaknesses in the theoretical method. Based on these findings, we can assert that we have established a reliable theoretical methodology that can be applied to other systems. In particular, the high-resolution capabilities of the experimental setup allowed the precise observation of the SO-induced splitting of the Ω-components of the electronic ground state, which had not been resolved in previous studies.

[1] Thissen R *et al.* 2011 Phys. Chem. Chem. Phys. **13** 18264
[2] Sabzyan H *et al.* 2014 J. Iran. Chem. Soc. **11** 871
[3] Šedivcová T *et al.* 2006 J. Chem. Phys. **124** 214303
[4] Mrugała F *et al.* 2008 J. Chem. Phys. **129** 064314

Resolving the fine structure branching ratio in K^- photodetachment

X. Urbain[1], R. Marion[1,2] and M. Génévriez[1]

[1] *Institute of Condensed Matter and Nanosciences, Université Catholique de Louvain, Louvain-la-Neuve, 1348, Belgium*
[2] *Royal Observatory of Belgium (ROB-ORB), Brussels, 1180, Belgium*

We report the experimental determination of branching ratios among the $4s\,^2S_{1/2}$ ground state and fine structure resolved $4p\,^2P_{1/2,3/2}$ states in the photodetachment of K^-. A strong interference phenomenon occurs in alkali-metal anions at such thresholds, which has been extensively studied both experimentally [1,2] and theoretically [3,4]. The fine structure components could be separately measured by analyzing the fluorescence of the $4p\,^2P_{1/2,3/2}$ states [2]. This measurement relied on a proper calibration of the photon detection efficiency and solid angle determination.
Instead, we base our measurement on the 4π detection of photoelectrons accompanying the different final states, and rely on a priori knowledge of the channel-specific asymmetry parameters to fit the radial electron distribution at the detector with the corresponding analytical expressions. The measured branching ratios agree well with previous determinations obtained by indirect techniques.

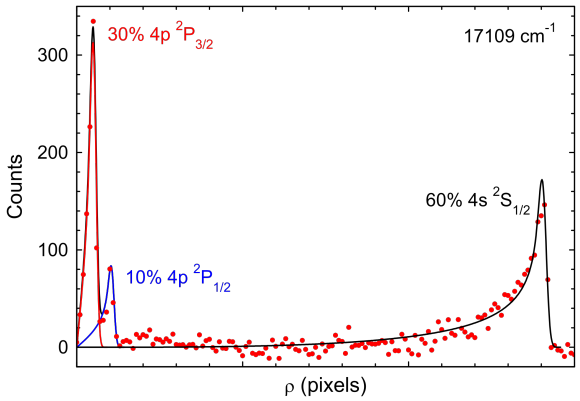

Figure 1: Radial distribution of photoelectrons recorded by velocity map imaging 22 cm^{-1} above the K($4p\,^2P_{3/2}$) + e$^-$ threshold.

[1] Slater J, Read F H, Novick S E, and Lineberger W C 1978 *P*hys. Rev. A **17** 201
[2] Rouze N and Geballe R 1983 *P*hys. Rev. A **27** 3071
[3] Lee C M 1975 *P*hys. Rev. A **ll** 1692
[4] Greene C H 1990 *P*hys. Rev. A **42** 1405

Understanding chromosomal structure from physical principles: scaling laws and microphase separation

E. Carlon[1], M. Segers[1], L. Remini[2] and A. Parmeggiani[2]

[1]*Soft Matter and Biophysics, KU Leuven, B-3001 Leuven, Belgium*
[2]*Laboratoire Charles Coulomb (L2C), Univ Montpellier, CNRS, Montpellier, France*

Each human cell contains about 2m of DNA packed in a nucleus of a few micrometers in size. How are long DNA molecules organized? This is a question of central interest as the three-dimensional chromosomal organization has a strong influence on several genomic processes such as transcription or replication. We have recently analyzed super-resolution microscopy data in which several specific DNA sites are tagged by fluorescent molecules. By recording the emitted fluorescence, the three-dimensional spatial location of the tagged loci can be determined, thereby providing information on the physical structure of the chromosomes. Inspired by polymer physics models, our analysis centers around distance distributions between different tags. We show that for any specific genomic site, there are (at least) two different conformational arrangements, implying coexisting distinct topologies which we refer to as phase α and phase β. These two phases show different scaling law behaviors indicating how DNA is arranged within each of them. We show that a simple heterogeneous random walk model captures the main behavior observed in experiments and brings considerable insights into chromosomal structure.

[1] Remini L *et al* 2024 *Phys. Rev. E* **109** 024408
[2] Remini L *et al* 2025 *J. Chem. Phys.* **162** 054110

Towards *in vivo* radiation sensing using radiation-sensitive ultrasound contrast agents

B. Carlier[1,2], U. Himmelreich[1], and E. Sterpin[2]

[1]*Laboratory of Biomedical MRI, KU Leuven, Leuven, 3000, Belgium*
[2]*Laboratory of Experimental Radiotherapy, KU Leuven, Leuven, 3000, Belgium*

Owing to a century of technological improvements, external beam radiotherapy has become one of the most effective cancer treatment strategies. In addition, the introduction of hadron therapy, where the radiation beam consists of charged particles instead of high-energy photons, enabled higher tumor conformity thanks to the finite particle range (Bragg peak). However, the steep dose gradients associated with these advanced treatments make them prone to uncertainties. While the latter can be considered during treatment planning by means of margin recipes or robust optimization techniques, such approaches inevitably increase healthy tissue exposure and resulting side effects. Hence, accurate treatment verification is of paramount importance to ensure correct treatment delivery and minimize the required treatment margins.

For this purpose, *in vivo* dosimetry and range verification techniques have become increasingly important. Yet, current solutions suffer from a variety of limitations, ranging from poor performance to complex development and a cumbersome workflow, hampering their clinical implementation. Therefore, we proposed a novel technique for *in vivo* radiation sensing based on the ultrasound imaging of radiation-sensitive contrast agents. In particular, superheated nanodroplets were developed that can be vaporized by different types of ionizing radiation depending on their degree of superheat [1,2]. The resulting microbubbles generate strong ultrasound contrast from which we derive the radiation deposition.

In this presentation, I will describe the evolution of nanodroplet-mediated ultrasound-based radiation sensing from its original conception to the first *in vivo* proof-of-concept within the context of proton range verification (figure 1) [3].

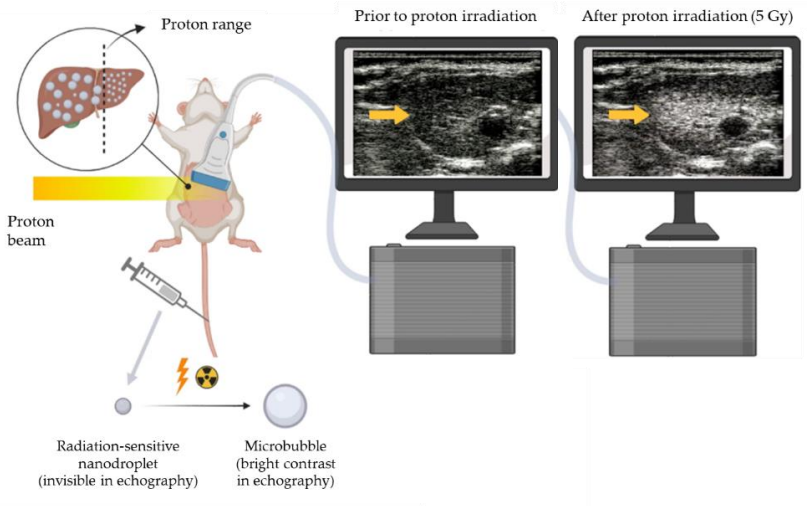

Figure 1: *In vivo* proof-of-concept of nanodroplet-mediated ultrasound-based proton range verification in the liver of a healthy rat.

[1] Carlier B*, Heymans S* *et al* 2020 Phys. Med. Biol. **65(6)** 065013
[2] Heymans S*, Carlier B* *et al* 2021 Med. Phys. **48(4)** 1983
[3] Carlier B *et al* 2024 Phys. Med. Biol. **69(20)** 205014

TOF-SIMS as a tool to study the alteration of membrane lipids in breast cancer cells after X-Ray and UHDR proton irradiation

C. Rossi[1,2], A.-C. Heuskin[2], and L. Houssiau[1]

[1]*UNamur, Namur Institute of Structured Matter, Rue de Bruxelles 61,5000 Namur, Belgium*
[2]*UNamur, NAmur Research Institute for Life Science, Rue de Bruxelles 61, 5000 Namur, Belgium*

Nowadays, breast cancer is a major health concern worldwide, with radiotherapy being one of the primary treatment modalities. Understanding the effects of ionizing radiation at the lipid membrane level is crucial, as membrane lipids play a vital role in maintaining cell integrity and signaling. FLASH radiotherapy has emerged as a promising technique for cancer treatment. One hypothesis proposed to explain the underlying mechanisms of the FLASH effect suggests that Ultra-High-Dose-Rate (UDHR) irradiation may reduce lipid peroxidation [1]. It is well-established that exposure to ionizing radiation at conventional dose rates can induce lipid alterations through the process of lipid peroxidation. But what impact does UHDR irradiation have?

Time-of-Flight Secondary Ion Mass Spectrometry (ToF-SIMS) is a powerful tool that can provide deeper insights into this hypothesis. ToF-SIMS is widely recognized in biological research for its ability to analyze the molecular composition of biological samples with submicron spatial resolution and high mass resolution. This technique has been effectively used to detect and characterize various biomarkers in cancer and other diseases, both in cells and tissues [2].

In this study, we aim to investigate the effects of X-ray irradiation on membrane lipids in breast cancer cells to establish an appropriate sample preparation method for studying the alteration of membrane lipids following UHDR proton irradiation. For this purpose, MDA-MB-231 breast cancer cells were exposed to X-ray radiation, and the resulting changes in the lipid profile of their membranes were analyzed using ToF-SIMS. These data provide insights into the molecular responses of cancer cell membranes to X-ray exposure, contributing to a better understanding of the cellular effects of radiotherapy. The next steps of this work will be to analyze breast cancer cells after proton irradiation in a conventional and UHDR mode, for different LET and dose rates, with ToF-SIMS to establish their lipid signature before and after irradiation.

[1] P. Froidevaux et al., “FLASH irradiation does not induce lipid peroxidation in lipids micelles and liposomes”, Radiation Physics and Chemistry, vol. 205,2023.
[2] M. Nabi *et al*., “Mass spectrometry in the lipid study of cancer”, Expert Review of Proteomics, vol.18, pp. 201–219,2021.

Design of a new 2D amorphous Silicon-based detector for Particle Therapy

K. El Achi[1], E. Cortina Gil,[1] A. Warnier[2], V. De Beco[2], S. Rossomme[2]

[1]*Université Catholique de Louvain, Louvain-la-Neuve, 1348, Belgium*
[2]*IBA Dosimetry, Louvain-la-Neuve, 1348, Belgium*

Particle therapy is a type of external radiotherapy that uses proton or carbon ion beams for cancer treatment to combat chronic and malignant cancers [1]. Using ultra-high dose rate (UHDR) conditions, FLASH therapy is a new treatment modality that is currently being studied by several groups. The treatment delivers high doses in a short period (40 Gy/s) and is highly effective against tumor cells while maintaining healthy cells [2]. This work aims to develop a high-resolution 2D a-Si detector for clinical routine in particle therapy. Amongst semiconductor materials, amorphous silicon (aSi) is characterized by durable radiation hardness [3]. The active region will comprise a p-n junction that is composed of a lightly p-doped bulk aSi and highly n-doped implants. Monte Carlo simulation will be used to compute the response of the active region pertaining to the different beam modalities. Early irradiation measurements using a diode performed at different proton beam intensities were done to validate simulation accuracy. The measured values using an electrometer show pristine charge linearity and close correlation with the simulation estimation, where the measurement falls in between the 2σ approximation with a 10% offset from the most probable value.

Keywords: Solid-state detector, Medical Dosimetry, Particle Therapy, Quality Assurance

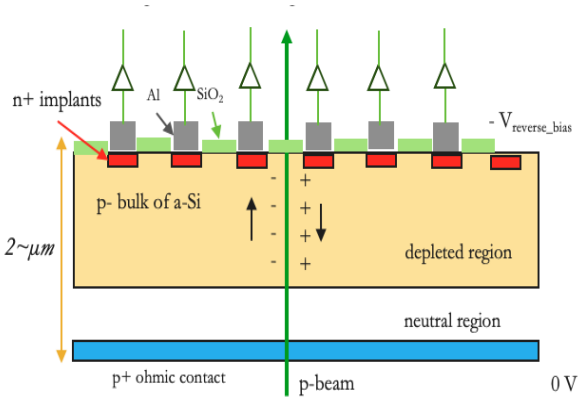

(a) Proposed detector design for an amorphous Silicon detector with a narrow depletion zone that can be expanded via a reverse bias voltage.

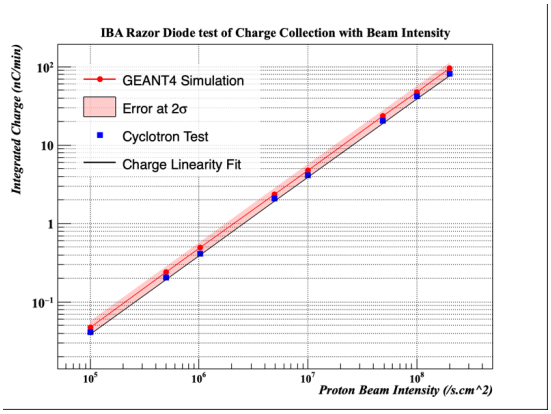

(b) Results of Geant4 Simulation with 2σ estimate and experimental results of the charge generated integrated for 1 min for each proton beam intensity for the IBA Razor Diode.

[1] E. C. Halperin, "Particle therapy and treatment of cancer," The lancet oncology, vol. 7, no. 8, pp.676–685,2006.

[2] B. Lin, D. Huang, F. Gao, et al., "Mechanisms of flash effect," Frontiers in Oncology, vol. 12, p. 995 612,2022.

[3] N. Wyrsch and C. Ballif, "Review of amorphous silicon-based particle detectors: The quest for single particle detection," Semiconductor Science and Technology, vol. 31, no. 10, p. 103 005, 2016

Monte Carlo study of high-field transverse relaxation induced by iron oxide nanoparticles coated by a slow water diffusion layer

Éléonore Martin[1], Yves Gossuin[1], Quoc Lam Vuong [1]

[1]*Biomedical Physics Unit, UMONS, Bâtiment 6, 25 Avenue Maistriau, 7000 Mons, Belgium*

Superparamagnetic iron oxide nanoparticles (SPIONs) are nanosize crystals of magnetite or maghemite. Their high saturation magnetisation and null remnant magnetisation make them particularly suitable to be used as contrast agents in nuclear magnetic resonance. Indeed, under the static magnetic fields typically used for NMR, they produce magnetic inhomogeneities, which modify the water relaxation rate where they are located. This in turn changes the pixel intensity in the area.

There is a variety of theoretical models that quantitatively predict the relaxation rate induced by such nanoparticles [1]. An important parameter is the diffusion coefficient of water molecules. However, these models only consider relaxation in a homogeneous medium, while SPIONs are usually coated with a layer of polymer. This coating is sometimes permeable to water and its water diffusion coefficient is usually smaller than that of bulk water. This inevitably affects the contrast induced by such nanoparticles [2]. Because they are complex to model analytically, numerical simulations are useful tools for studying the impact of these diffusion constraints on SPION-induced contrast.

This work hence aims at simulating, through Monte Carlo techniques, the influence of the nanoparticle polymer coating on SPION-induced T_2 NMR relaxation at high field. By varying the coating layer thickness and diffusion coefficient, it is shown that, especially with small SPIONs, thick coatings with slow diffusion lead to an increase in the water relaxation rate. This in turn leads to an increase in contrast. Our results indicate that efforts to produce thick coatings, permeable to water but with low diffusion coefficients, could improve the performance of SPIONs as contrast agents.

R (nm)	No coating	Thickness = R/4	Thickness = R/2	Thickness = R	Thickness = 2R
	R_2 (s^{-1})	R_2 (s^{-1})	R_2 (s^{-1})	R_2 (s^{-1})	R_2 (s^{-1})
7,5	36,00 ± 0,30	48,2 ± 4,1	61,9 ± 5,7	91,25 ± 0,35	73,3 ± 1,5
10	61,7 ± 0,7	71,7 ± 1,0	84,5 ± 1,7	94,2 ± 2,4	100,8 ± 1,2
20	124,8 ± 1,7	124,8 ± 1,8	117,7 ± 4,8	111,1 ± 2,7	103,2 ± 1,7
40	131,5 ± 1,0	127,6 ± 3,9	128,1 ± 4,0	127,8 ± 3,3	128,23 ± 0,26
50	114,7 ± 0,9	115,5 ± 2,2	112 ± 13	116,5 ± 1,9	125,9 ± 3,2
100	57,2 ± 3,4	57 ± 6	54,9 ± 1,3	67,5 ± 3,3	68,6 ± 2,4
160	27,7 ± 0,9	28,8 ± 0,5	29,2 ± 0,5	32,6 ± 2,5	36,1 ± 3,2
200	18,9 ± 2,5	17,9 ± 1,7	19,63 ± 0,39	20,2 ± 0,8	24,2 ± 1,6
320	7,8 ± 0,8	8,53 ± 0,27	7,9 ± 0,7	8,80 ± 0,16	9,9 ± 0,8
400	5,04 ± 0,10	4,97 ± 0,40	5,47 ± 0,37	5,52 ± 0,44	6,55 ± 0,35
420	4,70 ± 0,12	5,09 ± 0,41	4,7 ± 0,5	5,05 ± 0,26	6,13 ± 0,10
600	2,22 ± 0,10	2,19 ± 0,10	2,28 ± 0,13	2,64 ± 0,05	3,03 ± 0,06

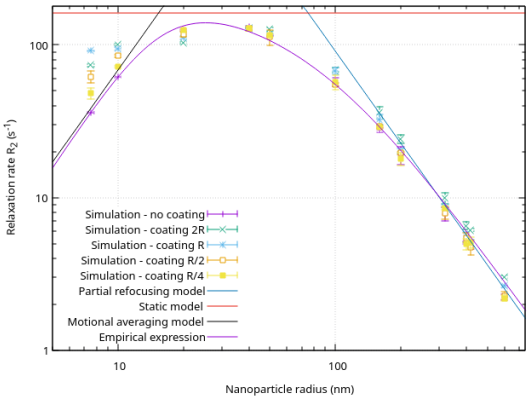

Figure 1: Simulated impact of the particle size and coating thickness on the relaxation rate induced by iron oxide nanoparticles. The diffusion coefficients in the solvent and in the coating are respectively $3 \cdot 10^{-9} m^2/s$ and $3 \cdot 10^{-10} m^2/s$. The particle magnetic volume fraction is $3.14 \cdot 10^{-6}$.

[1] Vuong Q.L., Gillis P. *et al* 2017 *WIREs Nanomed Nanobiotechnol* **e1468** 10.1002/wnan.1468

[2] Peng Y., Li Y. *et al* 2023 *Nanomed* **54** 10.1016/j.nano.2023.102713

Electrical stress on metallic nanoring based networks for flexible transparent electrodes

G. Vanoppen and B. Cleuren

UHasselt, Faculty of Sciences, Theory Lab, Agoralaan, 3590 Diepenbeek, Belgium

Transparent conductive electrodes (TCEs) are essential materials for a wide range of next-generation electronic and optoelectronic devices such as touch panels, displays and solar cells [1]. The most commonly used TCEs are based on indium tin oxide (ITO), which is not only rare, expensive and not eco-friendly to extract, but also extremely brittle, making it unsuitable for flexible devices. Therefore, there is a strong demand for alternative TCEs that are not only transparent and conductive, but also flexible and low-cost. Networks of metallic nanowires (NWs) are considered as one of the most promising alternatives to ITO.

While most of the scientific literature focusses on straight NWs (so-called nanorods), nanowires can also be manufactured in a circular shape (so-called nanorings) [2]. Due to their different geometry, nanorings have no dead ends in the percolation network. This could not only result in improved conductive properties but also reduce the occurrence of hot spots, leading to more durable electrodes [3].

In this work, we investigate the durability of an in silico network of nanorings (like in figure 1) by subjecting them to electrical stress, which seems to be one of the most important factors influencing their durability. The model for electrical stress is simple yet effective, as it is able to reproduce the main response features of an experimental sample under electrical stress. We also compare our results with those of a network of straight nanorods from [4], who used the same stress model. Compared to the nanorod networks presented in that study, we found nanoring networks that were better able to withstand the electrical stress.

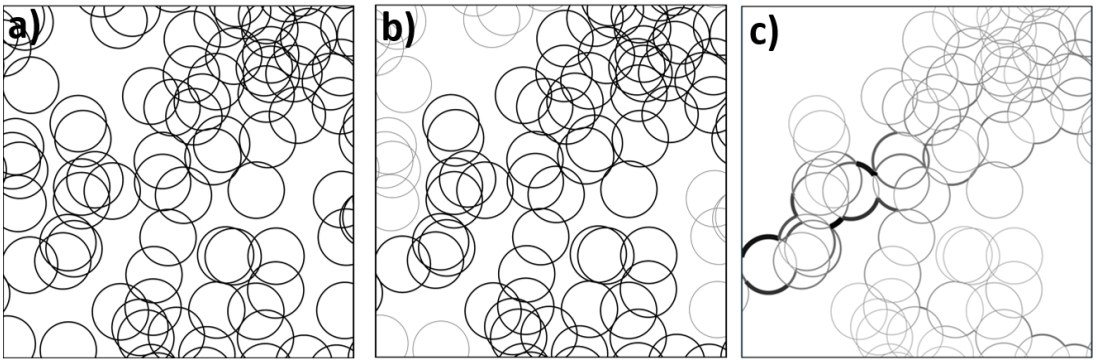

Figure 1: An example of a nanoring network a) and its percolating cluster b). A voltage difference is placed between the vertical terminals, which results in current flowing through the percolating cluster. These currents are illustrated in c), where thicker and darker lines indicate a higher current.

[1] Kumar *et al* 2022 *Mater. Today Commun.* **33** 104433
[2] Li Z *et al* 2020 *Micromachines* **11** 236
[3] Azani M and Hassanpour A 2018 *Chem. Eur. J.* **24** 19195
[4] Grazioli D *et al* 2024 *J. Compos. Sci.* **245** 110304

AI & teaching: case studies in optics class

M. Lobet[1,2]

[1] *Namur Institute of Structured Matter (NISM), University of Namur – Rue de Bruxelles, 61, Namur*

[2] *School of Engineering and Applied Sciences, Harvard University, Cambridge, Massachusetts 02138, USA*

Generative AI has become accessible to the many thanks to the explosion of ChatGPT in November 2022. After some original rejections, most of institutions now face the new reality of the accessibility of generative AI tools to the students. The presentation will discuss various experiments ran at University of Namur, with 1st bachelor in biological and veterinarian sciences in an optics introductory class. Successful and failed experiments, numerical skills of the students, pedagogical design will be discussed in several cases studies experimented at UNamur, with various supporting data.

"The Fun of Physics": a book for informal education

C. Fiolhais

Professor emeritus of the University of Coimbra, Portugal

In 1991, I published my first book, with the Portuguese title «*Física Divertida*» (in English, "The Fun of Physics"), in the Gradiva Publishing House, Lisbon, containing, by chronological order, a variety of stories from the history of Physics. The origin were lectures delivered to schools across the country. There were many references to experiments and everyday life situations, tempered with some humour.

The book turned out to be a big success with seven editions in Portugal (more than 25 000 copies sold), a Brazilian edition by the University of Brasilia, and Spanish and Italian translations. In 2005 a sequel followed, with stories on modern physics ("New Fun of Physics"), which also sold well. Recently (2024), a revised edition of the two books in a single volume appeared under the title «*Toda a Física Divertida*» («All Physics is Fun»).

I shall present not only some of the book contents but also strategies, open to discussion, on informal education of Physics based not only on my book but on my experience along decades in science communication for the general public.

The Physics Project Days
- A workshop to promote gender equality in physics

A. Benecke[1], D. Block[2], J. de Favereau[1], F. Greiner[2], M. Hein[3], and R. Kogler[4]

[1]*UCLouvain, Louvain-la-Neuve, 1348, Belgium*
[2]*Christian-Albrecht-Universität zu Kiel, Kiel, 24118, Germany*
[3]*RWTH Aachen Universität, Aachen, 52062, Germany*
[4]*DESY, Hamburg, 22607, Germany*

Promoting gender equality in physics, particularly through educational initiatives, is crucial given the low representation of women in the field, as evidenced by enrollment statistics. To address this, we initiated the Physics Project Days (PPD), a four-day workshop tailored for schoolgirls. This program aims to foster interest in physics and establish cross-school networks. Through hands-on experimentation in various physics disciplines, including particle physics, laser physics, and nanoscience, participants engage with cutting-edge research topics. As of today the PPD happen in 4 different locations: Kiel, Hamburg, and Aachen in Germany and Louvain-La-Neuve in Belgium. The PPD undergo rigorous evaluation to ensure its effectiveness and are recognized as a valuable tool for gender equality work by the German Research Foundation since 2015.

“Women in their element” – What happens when the history of the periodic system focuses on women?

B. Van Tiggelen [1]

[1]*Science History Institute, Philadelphia 19106, USA – Paris, 75005, France*

The International Year of the Periodic Table of the Chemical Element was set in 2019, coinciding intentionally with the 150th anniversary of Mendeleev's first publication of the Periodic System. This triggered many publications, meetings and projects with a historical viewpoint, often repeating the canons of heroes (D. I. Mendeleev, L. Meyer, H. Moseley, N. Bohr, … etc. to name a few of the usual suspects). What happens when the history of the periodic system is written with the explicit constraint of focusing on underrepresented groups, such as women?

This presentation will reflect on the experience of our collective volume “Women in their Element” which showcased 38 stories of female scientists who contributed to the Periodic System in a variety of different ways [1]. Few existing texts deal with women's contributions to the Periodic Table. A book on women's work can help make historical women scientists more visible [2], as well as shed light on the multifaceted character of the work on the chemical elements and their periodic relationships. Stories of female input, the editors believe, will contribute to the understanding of the nature of science, of collaboration as opposed to the traditional depiction of the lone genius.

[1] Lykknes, A and Van Tiggelen, B 2019 *Women in their element. Selected women’s contribution to the Periodic System*, Singapore: World Scientific Publishing. ISBN: 978-9811206283
[2] Van Tiggelen, B and Lykknes, A 2019 Celebrate the women behind the periodic table, *Nature* **565** 559-561. doi: https://doi.org/10.1038/d41586-019-00287-7

Understanding Nuclear Physics at different stages or education: looking for operational invariants

E. Tartinville[1] and G. Carvalho[1]

[1]*Science Education Laboratory, Catholic University of Louvain, Louvain-la-Neuve, 1348, Belgium*

This master's thesis investigates students' misconceptions in nuclear physics and how these evolve across various educational stages. Using a questionnaire administered to first-year bachelor students, master's students in physics, and future secondary school teachers, the study identifies persistent alternative conceptions regardless of academic level, though it also notes improvements in conceptual understanding with advanced education. The work is framed by the **Theory of Conceptual Fields** [1] and includes a didactic and societal rationale for teaching nuclear physics. The author highlights a lack of solid conceptual training for future teachers and provides recommendations to enhance physics education. An appendix offers an analysis of physics textbooks used in schools.

[1] Vergnaud, G 2009 *Human Development:* **52** 83-94